Identifying novel variation in root anatomical traits for waterlogging and drought tolerance and their genetic basis in wheat and barley

Shiah Alasimi

Thesis submitted to the University of Nottingham for the degree of

Doctor of Philosophy

September 2025

Division of Plant and Crop Sciences

School of Biosciences, University of Nottingham

Sutton Bonington Campus

LE12 5RD, UK

DECLARATION

I hereby declare that the research work presented in this thesis, entitled “Identifying novel variation in root anatomical traits for waterlogging and drought tolerance and their genetic basis in wheat and barley”, has been carried out by me at University of Nottingham under the supervision of Dr John Foulkes and Dr Guillermina Mendiondo. The work is composed solely by me except for the field experiments in Chapter 5 where the measurements of greenhouse gases and physiological traits were partly carried out by Marcela Moroyoqui-Parra, and no part of the thesis has been submitted, in whole or in part, earlier for any other degree of any University.

Place: University of Nottingham, Sutton Bonington Campus

Date: 15 September 2024

Shiah Alasimi

Acknowledgements

I dedicate this work to my parents, who have always been my source of strength and guiding light. I would like to express my deepest gratitude to God for granting me the strength, ability, and opportunity to complete this research project. This challenging journey would not have been possible without the support of several respected individuals who stood by me and provided me with endless encouragement. To all of them, I offer my sincere thanks and appreciation.

First and foremost, I would like to express my profound gratitude to my supervisors, Dr. John Foulkes and Dr. Guillermina Mendiondo , for their invaluable advice, unwavering support, and patience throughout my studies. Their continuous guidance and thoughtful care have greatly contributed to my success. I am truly honored to be a part of their team. I would also like to extend special thanks to my family, particularly my dear mother, who has always been my inspiration and source of strength, as well as my sister Hessah and my brother Bader for their constant support and encouragement every step of the way. To my beloved husband, who has been my greatest support and companion on this journey, thank you for your patience, understanding, and the boundless love and encouragement you have given me through every challenge. Words cannot express how much I appreciate everything you've done for me.

To my precious daughters, Sarah and Maha, who filled my life with love and laughter, making the difficulties much easier to bear. I dedicate this achievement to both of you, as your love fueled my energy and hope throughout this journey.

I would also like to thank Dr Darren Wells, Dr Jonathan Atkinson and Dr Umar Mohammed, for their training and assistance in the lab, as well as my colleagues , Dr Marcela Moroyoqui Parra , Dr Kamal Swarup, Dr Riccardo Fussi and the glasshouse team (Mark Meacham, Sue Flint and Catherine Tomlinson) for their constant support and contributions both in the lab and in the glasshouses.

I cannot forget to thank my dear friends Abrar, Khulud , Dalia, and Dalal, who helped me cope with the challenges of being far from home, and whose presence brought comfort and support during this journey.

Finally, I would like to express my heartfelt gratitude to my beloved country, The Kingdom of Saudi Arabia, and my esteemed university, Prince Sattam Bin Abdulaziz University, for granting

me the opportunity to pursue my PhD at The University of Nottingham. The support of my homeland has been the cornerstone of this achievement.

Table of Contents

List of Figures

7. Sectioning: Thin slices are cut for microscopic study.

8. Staining: Sections are stained to highlight tissues.

9. Mounting & Observation: Sections are mounted on slides and observed under a microscope. After imaging, the sections are analyzed using image analysis software.

Figure 3.1 A schematic of the N-degron pathway. This process illustrates ubiquitin-mediated targeted proteolysis, where specific protein substrates are tagged with ubiquitin for degradation by the proteasome. This pathway is a key mechanism for protein control and regulation.

Figure 3.2 This figure displays a cross-section of a root, analyzed using the RootScan software. The image highlights key anatomical features and their corresponding measurements: Total cortical area (TCA), Total stele area (TSA), Cortex cell area (CCA), Percentage of cortex that is aerenchyma (PercCisA%), and Percentage of stele that is metaxylem (PercSisMX).

Figure 3.3 Top row showing root cross-section under control conditions and the bottom row under waterlogging conditions for adventitious roots at 4 to 6 cm from the base of the stem for four spring barley genotypes using Nikon microscope.

Figure 3.4. (A) (percCisA%) Percentage of cortex as aerenchyma, (b) AA, mm^2 = Aerenchyma area, (C) CCA, mm^2 = Cortex cell area, (D) TCA; mm^2 = Cortex area, (E) TSA; mm^2 = Stele area and (F) (percSisMX%) = Percentage of stele that is metaxylem at 4 to 6 cm depth for tree mutant lines of barley Sebastian and wild type Sebastian in 2019 ,2020 ,2021 and 2022 under control and waterlogging conditions.

Figure 3.5 Root Cortical senescence (RCS) traits for four barley genotypes under control and waterlogging conditions in four individual experiments. AA (aerenchyma area), percCisA (percentage root cortical aerenchyma), (A) experiment 1,(B) experiment 2, (C) experiment 3 and (D) experiment 4.

Figure 4.1 REML statistics from the cross-experiment analysis for the Root Cortical senescence (RCS) traits for cv Paragon and three near-isogenic lines of wheat and cv Sebastian and three mutant lines and two elite lines (Sassy and Irina) of barley under control (fully irrigated) and drought conditions measured at antheses (Values are

means from two independent experiments in 2021 and 2022-23). AA (aerenchyma area, mm^2), percCisA (percentage root cortical aerenchyma, mm^2), CCA (cortex cell area, mm^2), percSisMX (percentage metaxylem), TCA (total cortical area, mm^2) and TSA (total stele area, mm^2).

Figure 4.2 Top row showing root cross-section under control conditions (well irrigated) and the bottom row under drought conditions for roots at anthesis using Nikon microscope. For cv Paragon and three near-isogenic lines of wheat; A (Paragon), B (WB TK0018-PFI), C (WB TK0019-PFI) and D (WB TK0020-OG).

Figure 4.3 Top row showing root cross-section under control conditions (well irrigated) and the bottom row under drought conditions for roots at anthesis using a Nikon microscope.A (WT Sebastian), B (*prt6k*), C (*prt6i*) and D (*prt6 ubrboxc*)

Figure 4.4 Top row showing root cross-section under control conditions (well irrigated) and the bottom row under drought conditions for roots at anthesis using Nikon microscope for two elite lines (Sassy and Irina) A (WT Sebastian), B (Irina), C (Sassy).

Figure 4.5 Green area (cm^2 $plant^{-1}$) and biomass for main shoot and total of plant for *cv* Paragon and three near-isogenic lines of wheat; and for cv Sebastian, three mutant PRT6 lines and two elite lines (Sassy and Irina) of barley under control (fully irrigated) and drought conditions measured at anthesis

Figure 4.6 Mineral concentration in barley grain: Sebastian wildtype and three PRT6 mutant lines under drought and irrigated conditions. Content of A) boron (B), B) calcium (Ca), C) cooper (Cu), D) iron (Fe), E) potassium (K), F) magnesium (Mg), G) manganese (Mn), H) sodium (Na), I) phosphorus (P), J) zinc (Zn) from the grain of barley control and mutants in a glasshouse experiment over 2021 and 22 under control (C) and drought treatment (T). ppm: parts per million (ppm). Error bars represent standard error of difference of the means (S.E.D.).

Figure 5.1 Mean across the 2 years for A) grain yield, B) plant height, C) biomass of main shoot at physiological maturity and D) infertile shoots per plant at physiological maturity**.** Error bars represent standard error of mean.

Figure 5.2 Normalized Difference Vegetation Index (NDVI) for WT Sebastian and three mutant lines of barley (*prt6k*, *prt6i*, *prt6ubrboxc*) for the PRT6 gene during grain filling in field trials in A) 2022 and B) 2023. Error bars represent the Standard Error of the Mean (SEM). Legends indicate the genotype for the barley PRT6 mutant lines and the Sebastian wildtype . NDVI values were used as a proxy for canopy greenness

Figure 5.3 Soil CO_2, CH_4 and N_2O fluxes (m^{-2} h^{-1}) during the field trial in 2023. Error bars represent standard error of difference of the means (S.E.D).

List of Tables

area, mm^2), percSisMX (percentage metaxylem), TCA (total cortical area, mm^2) and TSA (total stele area, mm^2).

Table 4.3. Leaf chlorophyll content (SPAD) for cv Paragon and three near-isogenic lines of wheat; and for cv Sebastian (wt) , three mutant *prt6* alleles and two elite lines (Sassy and Irina) of barley under control (fully irrigated) and drought conditions measured weekly in 2021

Table 4.4 Fertile tillers per plant for cv Paragon and three near-isogenic lines of wheat and for cv Sebastian and three mutant lines and two elite lines (Sassy and Irina) of barley under control (fully irrigated) and drought conditions measured weekly in 2021. **Table 4.5.** Leaf chlorophyll fluorescence for cv Paragon and three near-isogenic lines of wheat and for cv Sebastian and three mutant lines and two elite lines (Sassy and Irina) of barley under control (fully irrigated) and drought conditions measured weekly in 2021

Table 4.6. Green area (GA, cm^2) and biomass (g) per main shoot (MS) and per plant (PL) for cv Paragon and three near-isogenic lines of wheat; and for cv Sebastian and three mutant lines and two elite lines (Sassy and Irina) of barley under control (fully irrigated) and drought conditions measured at anthesis in 2021

Table 4.7 Biomass (g) for main shoot and total of plant, number of fertile, number of infertile and plant height (cm) for cv Paragon and three near-isogenic lines of wheat; and for cv Sebastian and three mutant lines and two elite lines (Sassy and Irina) of barley under control (fully irrigated) and drought conditions measured at harvest in 2021.

Table 4.8 Grain number per main shoot, grain number per plant, grain weight per main shoot, grain weight per plant and harvest index for cv Paragon and three near-isogenic lines of wheat; and for cv Sebastian and three mutant lines and two elite lines (Sassy and Irina) of barley under control (fully irrigated) and drought conditions measured at harvest in 2021.

Table 4.9. Leaf chlorophyll content (SPAD) for cv Paragon and three near-isogenic lines of wheat; and for cv Sebastian (WT), three *prt6* alleles and two elite lines

(Sassy and Irina) of barley under control (fully irrigated) and drought conditions measured weekly in 2022 Table 4.10 Fertile tillers per plant for cv Paragon and three near-isogenic lines of wheat; and for cv Sebastian, three *prt6* alleles and two elite lines (Sassy and Irina) of barley under control

(fully irrigated) and drought conditions measured weekly in 2022

Table 4.11. Leaf chlorophyll fluorescence (quantum yield, QY) for cv Paragon and three near-isogenic lines of wheat; and for cv Sebastian and three mutant lines and two elite lines (Sassy and Irina) of barley under control (fully irrigated) and drought conditions measured weekly in 2022

Table 4.12 Green area (GA, cm^2) and biomass (BM, gram) per main shoot and per plant for cv Paragon and three near-isogenic lines of wheat; and for cv Sebastian, three *prt6* alleles and two elite lines (Sassy and Irina) of barley under control (fully irrigated) and drought conditions measured at anthesis in 2022

Table 4.13 Biomass (g) for main shoot and total of plant, number of fertile, number of infertile and plant height for cv Paragon and three near-isogenic lines of wheat; and for cv Sebastian, three *prt6* alleles and two elite lines (Sassy and Irina) of barley under control (fully irrigated) and drought conditions measured at harvest in 2022.

Table 4.14 Grain number for main shoot, total of grain number per plant, grain weight in main shoot and total of grain weight per plant and harvest index for cv Paragon and three near-isogenic lines of wheat; and for cv Sebastian and three mutant lines and two elite lines (Sassy and Irina)

Table 4.15 Correlations between the different elements in the barley grains under (A) control and (B) drought conditions. *p < 0.05, **p < 0.01, ***p < 0.001, italics < 0.10.

List of Abbreviations

%	Percentage
°C	Degree centigrade
AGDM	Above-Ground Dry Matter
AA	Aerenchyma area
Cm	Centimetre
CCA	Cortical cell area
DM	Dry Matter
DNA	Deoxyribonucleic acid
Ds	Duration of spike growth
DTA	Days to anthesis
DTM	Days to maturity
DW	Dry Weight
FAO	Food and Agriculture Organization
FE	Fruiting Efficiency
Fs	Fraction of this above-ground dry matter partitioned to the spike averaged over the spike growth period
FW	Fresh Weight
G	Grams
G	Genotype
GA	Green Area
GAI	Green Area Index
GLM	General Linear Model
Glu	Glume
GN	Grain Number
GS	Growth Stage
GS65	Anthesis (Zadoks growth scale)
GS65+7d	Seven days after anthesis (Zadoks growth scale)
GS87	Physiological Maturity (Zadoks growth scale)
GW	Grain Weight

GY	Grain Yield
H	Hours
H^2	Broad-sense heritability
Ha	Hectare
HI	Harvest Index

Abstract

Climate change threatens crop yields and food security through changes in rainfall patterns associated with increased frequency of waterlogging and drought. In plants, the Ubiquitin mediated proteolysis, through the Plant Cysteine Oxidase (PCO) branch of the PRT6 N-degron pathway, has been identified as a key regulator of plant developmental and environmental responses. Much of the molecular understanding in the PRT6 N-degron pathway has been established in the genetic model *Arabidopsis thaliana*. However, there is also evidence that at least some of the molecular components of this pathway are conserved in cereals. For example, it has been shown that this pathway controls sensing low oxygen levels during waterlogging as well as affecting responses to drought and salinity in barley. The N-end rule pathway controls plant responses to hypoxia by regulating the stability of the group VII ethylene response factor (ERFVII) transcription factors, controlled by the oxidation status of amino terminal (Nt)-cysteine (Cys).

Root cortical senescence (RCS) is known as a type of programmed cell death found in the *Triticeae* tribe and studies suggest that RCS reduces water and nutrient uptake, respiration, and radial hydraulic conductance of root tissue. However, it has been argued that RCS can improve growth under suboptimal availability of water and nutrients, and that it can enable the development of crop varieties with improved drought tolerance. However, how the N-degron pathway may affect root cortical senescence traits in barley and wheat is not fully understood. The objectives of this study were firstly to evaluate the genetic variation of RCS traits and above-ground physiological traits of barley mutants for the PRT6 gene regulating the N-degron pathway under optimum and waterlogged conditions in controlled environment experiments. Secondly, to quantify the genetic variation of RCS traits and aboveground physiological traits and yield and yield components of barley mutants for the *Prt6* gene, as well as of wheat Paragon x Watkins landrace lines, under well-watered and drought-stressed conditions in glasshouse experiments. Thirdly, to quantify the soil greenhouse-gas emissions and physiological traits, yield and yield components in the barley PRT6 mutant lines and the wild type in two field experiments under rain-fed

conditions. The mutant PRT6 barley lines in these experiments are in the spring barley Sebastian background with three PRT6 allele mutations tested: *prt6k, prt6i and prt6 ubrboxc*.

Three barley lines containing mutants alleles for the PRT6 gene in barley (*prt6i*, *prt6k* and *prt6 ubrboxc*) and the Sebastian WT parent were phenotyped under controlled and waterlogging conditions in four controlled-environment experiments, and under well-irrigated and drought conditions in two glasshouse experiments. In addition, these lines were phenotype under rainfed conditions in two field experiments. Furthermore, three Paragon × Watkins landrace lines and the wild type Paragon were phenotype under well-watered and drought conditions in the two glasshouse experiments. In each experiment, the quantification of root anatomical traits, including total aerenchyma area and percentage aerenchyma tissue area in root cross-sections, was carried out for the genotypes (calculated as the percentage of air spaces using images of root cross-sections). Above-ground traits, including leaf chlorophyll content (SPAD), tiller number, dry matter accumulation and yield and yield components at harvest were also measured. In addition, greenhouse gas emissions, including CO_2 and N_20, were measured in the field experiments.

Results in CE and glasshouse experiments showed the percentage root aerenchyma area was increased under abiotic stress (waterlogging or drought), and for barley genotypes the increases were greater in the *prt6i* alleles than in the Sebastian wild type. In the present experiments, leaf chlorophyll content retention was not enhanced in the *PRT6* mutants compared to the Sebastian WT nor was shoot number per plant or plant height enhanced under waterlogging. So, positive effects on improved shoot growth under waterlogging for these *PRT6* mutants could not be confirmed in the present experiments. The barley *prt6i* allele in the present glasshouse experiments did not respond significantly differently to the drought stress for above-ground traits, despite an increase in absolute area of root aerenchyma and percentage aerenchyma area in this line compared to the Sebastian wild type under drought. These results suggest that the percentage aerenchyma area alone is not a sufficient indicator of drought tolerance without taking into consideration other root and above-ground physiological traits. In the field experiments, biomass at maturity was higher in *prt6k*

compared to WT by 4%. Differences in the greenhouse gas emissions were found in the field trial in 2023. CO_2 and N_20 was higher in *prt6k* allele compared to the WT by 34% and 20%, respectively.

Future studies should explore the complex interactions between aerenchyma formation and other physiological processes to understand their comprehensive impact on waterlogging and drought resilience. One possible explanation for the lack of drought tolerance despite increased aerenchyma area % could be related to its impact on water transport in xylem vessels. Aerenchyma plays a role in facilitating gas exchange in roots, but its increase might interfere with the hydraulic conductivity of xylem vessels. This could happen if the formation of aerenchyma reduces the mechanical strength of roots or alters their ability to transport water efficiently from roots to shoots. Future studies should also address the application of RCS traits and PRT6 mutant alleles for plant breeding for waterlogging and drought tolerance. For example, by introgression of the PRT6 alleles into modern elite high-yielding potential backgrounds and by developing molecular markers for screening germplasm for haplotype variation in the PRT6 gene.

Chapter 1: Introduction and Literature Review

This chapter provides a comprehensive exploration of root traits and root cortical senescence in wheat and barley, focusing on how they influence plant growth, development, and resilience to drought and waterlogging. By examining these critical factors, the chapter will show how they contribute to optimising crop performance under challenging environmental conditions.

1.1 Global production of barley and wheat and major characteristics

Barley (*Hordeum vulgare* L.) Barley is the fourth largest cereal crop produced worldwide, with a production of 147 million metric tons in 2022/2023 (FAOSTAT, 2023). It is primarily used as animal feed, as well as in malting for beer and whisky production. On average over the past 10 years, 148.5 million tonnes of barley have been produced per annum globally (FAOSTAT, 2023). Barley is well adapted to growth at higher latitudes and even in semi-arid regions, making it widely distributed, including in extreme climates such as those of Ethiopia, Nepal and Mali, where it remains an important food crop (Cossani et al., 2011). Barley has a relatively short growing period, which makes it suitable for the short seasons at high latitudes. It can develop even more rapidly under stress, meaning that among cereal crops, barley is considered to be one of the most drought-stress tolerant (Gous et al., 2015) as the rapid development is a mechanism of drought escape. Barley is a C3 plant. In dry semiarid conditions, barley yields can be greater than wheat, rye or oats grown in the same conditions (Chapman and Carter, 1976). Barley is better suited to dry conditions, under which it can tolerate temperatures of 32°C and above.

Barley has spring and winter varieties, which are sown in the autumn and spring, respectively. Vernalisation response is conferred by vernalization response major genes (Chapman and Carter, 1976). While spring barley can progress to reproductive development without a period of cool ‘vernalizing’ days, winter barley requires vernalisation during typically 50-60 cool days, with temperature in the range 3-10 °C. Barley can grow in the temperature range of 3°C to

35°C, with the optimums being 24°C during the vegetative stage, and 30°C during flowering.

Barley cultivars can also be split between two-row and six-row varieties. Barley has three spikelets per rachis node. In 2-row barley varieties, the lateral two spikelets are completely sterile, whereas in six-row cultivars all three spikelets are fertile. This results in a broader spike with a hexagonal arrangement of spikelets along the rachis in six-row cultivars. The row-type is under the control of a single pair of recessive genes (*vers1* and *vrs2*), which make all three spikelets fertile and grain producing (Smith et al., 1999).

Bread wheat (*Triticum aestivum* L.) is consumed globally across many regions as a staple crop and is the third largest produced cereal after rice and maize. It provides about 20% of the carbohydrate and 20% of the protein in human diets (FAO, 2022). Wheat grain is used in making bread, pasta and biscuits, and is also used as a supplement in animal feeds (Sharma et al., 2020), as well as an alternative for bioethanol production (Talebnia et al., 2010). Hexaploid bread wheat can be classified as winter wheat (which requires a cool climate for vernalization before flowering) or spring wheat (which doesn't require vernalization), which are grown in different environments depending on the climate of adaptation. They can also be classified as high or low gluten content and/or hard vs. soft wheat depending on grain quality or grain texture, respectively. According to the quality of the wheat grains, they are used in making different food products. Wheat cultivars which have high gluten content are mainly used for bread-making because of their dough elasticity. Similarly, hard wheat is mostly used in bread or pasta (durum wheat) making, while soft wheat is generally used for biscuits and breakfast foods.

1.2 Impacts of climate change

Climate change has a significant impact on crops, which in turn affects food availability, access to food and food quality. The effects of climate change on agriculture and food supply are complex and can vary depending on temperature, carbon dioxide (CO_2) levels, extreme weather events and regional conditions (Raza et al., 2019). Changes in temperature, precipitation patterns, and the frequency of extreme weather events can disrupt crop growth and yield. Additionally, CO_2 concentrations are projected to rise to approximately 800 ppm by the end of this century, representing a two-fold increase. Greenhouse gas emissions, particularly CO_2, are primary contributors to the

greenhouse effect, leading to warmer average global temperatures, which in turn have significant implications for agriculture and food supply (Raza et al., 2019). It is predicted that the CO_2 concentration will elevate twofold, i.e., up to 800 ppm at the end of this century. Emission greenhouse gases, especially CO_2, are the main factors for the greenhouse effect and warmer average global temperatures (Vaughn et al. 2019). While some areas show no significant influence of climate variability, in substantial areas of the global breadbaskets, >60% of the yield variability can be explained by climate variability (Ray et al., 2015). Climate change can make conditions better or worse for growing crops in different regions. For example, changes in temperature, rainfall, and frost-free days are leading to longer growing seasons in some regions at higher latitudes. This may allow some farmers to plant longer-maturing crops with higher yield potential. On the other hand, more extreme temperatures and precipitation (floods and droughts) can reduce yields. Water availability is a crucial factor in agricultural productivity, and climate change can disrupt this balance. Gradual increases in carbon dioxide may result in more favourable conditions for photosynthesis that could increase the yields of some crops. However, in some regions, these potential yield increases are likely to be restricted by extreme events, particularly extreme heat and drought, during crop flowering. Crop production is projected to decrease in many areas during the 21st century because of climate changes (Raza et al., 2019). For example, high night-time temperatures in 2010 and 2012 affected maize yields across the USA (USGCRP, 2014). In some regions, the amount of food required to offset the effects of extreme climate variability is triple the region's current food reserves (Hasegewa et al., 2021). Better-targeted food reserves and other adaptation measures could help fill the consumption gap in the face of extreme climate variability.

To mitigate the effects of climate change on crops, various adaptation strategies can be employed. These strategies include changing crop cultivars, sowing time, cultivation techniques, and irrigation practices. Crop-level adaptation through plant breeding is expected to be key in minimizing future yield losses and ensuring food security (Xiong et al., 2022). Additionally, sustainable agricultural practices that preserve soil health

and reduce greenhouse gas emissions can help minimize agriculture's impact on climate change while also developing more viable solutions (Schmitt et al., 2022).

1.3 Effects of waterlogging in crops and control strategies

Waterlogging is the presence of excess water in the root zone, accompanied by anaerobic conditions and can have several detrimental effects on crops. The excess water inhibits gaseous exchange with the atmosphere, and biological activity uses up available oxygen in the soil air and water, also called anaerobiosis, anoxia or oxygen deficiency. Waterlogging therefore, lowers oxygen levels in the root zone, which inhibits plant growth and weakens the roots (Tian et al., 2021). Waterlogging increases the reduction potential of the soil and changes the chemical equilibrium of many elements, leading to the accumulation of toxic salts and a more alkaline soil (Tian et al., 2021; Pan et al., 2021). These conditions can hamper the growth of crops and make the soil less suitable for plant development. Waterlogging can cause the loss of nutrients from the soil, further impacting plant growth and development (Manik et al., 2019). Sustained waterlogging can lead to the death of certain crops and plants (Pan et al., 2021).

Waterlogging can delay the growth and development of crops, leading to a shorter growing season and potentially lower yields (Tian et al., 2021). Waterlogging can affect the germination of seeds and the establishment of young seedlings, leading to a poor crop stand and reduced yield potential (Pan et al., 2021) and can promote the growth of water-loving wild plants, which can compete with crops for resources and reduce overall yield. In addition, waterlogged conditions can make plants more susceptible to diseases and pests, further reducing crop yield (Manik et al., 2019). The effects of waterlogging on crops can vary depending on factors such as crop type, growth stage, soil salinity, nutrient levels, temperature, frequency of waterlogging and flooding (Pan et al., 2021). Understanding these factors and implementing appropriate soil and crop management practices can help mitigate the impact of waterlogging on crop productivity (Pais et al, 2023).

Farmers can take several measures to prevent waterlogging in their crops. Implementing proper surface and subsurface drainage systems can help remove excess water from the root zone and prevent waterlogging. This can be done through techniques such as surface drainage, subsurface drainage and mole drains (Manik et al., 2019). In cases of persistent waterlogging, installing drainage systems such as French drains can help remove excess water from the root zone (Bos and Boers. 1994; Chandio et al., 2013). Practising crop rotation can help improve soil health and prevent waterlogging. By alternating between different crops, farmers can reduce the risk of waterlogging and enhance the well-being of the soil (Kaur et al., 2020). Selecting crop varieties that are more tolerant to waterlogging can help mitigate the effects of excess water on plants. Genetic differences exist for tolerance of waterlogging in crops, and incorporating waterlogging tolerance into existing elite varieties can be an effective approach. Implementing various agronomic practices, such as sowing time, nutrient application, and plant growth regulators, can help alleviate the effects of waterlogging on crops. For example, early sowing and using vigorous crops can improve crop tolerance of waterlogging (Manik et al., 2019). Crops tolerate waterlogging better if they have good nitrogen status before waterlogging occurs. Applying nitrogen after waterlogging, when the crop is actively growing, can help replenish any nitrogen deficiencies caused by waterlogging (Manik et al., 2019). Creating raised beds or using ridge and furrow arrangements can help elevate the planting areas, reducing the risk of waterlogging (Bakker et al., 2005). Using berms, which are mounds of soil, can help hold back water or divert it elsewhere, preventing waterlogging in specific areas or beds.

1.4 Impact of drought on crop production strategies

Drought stress is one of the most significant challenges facing global agriculture, profoundly affecting the production of key staple crops such as barley and wheat. Both crops are vital for food security and economic stability, making it crucial to understand how drought impacts their growth and yield.

1.5 Reduced crop yields

Drought stress can severely impact barley yields by limiting water availability, which affects grain filling and overall plant growth. Barley plants, though relatively drought-tolerant compared to other cereals, still suffer reduced yields under prolonged water deficits. Drought conditions can lead to smaller grain size and lower grain weight, reducing overall productivity. On the other hand**,** wheat is particularly sensitive to drought stress, especially during critical growth stages such as flowering and grain filling. Water scarcity during these periods can lead to significant yield reductions. Drought stress affects the development of wheat spikes and kernels, resulting in poor grain formation and lower yield potential.

1.6 Impaired photosynthesis and growth

Both barley and wheat experience reduced photosynthetic activity under drought stress due to limited water availability. Water stress causes stomatal closure, reducing carbon dioxide uptake and slowing down the photosynthesis process. This directly impacts the growth and development of the plants, leading to stunted growth and reduced biomass accumulation.

1.7 Increased susceptibility to diseases and pests

Drought-stressed barley and wheat plants are more vulnerable to diseases and pests. Weakened plants have lower resistance to fungal infections, such as rusts and blights, and are more likely to suffer from pest infestations. This additional stress further compounds the negative impact on crop yields and quality.

1.8 The impact of drought on grain quality

The quality of grains produced under drought stress can be significantly affected. Barley and wheat grains may exhibit reduced protein content, lower starch quality, and poor milling characteristics. These changes can affect the nutritional value and market value of the grains, impacting both consumers and producers. To mitigate the impacts of drought, various adaptation strategies are essential. For instance, developing

drought-tolerant crop varieties is a critical approach. In addition to breeding resilient varieties, improving crop yield under drought conditions can also be achieved by implementing strategies that manipulate root systems. These methods help enhance water and nutrient uptake, further supporting crop performance in water deficit environments.

Drought tolerance is a complex trait influenced by various genetic factors. By screening and selecting drought-tolerant genotypes, which often exhibit better root traits and water uptake, crop yield can be improved under water-limited conditions. Drought tolerance indices, such as mean productivity index (MP), geometric mean productivity (GMP), and stress tolerance index (STI), can be used to identify genotypes with high yield performance under stress conditions (Tsegay et al., 2011). Root traits, such as root length, number of roots and cortical cell number and size, play a significant role in water uptake and nutrient absorption. By improving the root system architecture and/or anatomy through genetic selection and breeding, favourable alleles can be introduced into elite cultivars to create desired root phenotypes (Dutta and Ramendra, 2022).

Plant growth regulators (PGRs) have been shown to enhance crop yield under various abiotic stress conditions, including drought. Exogenous application of substances like salicylic acid and chlormequat chloride can alleviate the negative effects of drought stress and improve plant performance. For example, foliar application of salicylic acid has been found to improve barley performance under saline conditions (Pirasteh-Anosheh and Emam, 2019). Water stress can affect root development and function, leading to reduced crop yield. By implementing appropriate irrigation strategies, such as deficit irrigation or precision irrigation, the root system can be managed to increase water availability for the plants. This can help in maintaining root health and function, ultimately improving crop yield. Root signalling pathways play a crucial role in plant responses to environmental stresses, including drought. By understanding these pathways and manipulating them through genetic or chemical means, it may be possible to enhance root cortical senescence and improve crop yield under stress conditions (Slack, 2018).

1.9 Root system architecture traits in barley and wheat

Root traits refer to the morphological, anatomical and physiological characteristics of plant roots that influence their ability to acquire water and nutrients from the soil. Root traits are crucial for plant growth and development, as they determine the efficiency of water and nutrient uptake, as well as the plant's ability to anchor itself in the soil. Important root system architecture traits include root length, root length density, root diameter, root surface area, root branching, and root hair density. Root traits play a crucial role in plant growth and development, as well as in response to various abiotic stresses such as waterlogging and drought. Understanding the effects of these factors in cereals such as wheat and barley is essential for improving their productivity and resilience in the face of changing climatic conditions. Drought and waterlogging can lead to a reduction in root length, root surface area, and root hair density as well as maximum rooting depth in both wheat and barley, which can negatively affect their ability to acquire water and nutrients from the soil. For main root (primary root) axes barley typically has a relatively shallow and fibrous root system, whereas wheat generally features a deeper and more extensive root system. For lateral roots, barley roots tend to be more branched closer to the surface, whereas for wheat lateral roots are more spread out and can extend deeper into the soil. Barley root hairs are dense and concentrated near the root tip, whereas wheat root hairs are distributed along the root.

Optimising root system architecture, defined as the *in situ* space-filling properties or the spatial distribution of the root system within the rooting volume, is important for improving drought tolerance. A well-structured root system with a balanced distribution of roots can enhance water uptake (Lesmes-Vega et al., 2023). The most important root system architecture traits for improving drought tolerance in barley and wheat include:

1. **Root length and surface area:** Root length and surface area are key morphological traits that influence the total root system's foraging performance and water uptake capacity. Fine or lateral roots, which comprise the majority of the length

and surface area of root systems, are particularly important for water uptake in both herbaceous and woody plants (Wu et al., 2016; Comas et al., 2013).

2. **Root diameter**: The variation in root diameter between roots and along roots can affect root structure and the overall foraging performance of the root system. Fine root diameter is considered a useful trait for improving drought tolerance (Wu et al., 2016; Comas et al., 2013; Wasaya et al., 2014).

3. **Root length density**: Root length density, defined as the root length per unit volume of soil, is another important trait for improving drought tolerance. An extensive dataset of root lengths for many crops indicates that root length density is a key factor in plant productivity under drought conditions (Jung et al., 2019).

4. **Specific root length and specific surface area**: Specific root length (SRL, root length per unit root dry matter) and specific surface area (SSA, root surface area per unit root dry matter) are root traits that can provide a more functionally descriptive measure of water uptake capacity in proportion to the capacity for light interception. These traits are particularly useful for comparing different plant genotypes (Comas et al., 2013).

5. **Root angle and depth:** Root angle and depth can also play a role in improving drought tolerance. A deeper and more vertical root system with a steeper root angle can access deeper soil layers with more moisture, while a shallow and horizontal root system may be more efficient in capturing surface water (Chen et al., 2020).

1.10 Root cortical senescence traits

Root cortical senescence (RCS) refers to the decline and death of root cortical cells. It can lead to changes in root anatomy including aerenchyma formation, affecting respiration costs of maintaining roots and water uptake. Aerenchyma is a spongy tissue that forms spaces/air channels in the leaves, stems, and roots of halophytic plants (Diaz et al., 2018). Specific traits involved in RCS include aerenchyma area (AA), total cortical area (TCA), total stele area (TSA), and the ratios between these areas. Thus, the percentage of cortex which is aerenchyma (percCisA) and the percentage of stele which is metaxylem (percSisMx) can also be affected by root cortical senescence. The stele is the

central vascular cylinder of the root and functions in the transport of water, and nutrients, while the cortical parenchyma fulfils metabolic functions. Within the stele, metaxylem is the primary water-conducting tissue that develops later and forms the mature, functional xylem.

1.11 Root phenotyping methodologies

By understanding the relationship between root traits and waterlogging and drought tolerance, breeders can select for genotypes with more efficient root systems, leading to the development of improved wheat and barley varieties that are better adapted to water-limited environments. Root phenotyping can be used to improve abiotic stress in wheat and barley by identifying and selecting for specific root traits that contribute to enhanced water uptake and stress adaptation (Paez-Garcia et al., 2015). Phenotyping methods such as the soil-core break method and shovelomics can be used to estimate root length density, root number and root angle in the field (Boudiar et al., 2021). Field phenotyping for root traits has also been conducted using rhizotrons, mini-rhizotrons and assessments of root parameters from soil cores (root washing and root counts/image analysis), but these methods are time-consuming and labour-intensive and generally cannot be applied in experiments with large numbers of lines (Atkinson et al., 2018). Screening techniques for evaluating roots have been developed recently that have the potential to overcome these limitations, focusing on seedling root growth in germination paper pouch and wick systems (Kareem et al., 2022). The seedling root phenotyping pipeline described by Atkinson et al. (2015) revealed wheat seedling root traits that were positively linked to mature plant N uptake under low N conditions.

Methods for phenotyping root anatomical traits in field conditions on cross section of roots as aerenchyma area and root cortex area using such techniques as laser ablation tomography has been reported recently in maize and barley (Vanhees et al., 2020; Klein et al., 2020; Lynch and Strock, 2021; Lynch yet al., 2014).

1.12 Root cortical senescence and its role in plant stress responses

Root cortical senescence (RCS) is the process by which the cortical cells of plant roots undergo programmed cell death, leading to the degradation of the root cortex. Root cortical senescence is a crucial mechanism for plant adaptation to various environmental stresses, including drought and waterlogging. During root cortical senescence, the degradation of the root cortex is accompanied by the release of various enzymes and metabolites that can help the plant cope with stress. Drought stress can accelerate root cortical senescence in wheat and barley, leading to the degradation of the root cortex and the release of stress-related enzymes and metabolites.

During root cortical senescence, the outer layer of the root undergoes aging and degeneration. This process can potentially also have a negative impact on crop growth and development. To improve crops, it is important to understand the factors that contribute to root cortical senescence and its effects on plant growth and development, including impacts on the respiration costs of maintaining roots under abiotic stress and to develop strategies to optimise its expression. Potential approaches for manipulating root cortical senescence include genetic modification: Researchers have identified genes and proteins involved in root cortical senescence and have successfully modified these genes to delay the process in various plant species. By understanding the molecular mechanisms underlying root cortical senescence, scientists can develop crops with enhanced root longevity and improved overall performance. Environmental factors affecting root cortical senescence include:

1. Nutrient deficiencies or imbalances can accelerate root cortical senescence, leading to reduced crop productivity. Continuous monocropping can deplete soil nutrients and increase the risk of root diseases, both of which can contribute to root cortical senescence. Implementing crop rotation and diversification strategies can help maintain soil health, reduce disease pressure, and improve overall crop performance.

2. Water stress is a major factor contributing to root cortical senescence. Drought conditions can accelerate the aging process in the root cortex, leading to reduced water and nutrient uptake. Implementing efficient irrigation systems and practising

water-conserving techniques can help minimise water stress and improve crop performance. Implementing irrigation strategies to improve crop yield through root cortical senescence requires access to a reliable water source and proper infrastructure for water delivery. In regions with limited water resources or inadequate irrigation systems, these strategies may not be feasible or cost-effective.

1.13 The Cys-Arg/N-degron pathway: A key sensor of abiotic stress in flowering plants

The Cys-Arg/N-degron pathway, is a crucial component of the ubiquitin-proteasome system that regulates protein degradation. This pathway specifically targets proteins based on their amino-terminal residues, determining their stability and turnover within the cell. Here's an expanded explanation (Holdsworth et al., 2020; Kozlic et al., 2022). This pathway has been found to play a significant role in various aspects of plant growth, development, and stress responses, making it a potential target for improving crop performance and biotechnological applications. Manipulating the N-degron pathway can help plants better cope with various environmental stresses, such as drought, waterlogging, and salinity. For example, researchers have successfully engineered plants with improved drought and waterlogging tolerance by manipulation one of the key components of the Cys-Arg/N-degron pathway in barley (Mendiondo 2016; Vicente et al. 2017).

The N-degrons are defined operationally as components of substrate proteins that include an N-terminal "destabilizing" residue, an N-recognin (E3ligase specific for N-degrons) available N-terminus, and a Lys residue for ubiquitin addition (Gibbs et al. 2016). N-degron pathways operate in conjunction with the Ubiquitin Proteasome System (UPS) through pathway-specific E3 ligase N-recognins that shuttle substrates for ubiquitin-mediated degradation. The pathways exert important influences on cell biology, growth, development and environmental responses (Gibbs *et al*. 2011). The N-degron pathway in plants therefore involves a unique combination of E3 ligases, such as PROTEOLYSIS (PRT)6 and PRT1, which recognize non-overlapping sets of amino-terminal residues (Holdsworth et al., 2020). These pathways have been shown to regulate diverse aspects of growth and development, including the response to

flooding, salinity, vernalization (cold-induced flowering) and shoot apical meristem function.

To study and manipulate the plant N-degron pathway, researchers have developed a yeast-based functional assay that allows for straightforward analysis of N-degron-recognizing ubiquitin ligases and their substrates. This assay has been used to monitor the stability of coexpressed GFP-linked plant proteins with Arginine N-degrons, providing a valuable tool for understanding the interactions and functions of the N-degron pathway in plants (Kozlic et al., 2019). The N-degron pathway could be harnessed to enhance the performance of crops under various environmental conditions and stressors (Dissmeyer et al., 2019). Further research and development of tools for studying and manipulating the N-degron pathway in plants will be essential for unlocking its full potential in agricultural and biotechnological applications.

For example, by optimising the N-degron pathway, plants can be engineered to more efficiently use nutrients, such as nitrogen and phosphorus, from the soil. This can help reduce the need for synthetic fertilisers and minimise environmental pollution. Manipulating the N-degron pathway can also lead to increased crop yield and biomass production. For instance, researchers have successfully engineered plants with enhanced biomass production by modulating the N-degron pathway. In response to reduced oxygen or nitric oxide levels, the N-degron pathway can be stabilised, leading to the regulation of diverse aspects of growth and development, including the response to flooding, salinity, vernalization, and shoot apical meristem function. This suggests that oxygen and nitric oxide levels play a role in modulating the activity of the N-degron pathway. Proteins starting with tertiary destabilizing residues may need to be modified before they are targeted for degradation by the N-degron pathway. For example, the plant Arg/N-end rule pathway has been shown to regulate various developmental processes and flooding tolerance through the degradation of ethylene response factors, which require arginylation by ATE1/ATE2 before being targeted for degradation by PRT6. Understanding the regulation of the N-degron pathway in plants can provide insights into how to manipulate this pathway to improve crop performance.

The N-degron pathway, which mediates the degradation of ERFVII transcription factors, is a master oxygen-sensing mechanism. It regulates the transition between anaerobic conditions, such as those caused by waterlogging, and the normal aerobic growth of land plants (Giuntoli and Perata, 2018). Important work was accomplished in barley as one of the world's key cereals and as a representative monocotyledon species. The barley ERFVII family member BERF1, which is most closely related to Arabidopsis RAP2.12, was shown to be an N-degron pathway target in vitro, and its highly conserved N-degron sequence was shown to be a portable N-degron that confers instability to a C-terminally-fused GUS enzyme as an artificial protein-stability reporter in vivo. Therefore, BERF1 and its N-terminal Cys residue are also considered to act as a sensor for oxygenation and flooding status in barley. Reducing the expression of the N-recognin E3 Ub ligase PRT6 by RNAi in barley increased the expression of hypoxia-related genes and generated an enhanced waterlogging tolerance (Mendiondo et al., 2016). Transgenic barley with reduced PRT6 expression showed enhanced resistance to waterlogging; abiotic stresses, such as salinity, drought, and high temperatures (Vicente et al., 2017).

Understanding the role of the N-degron pathway in protein degradation during stress can provide insights into how to manipulate this pathway to improve crop performance The PRT6 N-degron pathway helps the plant detect and respond to abiotic stress by targeting specific proteins for degradation. This response includes modulating root development and stress adaptation mechanisms. Under stress conditions, the PRT6 N-degron pathway can influence the stability of transcription factors like BERF and RAF. These factors are critical for regulating genes involved in root development and stress responses. In addition, BERF and RAF have been reported to be substrates of this pathway *in vitro* (Mendiondo and Alasami et al manuscript under preparation). The PRT6-N-degron pathway integrates with BERF and RAF transcription factors to influence root cortical senescence and stress responses, providing a comprehensive overview of their interconnected roles in plant stress management.

By targeting specific proteins or engineering N-degron substrates, researchers may be able to enhance stress tolerance, growth, and development in crops, leading to increased yields and improved agricultural sustainability. Additionally, the N-degron

pathway has potential applications in biotechnology and therapeutics, as it can be harnessed to regulate the stability of proteins and other biological materials. Previous studies have identified Group VII-ERF transcription factors (GVII-ERFs) as the first N-degron pathway substrates in plants, acting as oxygen and NO sensors (Gibbs *et al*., 2014; Licausi *et al*., 2011). GVII-ERFs are strongly associated with plant growth, development, and responses to biotic and abiotic stresses (Gibbs *et al*., 2014; Mendiondo *et al*., 2016; Vicente *et al*., 2017; Hartman *et al.* 2019). Raza *et al.* (2019) summarized the role of GVII-ERFs in general stress tolerance, including biotic and abiotic stresses. Constitutive expression of wheat GVII-ERFs genes, such as *TaERF*1 and *TaERF3*, enhances tolerance to salt and drought stress (Rong *et al*., 2014; Zhu *et al*., 2014). We hypothesize that GVII-ERFs serve as key regulators of plant response to abiotic and biotic stresses through RCS formation in barley, mediated by the PRT6 N-degron pathway. While the identification and manipulation of PRT6 N-degron substrates are beyond the scope of this project, Mendiondo's lab has identified several GVII-ERFs as substrates *in vitro* in barley, including BERF and RAF (Alasami, unpublished). BERF1 and RAF are well-established regulators of plant stress responses. For example, ectopic expression of *RAF* in A. thaliana promotes resistance to *Ralstonia solanacearum* and enhances tolerance to salt stress (Jung et al., 2007). *BERF1* is involved in the ethylene-mediated fine-tuning of *knox3 (Bkn3*) and is expressed in root tissue in barley (Osnato et al., 2010). Schneider *et al.* (2018) demonstrated the upregulation of *RAF* and *BERF1* in a transcriptional analysis, highlighting their importance in root cortical senescence (RCS) development.

In summary, root traits and root cortical senescence are crucial for plant growth and development, as well as for their response to various environmental stresses. Drought and waterlogging can have significant effects on wheat and barley root traits and cortical senescence, which can ultimately impact their productivity and stress tolerance.

This six-chapter thesis provides a comprehensive investigation of the anatomical and physiological mechanisms underlying waterlogging and drought tolerance in barley and wheat. A primary focus is on the genetic role of the **PRT6 N-degron pathway**. The

thesis is structured to guide the reader logically from foundational knowledge to experimental findings and their broader implications.

Chapter 1: Introduction and Literature Review

This chapter reviews the literature on waterlogging and drought stress in cereal crops. It focuses on root system architecture, root cortical senescence (RCS), and the molecular basis of stress responses. The chapter concludes by identifying key research gaps and outlining the study's specific objectives and hypotheses.

Chapter 2: Materials and Methods

This section details the experimental materials and methods used across the study. It describes the specific barley mutant lines (*prt6k*, *prt6i*, *prt6 ubrboxc*), wheat near-isogenic lines (NILs), and the experimental designs and measurement protocols used in controlled-environment, glasshouse, and field settings.

Chapter 3: Waterlogging Stress in Controlled Environments

This chapter reports on growth-room experiments that investigated the effects of waterlogging stress on root anatomical traits in spring barley mutant lines and their parental wildtype. It explores how mutations in the PRT6 gene modulate RCS development and other root traits, and their impact on above-ground traits

Chapter 4: Drought Stress in Glasshouse Conditions

This chapter extends the investigation to drought conditions, examining both barley and wheat genotypes. It assesses genotype-by-treatment interactions for RCS and shoot-related traits across two glasshouse experiments, enabling a comparative analysis. It also examines the effects of PRT6 mutations on biomass and grain yield components.

Chapter 5: Field Validation and Greenhouse Gas Emissions

This chapter moves the research to field conditions, evaluating the effects of the PRT6 mutant lines on physiological responses and greenhouse gas (GHG) emissions under rain-fed conditions. It validates whether the effects observed in controlled environments are consistent under agriculturally relevant field settings.

Chapter 6: Synthesis and Future Perspectives

This final chapter integrates the findings from the previous chapters, critically evaluating the consistency of results and linking them back to the initial hypotheses. It discusses the broader implications for breeding climate-resilient cereal varieties and outlines potential directions for future research.

1.14 Objectives and hypotheses

This research aims to elucidate the role of root cortical senescence (RCS) in cereal crop adaptation to abiotic stress, with a particular focus on waterlogging and drought. By employing both genetically modified barley lines carrying mutations in the PRT6 gene and near-isogenic wheat lines (NILs) in the elite Paragon background, this study seeks to assess how specific genetic modifications influence the development and expression of RCS and associated above-ground traits determining biomass growth and grain yield. Through a combination of anatomical and physiological evaluations, the study aims to explore the potential utility of RCS as a trait conferring tolerance of waterlogging and drought stress in crop improvement programmes.

1.15 Specific Objectives

1- To characterise the root anatomical structures of mutant alleles of the PRT6 gene in spring barley (*prt6k, prt6i,* and *prt6 ubrboxc*) and NILs in spring wheat and their parental wildtypes (spring barley Sebastian and spring wheat Paragon) using microscopic and image-based methods, with particular emphasis on the extent and pattern of RCS under controlled water logging and drought stress conditions compared to unstressed control plants.

2- To evaluate the physiological responses (e.g., leaf chlorophyll retention, NDVI, biomass , grain yield and yield components) of both barley and wheat genotypes under waterlogging and drought conditions compared to unstressed controls and determine whether RCS expression correlates with above-ground performance.

3- To investigate inter- and intra-species variation in RCS expression between barley and wheat lines, thereby determining whether RCS functions as a .conserved or species-specific adaptive trait

4- To assess the agronomic implications of RCS expression in the context of plant performance and stress tolerance in field experiments, and explore whether lines exhibiting enhanced RCS in controlled-environments maintain superior growth under field conditions.; and to test whether genotypes showing differences in RCS traits differ in the flux of green-house gases (CO_2, N_2O and CH4) from the soil in the field.

5-To build a conceptual framework linking genetic background, anatomical plasticity, and physiological adaptation—thereby informing breeding strategies for stress-resilient cultivars.

1.16 Research Hypothesis

1- To test the hypothesis that targeted disruption of the PRT6 gene (PRT6 mutant lines *prt6k*, *prt6i* and *prt6 ubrboxc*) in barley and introgressions of specific genomic regions in wheat NILs will result in measurable differences in the development and expression of root cortical senescence (RCS). Specifically, they will increase root cortical senescence and aerenchyma area.

2- To test the hypothesis that there is a relationship between **r**oot cortical senescence and expression of the PRT6 gene in the mutant lines affecting the N-degron pathway, such that the mutant lines with reduced expression of the PRT6 gene show greater root cortical sencescence, aerenchyma formation and response to waterlogging than the Sebastian wild type in spring barley.

3- To test the hypothesis that the three mutant lines *prt6k*, *prt6i* and *prt6 ubrboxc* for the PRT6 gene increase root cortical senscence and aerenchyma area and this leads to increased water uptake and above-ground biomass under drought compared to the wild type Sebastian parent in barley.

4- To test the hypothesis that there is a relationship between **r**oot cortical senescence and expression of the PRT6 gene in the mutant lines affecting the N-degron pathway, such that the mutant lines with reduced expression of the PRT6 gene show greater root cortical senescence, aerenchyma formation and above-ground biomass than the Sebastian wild type in spring barley in field conditions under drought conditions.

5- To test the hypothesis that there is a relationship between **r**oot cortical senescence and expression of the PRT6 gene in the mutant lines affecting the CO_2 production by root maintenance respiration, such that the mutant lines with reduced expression of the PRT6 gene show greater root cortical senescence, aerenchyma formation and hence reduced CO_2 emissions associated with maintenance compared to the Sebastian wild type in barley.

1.17 Rationale for the investigation of the three PRT6 mutant lines in the study

The choice of the three PRT6 mutant alleles, *prt6k*, *prt6i*, and *prt6 ubrboxc,*was a deliberate and strategic decision grounded in both functional genomics rationale and experimental feasibility. These alleles were identified from a Targeting Induced Local Lesions IN Genomes (TILLING) population in the spring barley cultivar Sebastian, a widely adopted background in abiotic stress research due to its consistent field performance and well-characterized genomic resources (Mendiondo et al., 2016). All three alleles harbour missense mutations, each altering a single amino acid residue within conserved regions of the PRT6 gene. The PRT6 gene encodes an E3 ubiquitin ligase that plays a pivotal role in the Cys-Arg/N-degron pathway, a proteolytic system that regulates the stability of stress-response transcription factors, particularly the group VII ERFs, in response to cellular oxygen availability (Gibbs et al., 2014; White et al., 2017). This pathway has been shown to act as a molecular oxygen sensor, directly linking oxygen status to downstream stress-responsive gene expression (Vicente et al., 2017; Holdsworth et al., 2020

While full loss-of-function (non-sense or knockout) alleles are often ideal for establishing gene function, they were not available in viable homozygous form in this population. This limitation is not unexpected, as complete disruption of PRT6 is associated with pleiotropic developmental defects, embryonic lethality, or compromised root architecture in several plant species (Weits et al., 2020). The use of missense alleles, on the other hand, offers a balanced approach: they are viable, stable, and likely to represent partial functional disruptions, allowing the dissection of quantitative phenotypic effects across environmental gradients. To further justify their inclusion, in silico protein domain prediction and cross-species alignments were conducted. These analyses confirmed that the mutated residues reside within conserved motifs, particularly adjacent to the UBR domain critical for substrate recognition and ubiquitin ligase activity. Such conservation across barley, rice, and Arabidopsis supports their likely functional importance (Graciet et al., 2009; Bailey-Serres et al., 2022). Moreover, pilot phenotyping of these lines under waterlogging stress in preliminary trials revealed allele-specific variability in root cortical senescence (RCS) and shoot growth traits, indicating that each allele might confer a unique physiological response. This variability is instrumental for testing the central hypothesis of this study—that the N-degron pathway influences both root anatomical traits and above-ground traits in a genotype-dependent manner.

By selecting three biologically informative and tractable PRT6 alleles, this study integrates molecular genetics with applied plant physiology, enabling a deeper exploration of the gene–trait–environment nexus. This approach is aligned with contemporary frameworks in functional genomics, which increasingly favour allele series analysis over binary knockout models to reveal gene function under complex stress scenarios (Bailey-Serres et al., 2022; Holdsworth et al., 2020).

Chapter 2: Materials and Methods

2.1 Plant material

We utilised a range of genetic resources to investigate drought responses in this project. For barley, we used the spring wild-type Sebastian and three mutant alleles in the *PRT6* gene: *prt6k*, *prt6i*, and *prt6 ubrboxc*. For wheat, we used three near-isogenic lines (NILs) in the spring wheat cultivar Paragon background, along with the Paragon parental cultivar itself. These resources were used in glasshouse and field experiments to quantify responses to drought.

Barley

The spring barley wild type Sebastian and three mutant alleles in PRT6 gene named *prt6k, prt6i, prt6 ubrboxc* were provided by Dr Mendiondo's laboratory at University of Nottingham (**Fig. 2.1**). In addition, the commercial spring barley cultivars Irina and Sassy from KWS were used as control cultivars in the UK.

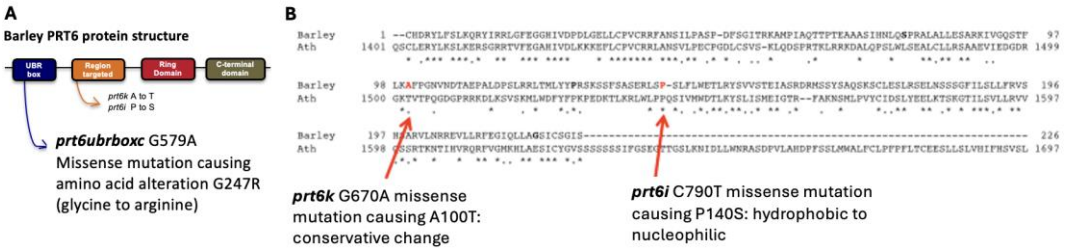

Figure 2.1 Barley PRT6 gene representation of conserved domains showing the two regions targeted**. A)** The schematic diagram which illustrates the locations of the mutant alleles *prt6k*, *prt6i*, and *prt6 ubr boxc.*. **B)** A protein sequence alignment of barley PRT6 and the model plant *Arabidopsis thaliana*. The alignment reveals a high degree of protein sequence conservation, suggesting a shared functional role across these species (Mendiondo *et al* 2016)

TILLING lines containing mutant alleles of PRT6 were developed from the HorTILLUS (*Hordeum vulgare*-TILLING-University of Silesia) population of spring barley cultivar 'Sebastian' created in Department of Genetics, University of Silesia, after double treatment of seeds with sodium azide (NaN3) and N-nitroso-N-methylurea (MNU). Mutations were identified in the PRT6 gene, giving a mutation density of 1mut/605 base pairs. Three of these were chosen (*prt6i*, *prt6k*, *prt6 ubrboxc*) that led to amino

acid substitutions, theoretically resulting in an unaffected full-length protein. For mutation identification, PCR was carried out using genomic DNA from eightfold DNA pools using the primers as described by Mendiondo et al. (2016). DNA from each individual from positive bulks was then analysed separately to identify single plants carrying mutations within the TILLING region. Seeds from M2 plants carrying mutations in the PRT6 gene were used for developing homozygous TILLING lines, which were then backcrossed with Sebastian. The material was backcrossed to BC3 in a Sebastian background by AB InBev (Fort Collins, Colorado) thorough a collaboration between Mendiondo lab and AB InBev.

Wheat: Three wheat near-isogenic lines (NILS) in spring wheat cv. Paragon background as well as the Paragon parental cultivar were used in experiments quantifying responses to drought in the glasshouse and field performance. The three Paragon NILs used were:

1- WB TK0018-PFI

2- WB TK0019-PFI

3- WB TK0020-OG

Back-crossing was started from a recombinant inbred line (RIL) from a Watkins bread wheat landrace × Paragon cross. There were two rounds of back crossing with Paragon. Final BC2F2 NILs are BC3 equivalents (since the donor of the landrace Watkins allele is a Paragon x Watkins RIL chosen to have high Paragon background). Homozygotes were selected from selfed BC2 and were multiplied in pots and then as bulk seed in a 1 m plot. The BC2 NILs have approximately 87% Paragon background. This material was developed by Dr Simon Griffiths at John Innes Centre, UK. Paragon is a UK spring wheat cultivar released by RAGT seeds in 1999.

The three near-isogenic lines were included in the study since they were shown in previous field experiments to show high N uptake at harvest compared to the

Paragon wild type in low N treatments at University farm Nottingham and Rothamsted Research in the BBSRC Lola Wheat Improvement Strategic Programme. It was hypothesised that root cortical senescence may explain improved N uptake through effects of reduced maintenance respiration costs leading to increases in the root length of remaining healthy roots, hence increasing N uptake at depth; and that the same mechanism may potential apply to increased water uptake at depth under drought. Therefore, the four wheat genotypes were included in the experiment to compare differences amongst the genotypes and also to compare responses to drought to RCS traits between barley and wheat.

2.2. Waterlogging controlled-environment experiments

Four independent controlled-environment experiments were carried out each testing the three spring barley mutant PRT6 alleles (*prt6k*, *prt6i* and *prt6 ubrboxc*) and the Sebastian *cv*. parental wild type under controlled and waterlogging conditions. The procedure in each experiment was as below.

2.2.1. Seed sterilisation, germination and plant growth conditions

Firstly, all seeds were sterilised by adding 70% ethanol for 30 seconds followed by 50% bleach for 5 minutes. After that, seeds were washed with water and then put on filter paper in a Petri dish with water added and sealed with adhesive tape (Fig 2.2) and transferred to a growth room for 4 days at 4 °C. When the seeds started germination, they were transferred (10 barley plants per genotype) to modular trays filled with compost and kept in a growth room to grow (16 h day, day temperature 15 °C, and night temperature 12) and irrigated daily (for 14 days).

2.2.2 Waterlogging conditions

In this stage seedlings were transferred (5 plants per genotype) from compost to Hydroleca, A net was inserted into the pot and fastened to cover the top of the pots (allowing the shoots to growth through the net) and sealed with micropore tape. The entire pot was submerged in water for 22 days in the waterlogging treatment, but not in control.

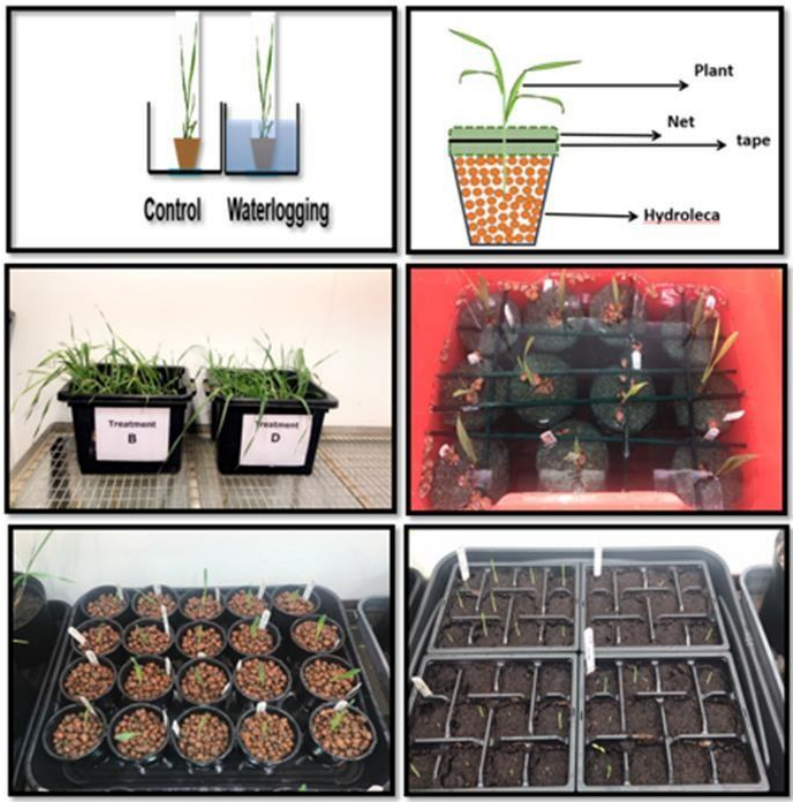

Figure 2.2 Waterlogging experiment setting. This figure shows seedling plants subjected to control and waterlogging conditions. The images depict the state of the seedlings before and after transplanting into pots. Panels illustrate seedlings under control conditions and under waterlogging stress. The images capture the impact of these conditions on plant morphology and overall health at different stages of growth.

2.2.3 Quantifying Root Cortical Senescence (RCS)

To quantify RCS in barley following waterlogging, the following steps were undertaken:

a) Sample Collection and Preservation: After 22 days from the onset of waterlogging, the net covering the pot was carefully removed (Fig 2.2). The hydroleca was gently poured out to expose the root system. Freshly developed adventitious roots, which had emerged from the base of the stem, were excised using sterilised scissors. The adventitious roots from each plant (waterlogged and control plants) were

placed in falcon tubes containing 70% ethanol and roots stored in the fridge until sectioning.

b) Root sectioning: Root samples (at 5 and 10 cm in length) from 38-day-old plants (22 days after onset of waterlogging) were obtained from two positions of the adventitious roots (5 cm and 10 cm from the root tip). The root samples were collected in water, placed in custom-designed polylactic acid moulds, and embedded with 5% agarose gel as described by Atkinson and Wells (2017). 250–300 µm thick sections of agarose-embedded roots were cut using a Vibrating Microtome Ci 7000smz-2 (Campden Instruments Ltd, England) with blade frequency of 65 Hz. Sections were stained with Calcofluor -white (0.3 mg ml^{-1}) for 1–3 minutes and rinsed with deionized water. Root sections were then imaged using an Eclipse Ti CLSM confocal laser scanning microscope (Nikon Instruments Inc, USA) using excitation and emission wavelengths of 440 nm and 540 nm, respectively (**Fig. 2.3**).

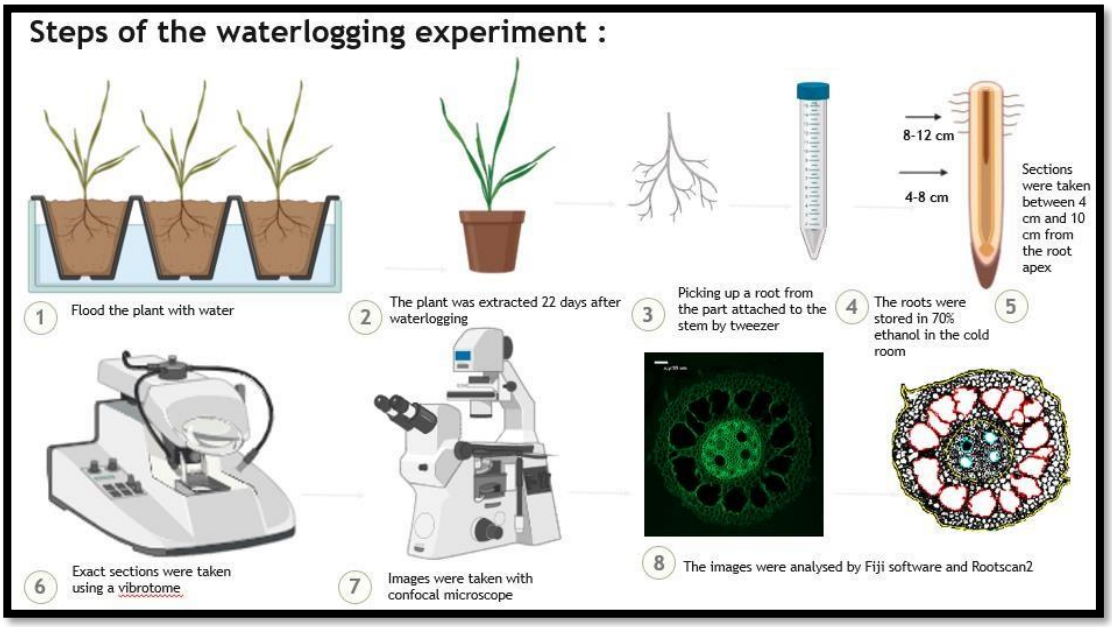

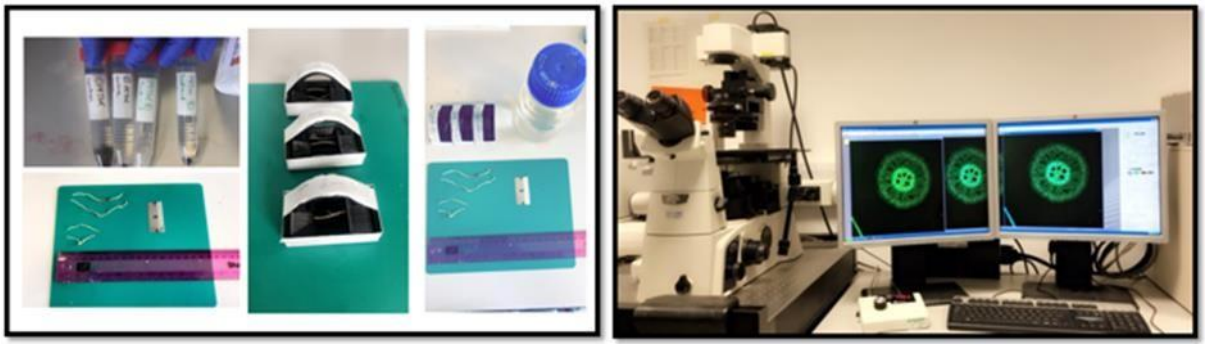

Figure 2.3 Imaging pipeline for root cortical senescence. (1) Plots flooded with water, (2) waterlogged plants sampled after 22 days, (3) adventitious roots collected, (4) roots preserved in 70% ethanol and stored in a cold room, (5) sections taken from 4-6 cm above root base, (6) sections prepared using a vibrotome, (7) images of root sections captured using Nikon microscope, (8) root images analysed using RootScan2 software. The aerenchyma area was measured to calculate the percentage of cortex that is aerenchyma (percCisA).

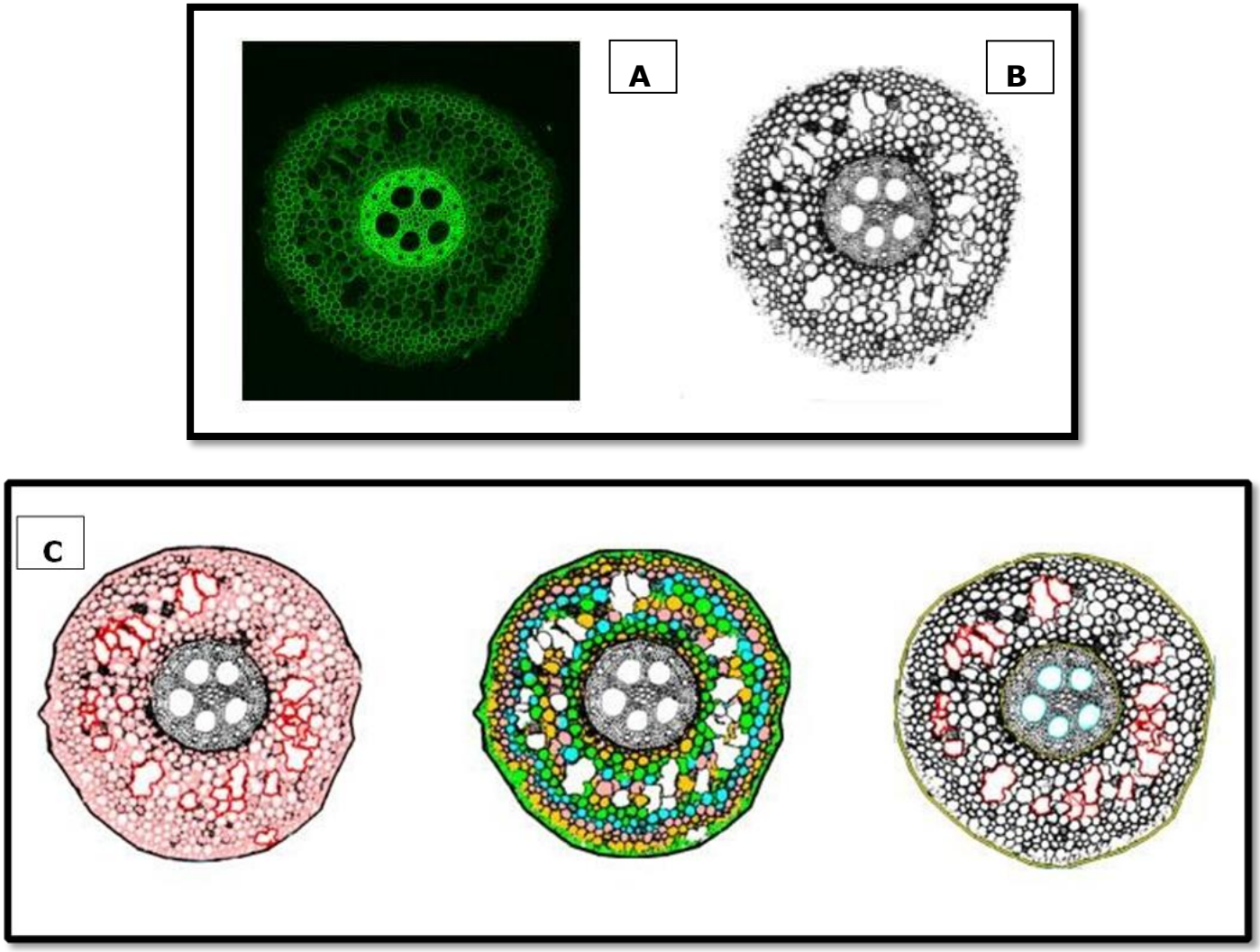

Figure 2.4. Illustrative pictures of sections of adventitious root. Panel A: confocal microscope picture. Panel B: Fiji program picture, step before image analysis. Panel C: Image analysis by Rootscan2 program.

2.2.4 Plant measurements

2.2.4.1 Leaf chlorophyll content and fluorescence

Leaf relative chlorophyll content (SPAD-502 meter, Minolta, Osaka, Japan) and fluorescence quantum yield (FP10 fluorometer, PSI, Czech Republic) were measured weekly from tillering (GS21) to stem elongation (GS32). Three readings were taken per plant (main shoot and tillers 1 and 2) in both control and waterlogged treatments (Pask *et al.,* 2012).

2.2.4.2 Tiller number

The main shoots were tagged after emergence. When the tiller buds grew out at the leaf axils and became visible tillers they were recorded. The tiller number of each plant was assessed every 2-3 weeks.

2.3 Glasshouse experiments in 2021 and 2022

2.3.1 Experimental design

In each experiment 10 genotypes were grown and tested under control and drought-stressed conditions. These comprised three wheat near-isogenic lines and the parental cultivar Paragon:

1. Paragon (WT)
2. WB TK0018-PFI
3. WB TK0019-PFI
4- WB TK0020-OG

And six spring barley genotypes, note the mutants alleles have been identified in Sebastian background:

5. Sebastian (WT)
6. *prt6k*
7. *prt6i*
8. *prt6 ubrboxc*
9. KWS Irina
10. KWS Sassy

In each experiment, there were two irrigation treatment levels (fully irrigated and droughted) and the ten genotypes were randomized in a 'split-plot' design with four replicates. There were two technical replicates for destructive samplings at anthesis (GS61) and harvest. The wheat and barley lines were kept together is two separate

blocks with the group of 10 genotypes. The irrigation treatment level was initiated approximately 20 days after transplanting at around flag-leaf emergence. Prior to this, all pots received the same weekly irrigation based on evapotranspiration in one sampling sub-replicate estimated through gravimetric analysis. The pots were weighed every 3 to 4 days on a balance (one replicate of each irrigation × genotype treatment combination). In the fully irrigated treatment, irrigation was applied weekly to maintain soil water content (SWC) to 90% of available water at field capacity (AWFC). In the droughted treatment, water was restricted from ca. 20 days after transplantation to maintain soil available water to 50% AWFC, and after GS61 to 25% AWFC (Tottman 1987; Zadoks et al. 1974). This represented a typical pattern of Mediterranean-type post-anthesis drought. Irrigation was applied by hand using a measuring cylinder at the soilpot level. To avoid any nutrient deficiencies all irrigation was applied with a complete nutrient solution.

In each experiment, before transplanting the bulk density (BD) of the soil medium was estimated in three additional 2 L pots (not used in the actual experiment) as: dry mass of oven-dried soil (g)/soil-pot volume (cm^3). The volumetric water content at field capacity (ϑ_{FC}) was calculated as: volume of water (m^3)/bulk volume of soil (m^3).
The available water at field capacity (AW_{FC}) is defined as ϑ_{FC} minus the water at the permanent wilting point (ϑ_{PWP}). In this study, ϑ_{PWP} was considered to be $\vartheta_{FC}/2$ (Dani and Wraith, 2000), so the water available at FC (AW_{FC}) is: $\vartheta_{FC} - (\vartheta_{FC}/2)$. Forty-eight hours before transplantation, the columns were irrigated to saturation and left to drain to ensure that at transplantation the soil was at FC.

All seeds were sterilized by adding 70% ethanol for 30 seconds followed by 50% bleach for 5 minutes. After that, seeds were washed with water and then put on filter paper in a Petri dish with water added and sealed with adhesive tape and transferred to a growth room for 4 days at 4 °C. When the seeds started germination, they were transferred (8 plants per genotype) to modular trays filled with soil medium of 80% sand 20% topsoil compost and kept in a growth room to grow (16 h day, day temperature 15 °C, and night temperature 12) and irrigated daily (for 14 days). After 14 days plants were transplanted into 2 L pots filled with a mixture of 80% commercial washed and 20% topsoil (sandy loam).

2.3.2 Growing conditions of plants

Initially, seeds were sterilized by immersing them in 70% ethanol for 30 seconds, followed by 50% bleach for 5 minutes. Post-sterilization, seeds were rinsed with water and placed on filter paper in a Petri dish with added water. The Petri dishes were sealed with adhesive tape and transferred to a growth room for 4 days. Once germination began, 16 plants per genotype were transferred to modular trays filled with Levington compost. These trays were maintained in a growth room with a 16-hour photoperiod, day temperatures of 15°C, and night temperatures of 12°C. The plants were irrigated daily for 14 days and then transplanted into 2 litre pots.

The sowing dates were 18 February 2021 and 5 August 2022. The plants were transferred from the modular trays to the glasshouse and transplanted into 2 litre pots (one plant per pot) containing soil medium (mixture of 80% sand 20% medium loam). Both experiments used a split-plot design with four replicates and two treatments (fully irrigated control and drought) as the 'main plot level. Herbicides and fungicides were applied as necessary to minimize the effect of weeds and diseases. No supplementary lighting was used.

2.3.3 Root cortical senescence sampling

At anthesis (GS61), freshly developed adventitious roots which had emerged from the base of the stem were excised using scissors. The roots from both well watered and droughted plants were collected and placed into Falcon tubes containing 70% ethanol for preservation. These tubes were then stored in the refrigerator (4^{o}C) to maintain the roots in good condition until further processing, specifically for sectioning as is described in Figure 2.3.

2.3.3.1 Root sectioning and imaging

Root cross-sections were prepared from adventitious roots at positions 4-6 cm from the top of the root in 38-day-old plants. Root samples were collected in water, placed in custom-designed polylactic acid moulds, and embedded with 5% agarose gel as described by Atkinson and Wells (2017). Sections, 250–300 µm thick, were cut using a Vibrating Microtome Ci 7000smz-2 (Campden Instruments Ltd, England) with a blade

frequency of 65 Hz. Sections were stained with Calcofluor White (0.3 mg/ml) for 1–3 minutes, then rinsed with deionized water. Imaging was conducted using an Eclipse Ti CLSM confocal laser scanning microscope (Nikon Instruments Inc, USA) with excitation and emission wavelengths of 440 nm and 540 nm, respectively.

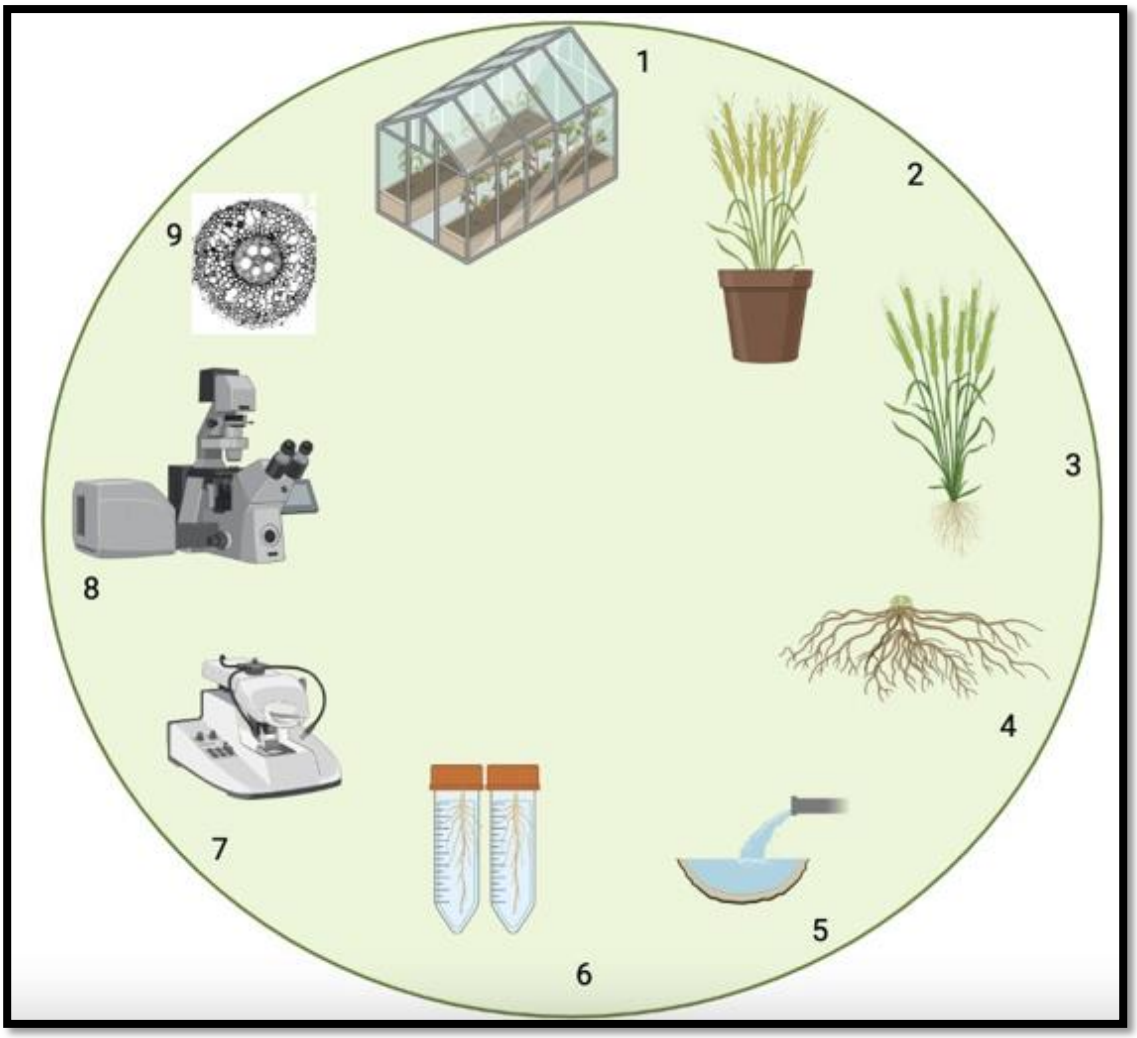

Figure. 2.5 Diagram representation of the steps in the root processing and imaging for root cortical senescence analysis

1. Root Extraction: Roots are carefully removed from the soil.

2. Washing: Roots are rinsed to remove all attached soil.

3. Fixation: Tissue is preserved to maintain structural integrity.

4. Clearing: Roots are treated to increase transparency.

5. Dehydration: Water is replaced gradually with ethanol.

6. Embedding: Roots are embedded in a supportive medium.

7. Sectioning: Thin slices are cut for microscopic study.

8. Staining: Sections are stained to highlight tissues.

9. Mounting & Observation: Sections are mounted on slides and observed under a microscope. After imaging, the sections are analyzed using image analysis software.

2.3.4 Above-ground plant measurements

2.3.4.1 Developmental stage

To quantify the impact of stress on crop development, the Zadoks scale (as described by Zadoks et al., 1974) was used. This scale categorizes crop development into several key growth stages, each representing distinct phases of growth. It is divided into two main phases: vegetative and reproductive, with specific sub-stages within each phase. For accurate assessment, the developmental stages including the onset of tillering (GS21), onset of stem elongation (GS31), and anthesis (GS61) were recorded using the decimal code of growth stages (GS) for each plant or main shoot.

2.3.4.2 Leaf relative chlorophyll content (SPAD)

Leaf relative chlorophyll content (SPAD) was measured every 7-14 for the newest fully emerged leaf on the main shoot from tillering (GS21) to physiological maturity (GS89) on each plant using a chlorophyll meter (SPAD-502; Minolta, Osaka, Japan). Three readings will take per plant in both well-watered and drought treatments.

2.3.4.3. Leaf chlorophyll fluorescence

The chlorophyll fluorescence as the quantum yield (QY) was measured every 7-14d for the newest fully emerged leaf on the main shoot from tillering (GS21) to physiological maturity (GS89) on each plant using a FluorPen FP 100 fluorometer (PSI, Czech Republic). Measurements were taken on three leaves per plant (main shoot and tillers 1 and 2) on the same dates as the leaf SPAD measurements.

2.3.4.4. Tiller number

The number of fertile and infertile tiller for each plant was counted every 14-21 days. Infertile shoots were classified as those for which all leaves were yellow or the newest emerging leaf was yellowing before anthesis; and after anthesis shoots without an ear.

2.3.4.5. Plant height

Plant height of the main shoot was measured to the tip of the ear with a ruler for each plant at physiological maturity.

2.3.4.6. Plant water uptake and water-use efficiency

Plant water uptake (WU; cumulative water used by the plant from transplanting to GS31) was calculated based on the weight of pot (one replicate of each irrigation x genotype treatment combination) at transplanting ($_T$) and harvest ($_H$) and also taking account of the amount of irrigation water added to each pot. It was assumed that drainage and soil evaporation were zero from transplanting to harvest.

$$WU\ (L) = \text{pot weight (kg)}_T + \text{Irrigation (L)} - \text{pot weight (kg)}_H \qquad \text{Equation 2.1}$$

Water-use efficiency (WUE) was calculated at harvest as:

$$WUE\ (g/L) = \text{AGDM at harvest (g plant)} / \text{Water uptake (L)} \qquad \text{Equation 2.2}$$

2.3.4.7. Plant growth analysis

For the samplings at anthesis (GS61) and physiological maturity (GS89), the fresh weight of the above-ground plant was measured, and the material was separated into fertile (those with some green area prior to GS61 or with an ear from GS61 onwards) and infertile (those with no green area prior to GS61 or without an ear from GS61 onwards) shoots. The fertile shoots were separated into flag-leaf, remaining leaf lamina, stem-and-leaf-sheath and the ear, and components weighed separately after drying for 48 h at 80 °C. The weight of the aboveground dry matter of the infertile shoots was also recorded. At harvest, the ears were hand-threshed, and the chaff and grain weighed separately after drying for 48 h at 80 °C. Grain number was measured using a seed counter (CONTADOR, Hoffman Manufacturing, Jefferson, OR, USA) and the weight was recorded after drying for 48 h at 80 °C.

2.3.4.8. Ionomic profiling of grain: analysis of mineral and elemental composition

Grain samples of the main shoot at physiological maturity (GS89) were analysed for the elemental concentrations of B, Na, Mg, Al, P, S, K, Ca, Mn, Fe, Co, Ni, Cu, Zn, As, Se, Rb, Mo, and Cd following the analytical methods described in Ziegler et al. (2013). Individual grain weight was also recorded for each sample analysed. A simple weight normalization procedure to correct measured sample concentrations for grain size was applied to introduce artefacts, especially for elements whose concentration is at or near the method detection limit. This could either be due to a systematic over or under reporting of elemental concentrations by the ICP-MS procedure or a violation of the assumption that all elemental concentrations scale linearly with weight. We used an alternative method to normalize for seed weight following the method recently reported in Shakoor et al. (2016). A linear model was developed modelling un-normalized seed concentrations against seed weight and the analytical experiment the seed was run in. The residuals from this linear model were then extracted and used as the elemental phenotype. For each element, the phenotypic measurement was taken as the median of the elemental concentrations from the two or eight seeds measured from each line (after outlier removal of measurements with a median absolute deviation of >10 where we had enough samples).

Chapter 3: The role of the PRT6 N-degron Pathway in Regulating Root Cortical Senescence during Waterlogging in Barley

3.1 Introduction

3.1.1. Climate change and its effects on crop production

Climate change will be a major factor influencing potential crop production in the coming decades, making strategies to enhance crop resilience essential for sustaining agricultural productivity. Barley production in the UK is second only to wheat, and contributes £20 B to the UK economy, including the beer and whisky industries. Modelling of climate scenarios has shown that barley production globally is set to decrease, as cereal demand continues to increase year on year. As such, it is critical to develop new breeding strategies to stabilize yield under environmental stresses.

Currently there is insufficient understanding of how crops sense and respond to abiotic stresses at the molecular level and new understanding is required to combat these challenges. In plants, the N-degron pathway (formerly named N-end rule pathway) was identified as a key regulator of plant developmental and environmental responses. The molecular understanding of the N-Degron pathway has been established in the genetic model *Arabidopsis thaliana*. There is evidence that at least some of the molecular components of the N-Degron pathways are conserved in cereals.

3.1.2. The PRT6 N-degron pathway

This chapter benefits from the molecular conservation of the PCO branch of the PRT6 N-Degron pathway across taxa, including between *A. thaliana* and barley, making feasible a comparative approach between these species to further unravel and exploit the N-Degron pathway in cereals. This pathway leads to selective and conditional removal of regulatory proteins by ubiquitin-mediated targeted proteolysis based on their N-terminal (Nt) amino acid motifs (Vicente et al.,2017). The presence of a destabilizing amino acid residue targets the substrate proteins for degradation (Fig. 3.1A and B). Proteins are synthesized with NtMet, but new Nt-residues can be exposed by peptidases, including methionine aminopeptidases (MAPs) or endopeptidases. Nt-residues act as primary destabilizing targets and are recognised by E3 ligases (Arg/N-

recognins) that allows ubiquitin addition to substrates and therefore targeted degradation by the proteasome. Peptidases can also expose the secondary residues, which are arginylated by arginyl-tRNA transferases (ATEs) to produce the primary destabilizing residues (Varshavsky, 2011; Dissmeyer, 2019). Peptidases can also expose Cys that can be oxidized by oxygen and NO, and oxidized Cys acts as a secondary destabilizing residue (summary Fig.3.1A). This Cys- division of the PRT6 N-Degron pathways is present in eukaryotes and has emerged as an important sensor of oxygen and nitric oxide (NO) (Fig 3.1B). Through collaboration with AB InBev, *prt6* mutant lines have been backcrossed into commercial barley lines and are tested for their, CE, glasshouse and field performance in this thesis. However, understanding the molecular basis of this through identification of the key PRT6 substrates will be critical for optimized targeting of this pathway. The first identified N-Degron pathway substrates in plants were the Group VII-ERF transcription factors (GVII-ERFs), identified in *A. thaliana* and were shown to be oxygen and NO sensors, acting through the Cys-PRT6 branch of the pathway (Fig. 3.1 B) (Gibbs et al., 2015).

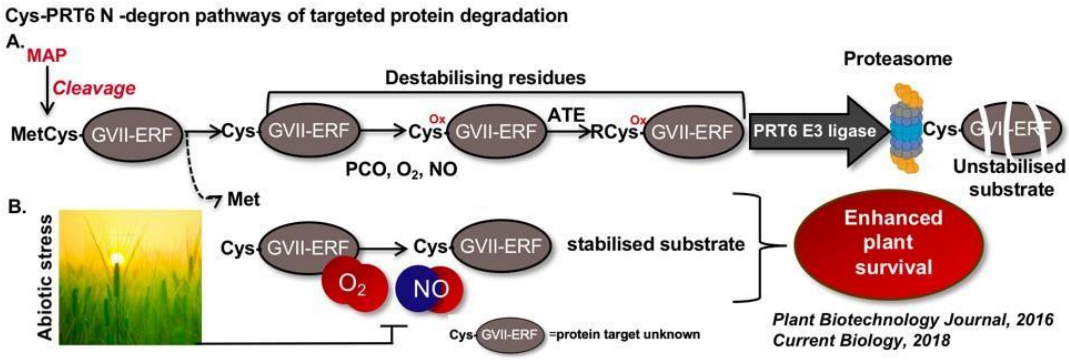

Figure 3.1 A. Simplified representation of the N-degron pathway associated with Cysteine oxidation of MC-substrate proteins. MAP, Methionine Amino-Peptidase; ATE, Arg-tRNA- protein transferase; PRT6 and PRT1 PROTEOLYSIS6 and 1; C-, C^{OX}-, R- protein substrate indicating different Nt-amino residues (C^{OX}, Cys-sulfinic acid; PCO, plant Cysteine oxidase); **B.** The Cys-PRT6 N-degron pathways controls homeostatic response of plants to low oxygen or NO through controlled degradation of group VII Ethylene Response Factor (GVII-ERFs) transcription factors. In the presence of both gases, Nt-cysteine is oxidized, allowing arginylation by ARGINYL TRANSFERASES (ATEs) which

permits recognition by the N-recognin E3 ligase PROTEOLYSIS 6 (PRT6) and degradation through the 26S proteasome. Absence of either O_2 or NO results in substrate stabilization. GVII-ERFs have previously been associated with plant responses to several abiotic stresses

This project leverages the conserved molecular nature of the PRT6 N-degron pathway across species, particularly between *Arabidopsis thaliana* and barley, allowing for a comparative approach to further investigate and utilize this pathway in cereals. The PRT6 N-degron pathway plays a key role in the selective removal of regulatory proteins via ubiquitin-mediated proteolysis, which is triggered by specific N-terminal (Nt) amino acid motifs. Proteins with destabilizing Nt-residues are targeted for degradation (Fig. 3.1A and B). Initially synthesized with Nt-Met, proteins may have new Nt-residues exposed by peptidases like methionine aminopeptidases (MetAPs) or endopeptidases. Some Nt-residues act as primary destabilizing elements and are recognized by E3 ligases (Arg/N-recognins), leading to the addition of ubiquitin and subsequent proteasomal degradation. Secondary residues, such as Asp (D) or Glu (E), are exposed and arginylated by arginyl-tRNA transferases (ATEs) to form primary destabilizing residues, while tertiary destabilizing residues Asn (N) and Gln (Q) must first be deamidated by specific Nt amidases (NTAN/NTAQ) before becoming destabilizing.

The tertiary destabilizing residue Cys can also be exposed and oxidized by oxygen or nitric oxide (NO), functioning as a secondary destabilizing residue due to its similarity to Asp (D). This Cys-related division of the PRT6 N-degron pathway is present across eukaryotes and serves as an important sensor of oxygen and NO. In collaboration with AB InBev, a PRT6 mutant has been backcrossed into commercial barley lines (three PRT6 alleles published and unpublished) and the mutant lines have been phenotyped and evaluated for controlled environment, glasshouse and field performance in Chapters 3, 4 and 5, respectively.

The identity of the second amino acid of these proteins (Cysteine, MC-) destines them for destruction under normal oxygen and NO levels (**Fig. 3.1A**). However, when oxygen or NO levels decline these proteins become stable and accumulate in the cell (**Fig.**

3.1B). The GVIIERFs have been strongly associated with a wide range of responses to plant growth, development, biotic and abiotic stress and have been implicated in multiple stress tolerances (discussed below) (Mendiondo et al., 2016). It has also been shown that GVII-ERF initial protein motif (MCGGAI-) is conserved in dicots and monocots (Fig.3A), making GVII-ERFs promising candidates to integrate in breeding strategies for stress tolerance in crops. In particular, constitutive expression of the wheat GVII-ERFs genes, *TaERF1* in *A. thaliana* and *TaERF3* in wheat enhances tolerance to salt and drought stress, while the *PATHOGENINDUCED ERF1* (*TaPIE1*) increases freezing stress tolerance in wheat. Thus, the GVII-ERFs may serve as the key regulators of plant response to abiotic and biotic stresses in barley through the PRT6 N-Degron pathway. Therefore, in this chapter, I will investigate the role of the PRT6 gene in the response to root cortical formation and response to a waterlogging treatment.

3.1.3. Root Anatomy: a key target for breeding strategies

Studying root anatomy is crucial for understanding the complex structure and function of roots in plants. This knowledge is essential for developing crops that are resilient to both biotic and abiotic stress (Deacon et al., 1986). Root anatomy study can help identify the role of different root traits in resistance to abiotic stress and understand the relationship between root anatomy and the impact of environmental stress on plant and crop growth (Robinson, 1990; Saengwilai et al., 2014). In previous work the role of the PRT6 gene in barley enhancing the tolerance to waterlogging was a focus in studies in the aerial part of the plant. However, in this chapter I will focus on the potential role of the PRT6 gene in shaping root anatomy traits like root cortical senescence (RCS). A recent paper demonstrated that RAF and BERF1, identified as putative substrates of the PRT6 N-degron pathway *in vitro*, were upregulated in a transcriptional analysis (Schneider *et al*., 2021). These findings suggest that PRT6, through its regulation of substrates, plays a crucial role in modulating the development of root cortical senescence (RCS).

Root cortical senescence (RCS) in plant roots is characterized by the formation of air spaces between cells, which alters the functionality of the tissue. Environmental stress

factors such as hypoxia, drought, and nutrient deficiency are known triggers of RCS (Postma & Lynch, 2011). During the development of RCS, living tissues in the root cortex are converted into air spaces, a process that reduces root respiration and the overall nutrient content. However, research has shown that this process promotes root development and enhances the plant's tolerance to environmental stress (Fan et al., 2003; Zhu, Brown & Lynch, 2010).

The functional implications of RCS are significant, as studies have identified three key aspects: (1) reduced root respiration, (2) decreased radial transport of nutrients and water, and (3) nutrient reallocation from senescing tissues to more active parts of the plant (Robinson, 1990; Schneider et al., 2017). These processes suggest that RCS plays a crucial role in optimizing root function under stress conditions by conserving energy and redistributing resources to sustain plant growth in adverse environments.

3.2 The specific objectives of this chapter are:

- To characterise the root anatomical structures of mutant alleles of the PRT6 gene in spring barley (*prt6k*, *prt6i*, and *prt6 ubrboxc*) and NILs in spring wheat and their parental wildtypes (spring barley Sebastian and spring wheat Paragon) using microscopic and image-based methods, with particular emphasis on the extent and pattern of RCS under controlled water logging conditions compared to unstressed .control plants.

- To evaluate the physiological responses (e.g., leaf chlorophyll retention, NDVI, biomass , grain yield and yield components) of both barley and wheat genotypes under waterlogging conditions compared to unstressed controls and determine whether RCS expression correlates with above-ground performance.

3.3 The specific hypotheses tested in this chapter are:

- To test the hypothesis that targeted disruption of the PRT6 gene (PRT6 mutant lines *prt6k*, *prt6i* and *prt6 ubrboxc*) in barley will result in measurable differences in the development and expression of root cortical senescence (RCS). Specifically, that they will increase root cortical senescence and aerenchyma area.

- To test the hypothesis that there is a relationship between root cortical senescence and expression of the PRT6 gene in the mutant lines affecting the N-degron pathway, such that the mutant lines with reduced expression of the PRT6 gene show greater root cortical senescence, aerenchyma formation and response to waterlogging than the Sebastian wild type in spring barley.

3.4 Materials and methods

The barley genotype Sebastian (TILLING) and near-isogenic lines with mutant alleles within the PRT6 gene were utilised for all experiments. Plants were grown under controlled conditions (15 °C/12 °C; 16-h photoperiod; 80% RH, 500 µmol/m^2/s metal halide lamps (HQI) supplemented with tungsten bulbs) at University of Nottingham , Sutton Bonington campus. Four independent controlled-environments experiments were carried out each testing the three spring barley mutant lines (*prt6k*, *prt6i* and *prt6 ubrboxc*) and the Sebastian *cv*. parental wild type under controlled and water logging conditions. The procedure in each experiment was as described in Chapter 2.2. The plant measurements were carried out as described in Chapter 2.2.

Statistical analysis across the four experiments was carried out using a Residual Maximum Likelihood (REML) linear mixed model in Genstat version 19 assuming replicates and experiments were random effects and genotypes and water logging treatments were fixed effects.

Figure 3.2. A. An Image illustrating the stages of the experiment in the phytotron chambers: the beginning, the initiation of flooding, and finally just before plant harvesting (from left to right). B. Images of the experimental plants at harvest, showing the differences in colour and height between different alleles, and the control plants under normal conditions and flooding conditions. C. Image showing the vibrotome device used for root cutting and slide preparation, along with a microscopic image of the section.

3.5 Results

3.5.1 Leaf chlorophyll content

The water logging, genotype and water logging x genotype effects were significant (P< 0.01; Table 3.1). Chlorophyll content in all genotypes was similar in the control at 0 days from waterlogging. WT and *prt6i* had approximately the same value of 42.3 to 42.8. compared to *prt6 ubrboxc* at 37.7. On day 20 after water logging, the decrease under waterlogging ranged from 4 to 6 SPAD units among genotypes (p= 0.001). When waterlogging conditions were applied for 20 days on plants, the highest chlorophyll content was for the WT (37.9) and *prt6i (37.7), then prt6 ubrboxc* and *prt6k* were lower and almost equal at 34.3 and 33.6, respectively. *prt6k* lost more leaf chlorophyll in response to water logging compared to the WT. There was no Time point x treatment x genotype interaction p=(0.087).

Table 3.1. REML analysis statistics for leaf chlorophyll content (SPAD), leaf number per plant, tiller number per plant and plant height for three spring barley mutant alleles (*prt6k*, *prt6i* and *prt6 ubrboxc*) and Sebastian at 0, 10, 13/14 and 20 days after application of waterlogging treatment under waterlogging and control conditions (mean values in four experiments).

treatment	Genotype	SPAD				Leaf number				Tiller number				Plant height (cm)			
		time point															
		0d	10d	13/14 d	20d	0d	10d	13/14 d	20d	0d	10d	13/14 d	20d	0d	10d	13/14 d	20d
Control	WT	40.69	41.71	43.61	41.96	3.8	7.284	10.281	11.538	1.4	2.444	3.864	4.588	26.74	36.24	41.22	41.9
	prt6k	42.19	43.01	44.26	45.28	3.208	5.557	7.054	8.182	1.25	2.062	2.952	3.875	19.03	27.54	32.31	36.14
	prt6i	43.45	46.42	46.94	41.97	3.294	7.075	7.583	9.5	1.176	2.583	2.882	3.889	24.35	37.33	41.88	48
	prt6 ubrboxc	38.96	41.41	44.37	45.37	3.833	6.247	8.897	10.818	1.417	2.526	3.792	4.875	20.13	27.94	31.92	33.23
Waterlogging	WT	42.28	41.96	40.98	37.91	3.25	7.033	10.373	12.067	1.357	3.478	4.75	5.7	24.81	34.22	40.17	40.87
	prt6k	39.95	38.14	39.23	34.26	3.185	5.405	6.984	8.071	1.37	2.3	3.36	4.105	18.29	23.67	28.3	30.96
	prt6i	42.75	34.3	37.39	37.73	3.529	6.968	9.878	10.25	1.471	3.333	3.824	4.778	22.34	32.77	40.53	46.25
	prt6 ubrboxc	37.7	38.09	37.36	33.56	3.615	5.892	8.127	8.786	1.577	2.273	3.704	5.053	18.06	25.69	30.95	59.94
F pr	Treatment	<0.001				0.448				<0.001				0.001			
	Genotype	<0.001				<0.001				<0.001				<0.001			
	Genotype*Treatment	0.006				0.035				0.001				0.129			
	Genotype*Treatment*Time point	0.087				0.064				0.221				0.767			

3.5.2. Leaf number per plant

The number of leaves per plant was measured at 0, 7, 13/14 and 20 d after onset of waterlogging. At 20 d, the WT in control conditions had more leaves per plant (11.5) than the *prt6k* line at 8.1, while *prt6i* (9.5) and *prt6 ubrboxc* (10.8) had intermediate values (p=0.001; Table 3.1). There was no main effect of water logging (p=0.448), although there was waterlogging × genotype interaction. At 20 d after waterlogging, the decrease under water logging was relatively greater for *prt6k* and *prt6 ubrboxc* compared to the WT: with values under water logging for WT of 12.0 leaves per plant, for *prt6i* of 10.3, for *prt6k* of 8.1 and for *prt6 ubrboxc* of 8.8. There was a trend for a waterlogging treatment × genotype × time point interaction (p= 0.064).

3.5.3 Tillers per plant

The number of tillers per plant was measured at 0, 7, 13/14 and 20 d after the onset of water logging. The results showed that at 20 d the *prt6 ubrboxc* line (4.9) and WT (4.6) had more tillers per plant than *prt6k* (3.9) and prt6i (3.9) (p< 0.001) under control conditions. Under waterlogging conditions, tillers per plant were overall increased slightly; tillers per plant were similar for *prt6 ubrboxc* 5.1 and WT 5.7, but lower and higher for *prt6k* 4.1 and *prt6i* 4.8, respectively (p= 0.001). There was treatment × genotype interaction (p=0.001) with the increase relatively greater for the WT compared to *prt6 ubr boxc* but no time point x treatment x genotype interaction p= (0.221).

3.5.4. Plant height

At the start of the experimental treatment (0 days after waterlogging), plant heights ranged from 18.3 to 26.0 cm. After 20 days under control conditions, both *prt6i* (24.8 cm) and WT (23.3 cm) showed similar plant heights, while *prt6k* (17.1 cm) and *prt6 ubrboxc* (13.1 cm) had significantly shorter heights (p = 0.001; Table 3.1). Under waterlogging conditions, the height increase between 0 and 20 days was greater for the *prt6* mutant lines compared to the WT. The final heights were 32 cm for *prt6 ubrboxc*, 24 cm for *prt6i*, 16 cm for WT, and 12 cm for *prt6k*. There was no significant

interaction between treatment and genotype (p = 0.129), nor between time point, treatment, and genotype (p = 0.767).

3.5.5. Root anatomical traits

The root anatomical traits measured at 38 days after sowing (22 days after the onset of waterlogging) included total cortical area (TCA), total stele area (TSA), cortex cell area (CCA), percentage of cortex that is aerenchyma (percCisA; %), and percentage of stele that is metaxylem (percSisMX) (Figs 3.3 and 3.4). In general, the mutant lines exhibited greater increases in most root cortical senescence (RCS) traits compared to the Sebastian WT under waterlogging conditions (Table 3.2).

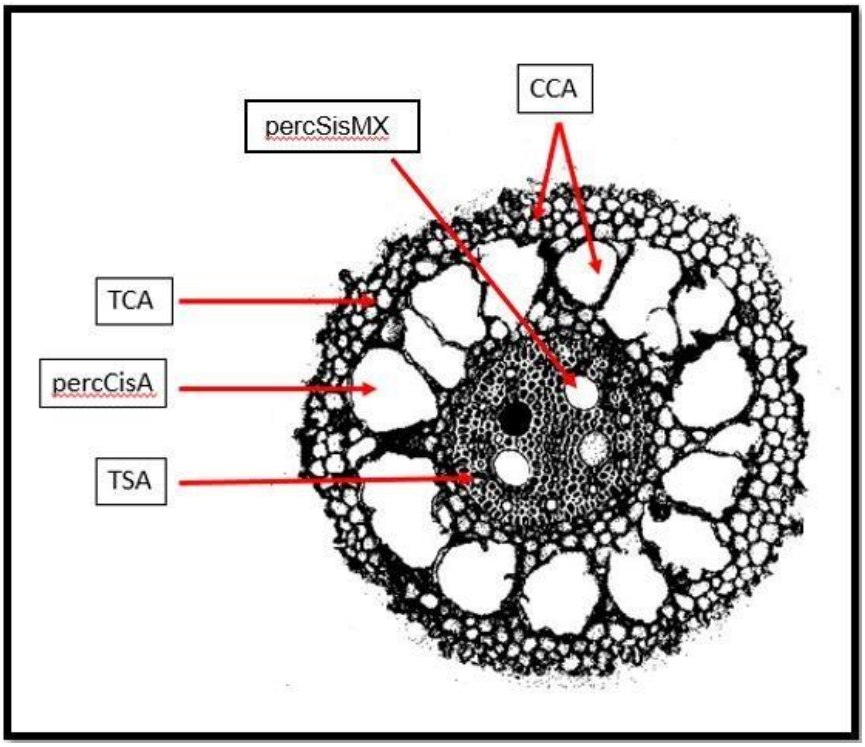

Figure 3.3 Representative root cross-section analysed using RootScan software. The image illustrates key anatomical parameters, including: Total Cortical Area (TCA), Total Stele Area (TSA), Cortex Cell Area (CCA), Percentage of Cortex that is Aerenchyma (PercCisA%), and Percentage of Stele that is Metaxylem (PercSisMX).

Table 3.2. The REML statistical analysis compared treatment differences in Root Cortical Senescence (RCS) parameters in adventitious roots across four for three mutant lines of spring barley and wild type Sebastian under control and waterlogging conditions, based on data from four independent experiments. The RCS parameters included: aerenchyma area (AA), percentage root cortical aerenchyma (percCisA), cortex cell area (CCA), percentage metaxylem in the stele (percSisMX), total cortical area (TCA), and total stele area (TSA).

RCS trait	Factor	Df (trt,resid.)	F ratio	P value
Log AA	Genotype	3, 246	14.19	<0.001
	WL treatment	1, 246	240.17	<0.001
	Genotype*treatment	3, 246	7.14	<0.001
PercCisA	Genotype	3, 246	9.73	<0.001
	WL treatment	1, 246	372.66	<0.001
	Genotype*treatment	3, 246	5.09	0.002
Log CCA	Genotype	3, 246	4.33	0.005
	WL treatment	1, 246	0.13	0.721
	Genotype*treatment	3, 246	3.96	0.009
PercSisMX	Genotype	3, 246	5.06	0.002
	WL treatment	1, 246	5.41	0.021
	Genotype*treatment	3, 246	2.03	0.111
Log TCA	Genotype	3, 246	1.58	0.194
	WL treatment	1, 246	1.81	0.179
	Genotype*treatment	3, 246	1.60	0.190
Log TSA	Genotype	3, 246	1.38	0.250
	WL treatment	1, 246	5.34	0.022
	Genotype*treatment	3, 246	1.58	0.195

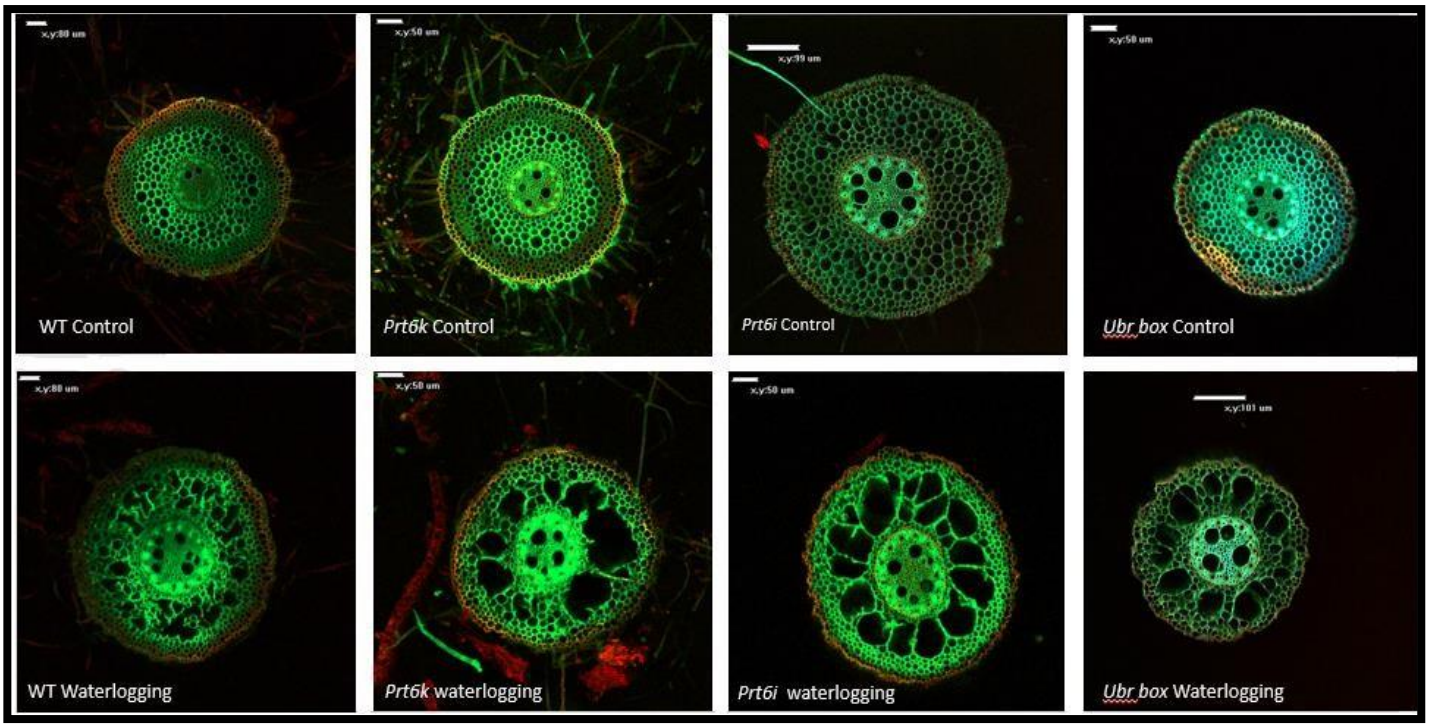

Figure 3.4 Representative root cross-sections for adventitious roots at 4 to 6 cm from the base of the stem for WT (Sebastian) and the three mutants alleles for the PRT6 gene under control conditions (top row) and waterlogging conditions (bottom row). Images were captured using a Nikon microscope

3.5.5.1 Percentage root cortical aerenchyma (PercCisA)

For percentage aerenchyma area genotypes ranged from 0 to 2.6% under control conditions and 9.5 to 14.4% under waterlogging conditions (p=0.001; Fig. 3.5 and 3.6). All the mutant lines had greater PercCisA than WT plants when the waterlogging treatment was applied. In the control, the highest percentage was for the *prt6k* (2.7) and *ubrboxc* (2.5) compared to WT (0.4) (p=0.001). The *prt6*i allele had lower percCisA compared to the other two mutant alleles. However, it was still higher than the WT plant (p=0.001). In the waterlogging treatment, the mutant lines showed larger responses in terms of increasing percCisA than the WT plant. For example, percCisA increased under waterlogging in *prt6k* to 18.5% and in *prt6i* to 17.5% compared to the WT at 9.59% (p=0.001).

3.5.5.2 Aerenchyma area (AA)

Aerenchyma area was increased in the mutant lines compared to the WT plants (p< 0.001). In the control treatment, *prt6k* was 0.00944 and WT 0.00086 mm^2 per root. When the plants were exposed to waterlogging the *prt6i* allele showed a slightly higher area (0.04168 mm^2) than *prt6k* and *prt6 ubrboxc* alleles (0.03546 and 0.02653 mm^2 per root, respectively) compared with the WT (0.0220 mm^2) (p=<0.001). There was a treatment × genotype interaction (p=<0.001), with a relative greater increase under waterlogging for *prt6i* compared to the WT.

3.5.5.3 Cortex cell area (CCA)

Under control conditions, cortex cell area per root was greater in the two mutant lines *prt6i* and *prt6k* (0.85 and 0.28 mm^2, respectively) compared to the *prt6 ubrboxc* line and the WT at 0.075 and 0.090 mm^2, respectively. Although the main effect of the water logging treatment was not statistically significant, there was a treatment x genotype interaction (p< 0.01). Under waterlogging *prt6i* showed a larger increase in CCA compared to the WT which did not increase significantly under waterlogging conditions compared to the control (P< 0.01).

3.5.5.4 Percentage steel as metaxylem (percSisMX)

Metaxylem has a role in the plant's response to water stress. It has been reported that under water stress, metaxylem cell number increased thereby improving root hydraulic conductivity, while the total cortical area was reduced (Strock et al., 2021). Averaging over the experiments, the percentage metaxylem was slightly greater for the mutant PRT6 lines than the WT under control conditions: *prt6 ubrboxc* (10.2 %), *prt6i* (9.1 %) and *prt6k* (8.5 %) compared to WT (7.8 %) (p=0.002). Under waterlogging, the percentage metaxylem overall increased slightly in mutant lines and the WT (P=0.021) with values in the range 8.3 - 11.8%.

The waterlogging treatment × genotype interaction was not statistically significant.

3.5.5.5 Total Cortex area (TCA)

Total cortex area in all three PRT^ mutant lines and the WT showed very similar values under control conditions ranging between 0.243 mm^2 (WT) to 0.225 mm^2 for *prt6i* (p= 0.194). Under waterlogging conditions, the genotypes were again not significantly different; the highest was *prt6i* (0.241 mm^2) and lowest was *prt6k* (0.217 mm^2) (p=0.174). There was no significant main effect of the water logging treatment or treatment × genotype interaction.

3.3.3.6. Total Stele area (TSA)

Total stele area showed no effect of genotype (p=0.250; Table 3.2). The main effect for the water logging treatment was significant (p=0.022), with a small increase under waterlogging (Fig. 3.5). There was no treatment x genotype interaction (p= 0.195).

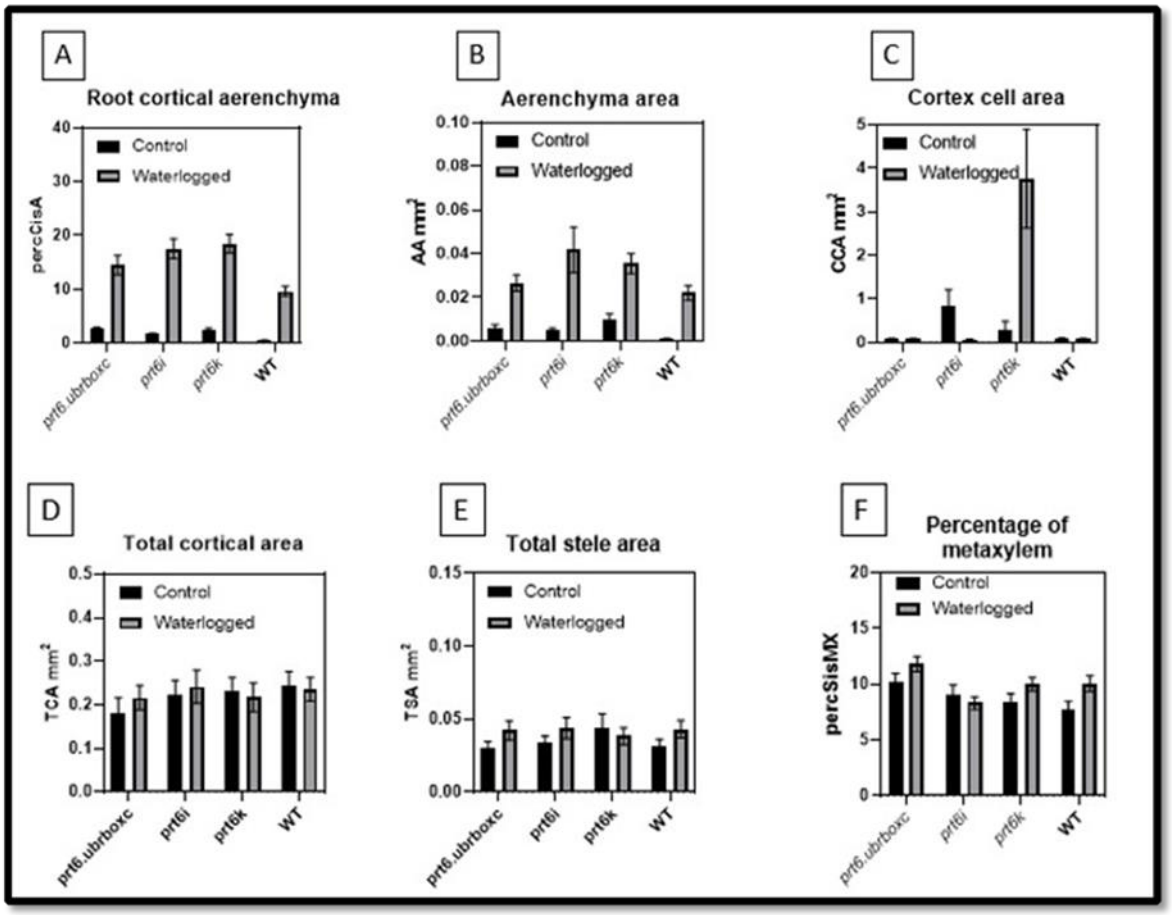

Figure 3.5. Root cortical senescence traits. (A) (percCisA%) Percentage of cortex as aerenchyma, (b) AA, mm^2 = Aerenchyma area, (C) CCA, mm^2 = Cortex cell area, (D) TCA; mm^2 = Cortex area, (E) TSA; mm^2 = Stele area and (F) (percSisMX%) = Percentage of stele that is metaxylem at 4 to 6 cm depth for three mutant lines of spring barley Sebastian and wild type Sebastian (values represent means of four experiments in 2019 ,2020 ,2021 and 2022) under control and waterlogging conditions. For statistical significance of Waterlogging, Genotype and Waterlogging × Genotype effects see **Table 3.3 A.**

Table 3.3 A Root Cortical Senescence (RCS) trait for four barley genotypes (WT Sebastian, and *prt6k*, *prt6i*, and *prt6 ubrboxc* mutant lines for the PRT6 gene) under control and waterlogging conditions across four independent experiments. The traits measured are Aerenchyma Area (AA) and Percentage of Cortex that is Aerenchyma (percCisA). Values are presented as means ± Standard Error of the Mean (SEM). Statistical significance was assessed using REML analysis (*p < 0.05, **p < 0.01).

RCS trait

Experiment 1	**Factor**	**df**	**F ratio**	**P value**
logAA mm^2	Genotype	3.8	4.71	0.035
	Treatment	1.8	10.30	0.012
	Genotype*treatment	2.8	2.81	0.119
PercCisA	Genotype	3.13	7.24	0.004
	Treatment	1.13	27.90	0.001
	Genotype*treatment	3.13	5.03	0.015
Experiment 2 Parameter	**Factor**	**df**	**F ratio**	**P value**
logAA mm^2	Genotype	3.89	2.09	0.107
	Treatment	1.89	11.72	0.001
	Genotype*treatment	2.89	1.57	0.213
PowerPercCisA	Genotype	3.110	3.26	0.024
	Treatment	1.110	164.57	0.001
	Genotype*treatment	3.110	3.97	0.010
Experiment 3 Parameter	**Factor**	**df**	**F ratio**	**P value**
PowerAA mm^2	Genotype	3.48	0.75	0.527
	Treatment	1.108	108.62	0.001
	Genotype*treatment	3.94	0.94	0.431
PercCisA	Genotype	3.48	20.27	0.001
	Treatment	1.48	680.39	0.001
	Genotype*treatment	3.48	16.42	0.001
Experiment 4 Parameter	**Factor**	**df**	**F ratio**	**P value**
AA mm^2	Genotype	3.59	8.57	0.001
	Treatment	1.59	59.39	0.001
	Genotype*treatment	3.59	1.52	0.218
PercCisA	Genotype	3.59	10.36	0.001
	Treatment	1.59	111.03	0.001
	Genotype*treatment	3.59	1.35	0.2688

Table 3.3B REML statistics comparing differences in the Root Cortical senescence (RCS) parameters in barley adventitious root formation and estimation of aerenchyma via Rootscan linked to the waterlogging treatment experiment from individual experiments for three mutant lines of spring and the Sebastian wild type. Output of root cross-section from RootScan software indicating AA (aerenquima area), percCisA (root cortical aerenchyma).

Genotype	Experiment 1				Experiment 2				Experiment 3				Experiment 4			
	AA		percCisA		AA		percCisA		AA		percCisA		AA		percCisA	
	Con	WL	Con	WL	Con	WL	Con	WL	Con	WL	Con	WL	Con	WL	Con	WL
Sebastian (WT)	0	0.014565	0	9.968	0	0.01296	0	8.406	0.00119	0.03372	0.68	15.23	0.00302	0.02962	0.986	6.928
prt6k	0.001673	0.001951	0.896	1.362	0.00992	0.01418	2.593	13.309	0.00208	0.03195	2.75	29.24	0.0179	0.06535	3.876	13.686
prt6i	0.000815	0.037533	0.544	19.594	0.00216	0.05172	1.261	17.115	0.00099	0.03868	1.23	34.5	0.01467	0.04771	2.834	10.293
prt6 ubrbox c	0.000519	0.016901	0.258	12.111	0.00692	0.01504	3.077	11.829	0.00165	0.02552	1.54	26.97	0.00969	0.04856	2.58	12.241
Genotype	**0.048**		**0.009**		**0.203**		**0.024**		**0.527**		**<0.001**		**<0.001**		**<0.001**	
Treatment	**0.006**		**<0.001**		**<0.001**		**<0.001**		**<0.001**		**<0.001**		**<0.001**		**<0.001**	
Genotype*Treatment	**0.116**		**0.029**		**0.011**		**0.01**		**0.431**		**<0.001**		**0.266**		**<0.210**	

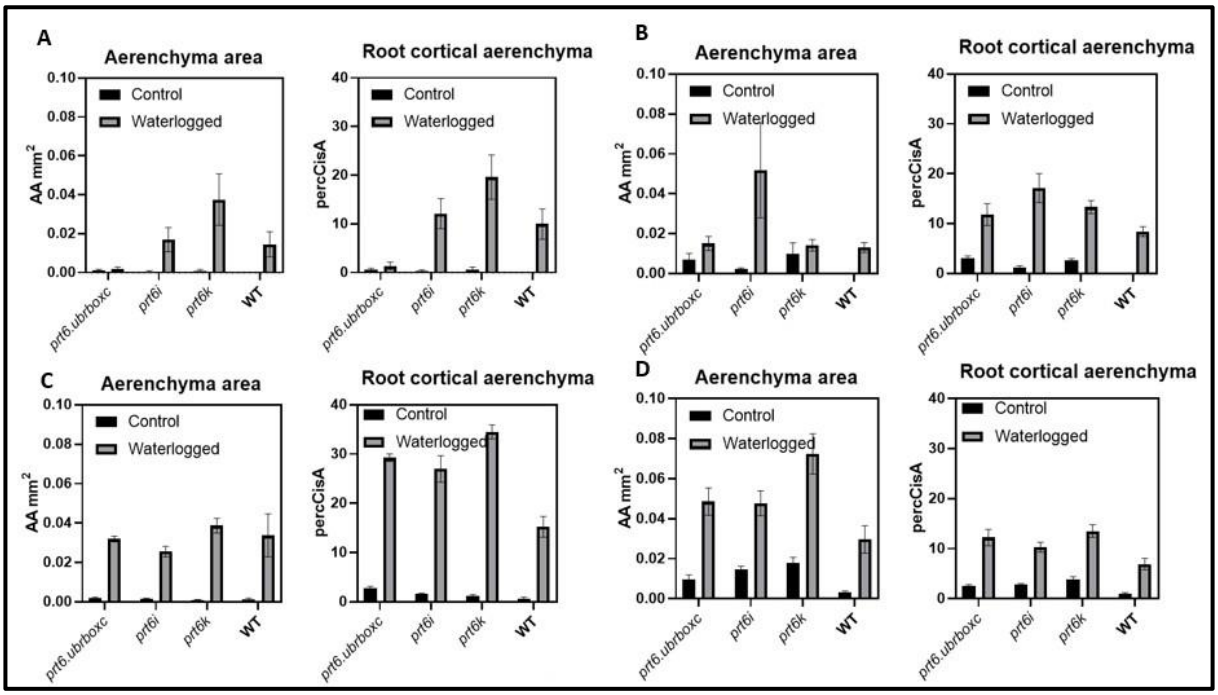

Figure 3.6. Root cortical senescence (RCS) traits for three mutant lines of spring barley and the Sebastian wildtype under control and waterlogging conditions in four individual experiments. AA (aerenchyma area), percCisA (percentage root cortical aerenchyma), (A) experiment 1, (B) experiment 2, (C) experiment 3 and (D) experiment 4. For statistical significance of Waterlogging, Genotype and Waterlogging × Genotype effects see **Table 3.3 B**.

Experiment 1

The results of the first experiment showed higher percentage of root cortical aerenchyma under waterlogging in *prt6k* at 19.6 and in *prt6i* 12.1 compared to the Sebastian WT at 10.0 (p=0.004; Fig. 3.6, Table 3.3). The percentage of cortical aerenchyma in control plants was similar in the mutant lines *prt6k* at 0.54 and *prt6 ubrboxc* at 0.60 and the WT at 0.30 (p=0.001). For aerenchyma area, the results showed a greater increase when applying waterlogging in genotype *prt6k* and *prt6i* compared to the WT (p= 0.035).

Experiment 2

The percentage of root cortical aerenchyma was again higher in the PRT6 mutant lines compared to the WT, by 3 to 9%. Under waterlogging conditions, the *prt6i l*ine had the highest percentage aerenchyma (17.1) (p=0.024) followed by *prt6k* (13.3), then *prt6 ubrboxc* (11.8) and the WT (6.0). Regarding AA, the *prt6i* line showed a trend for greater relative increase when waterlogging was applied compared to the WT and the other alleles (p=0.107).

Experiment 3

The percentage aerenchyma of mutant PRT6 lines was much higher than that of WT when waterlogging conditions were applied. Line *prt6k* was the highest, followed by *prt6k, prt6 ubrboxc* and *prt6i* (p=0.001). In control plants, the mutant PRT6 lines had greater root cortical senescence than the WT even in unstressed conditions (p=0.001). AA showed an increase in all four genotypes under waterlogging conditions compared to the control treatment. However, for AA the genotype effect and the waterlogging treatment × genotype effects were not statistically significant.

Experiment 4

The results again showed that the percentage of root aerenchyma in the mutant lines was higher than in the WT (P< 0.01). Under waterlogging the formation of aerenchyma increased in mutant PRT6 lines and the WT plants (P< 0.01). Under waterlogging the percentage aerenchyma for *prt6k* was 13.5, for *prt6 ubrboxc* was 12.2 and for prt6i was 10.3 compared WT at 6.9. The interaction was not statistically significant.

The AA was higher in the PRT6 mutant lines in the control conditions compared to the WT. For example, the *prt6k* line was higher than the WT in both the control or waterlogging conditions (p=0.001). AA increased with waterlogging (P< 0.01) but the interaction was not statistically significant.

3.6 Discussion

One of the main goals shared by plant breeders around the world is to maintain optimal crop performance under abiotic stress conditions. Root cortical senescence (RCS) is a promising trait for plant breeding programs to improve crop performance under abiotic stress, particularly waterlogging and drought stress. Recent research highlights a strong coordination between a plant's above-ground and below-ground organs. By incorporating root cortical senescence as a key characteristic into breeding programs, breeders can develop crops with a more efficient root system. This trait allows for the programmed death of root cells, creating air channels that enhance oxygen transport to the rest of the plant, helping it survive and thrive in waterlogged conditions. By selecting for this trait, breeders can create more resilient crops that maintain optimal performance and yield in a changing climate . In previous work, in response to waterlogging, transgenic barley plants showed sustained biomass, enhanced yield, retention of chlorophyll and enhanced induction of hypoxia-related genes (Mendiondo et al., 2016). *PRT6* RNAi plants also showed reduced chlorophyll degradation in response to continued darkness, associated with waterlogged conditions. Barley Targeting Induced Local Lesions IN Genomes (TILLING) lines, containing mutant alleles of *PRT6*, also showed increased expression of hypoxia-related genes and phenotypes similar to RNAi lines.

RCS is a type of programmed cell death found in the *Triticeae* tribe. Studies suggest that RCS reduces nutrient uptake, nutrient content, respiration, and radial hydraulic conductance of root tissue. However, it has been argued that RCS can improve growth under suboptimal availability of nutrients, and that it can enable the development of crop varieties with improved soil resource acquisition. For example, Robinson (1990) argued that RCS could be beneficial if mineral nutrients are remobilized from senescing cells to support new root growth.

The mutant PRT6 barley genotypes in this experiment are the spring barley Sebastian with three PRT6 allele mutations: *prt6k, prt6i and prt6 ubr boxc.* Previous work showed that reduced expression of *prt6k* and *prt6i* was associated with enhanced retention of chlorophyll and green under water-logging conditions (Mendiondo et al., 2016) as mentioned above. In the present experiments, however, leaf chlorophyll content retention was not enhanced in the PRT6 mutants compared to the Sebastian WT nor was shoot number per plant or plant height

enhanced. So the previously reported effects on shoot growth under water logging for these PRT6 mutants could not be confirmed. In the present study, root cortical senescence traits were characterised for the first time for these PRT6 mutant lines compared the WT under water-logging conditions. It was hypothesised that plants with enhanced RCS have reduced nutrient requirement of root tissue for optimal plant growth and reduced total cumulative cortical respiration and increased total carbon reserves and therefore may be better adapted to survive under low O_2 conditions (Schneider et al, 2017).

In the present study absolute area and percentage area of root cross-sections was observed consistently to increase under waterlogging compared to control conditions in four controlled-environment experiments. Previous studies have shown that waterlogging/ hypoxic conditions induce aerenchyma formation to facilitate gas exchange. For example in sunflower, increased root cortical senescence under waterlogging was reported and it was suggested that ethylene and reactive oxygen species, as regulatory signals, might also be involved in these adaptive responses. However, the interrelationships between these signals have seldom been reported. They showed that programmed cell death was involved in aerenchyma formation in the stem of *Helianthus annuus*. Lysigenous and aerenchyma formation in the stem was induced through waterlogging, ethylene and ROS. Further work in barley may be justified to test if a similar mechanism may be underlying RCS formation under waterlogging.

Present results overall showed that the PRT6 mutants had higher expression of RCS under waterlogging compared to the Sebastian WT and also RCS increased relatively more compared to the WT under waterlogging, e.g., for AA and PercCisA. The effects of genotype on total cortical area, total stele area and percentage of root as metaxylem were generally small in the experiments and unlikely to be large enough to explain the differences in tolerance in waterlogging tolerance previously reported by Mendiondo et al. (2016) between PRT6 mutants and Sebastian (2016). However, the cortical cell area showed a much larger increased under waterlogging conditions in *prt6i* and particularly in *prt6k* compared to the WT. It can be speculated that the *prt6i* allele may play a role in increasing cortical cell area under hypoxia and further experiments seems justified to test whether this was the case.

Chapter 4: Root Cortical Senescence Traits and their Relationship with Plant Growth under Well-watered and Drought Conditions in Wheat and Barley

4.1 Introduction

Drought stress significantly affects the production of wheat and barley, affecting various physiological processes such as development, photosynthesis, growth and metabolism, ultimately leading to reduced grain yield. The frequency and severity of droughts are expected to increase due to global warming and climate change, exacerbating these challenges (Li et al., 2018; Otkin et al., 2019). Recent evidence indicates that drought has severely affected crop yields in various regions. For instance, in 2024, approximately 21% of barley and 25% of spring wheat production in the U.S.A. was affected by drought conditions (USDA, 2024; NOAA, 2024) reflecting considerable variability in soil moisture and crop conditions across different states (USDA, 2024).

Drought stress is particularly detrimental during critical stages of growth affecting grain number and grain development, such as the phase between spike emergence and anthesis and the initial stages of grain filling. These stages are crucial for determining grain number, potential grain weight and final yield, and drought during these periods can lead to significant yield reductions (Martínez-Fernández et al., 2023; González-Zamora et al., 2023). For example, a recent study comparing drought impacts in Spain and Germany found that drought conditions significantly reduced wheat and barley grain yields, with some regions experiencing up to a 30% decline in productivity (Martínez-Fernández et al., 2023). Efforts to mitigate these impacts include developing drought-tolerant varieties. An international collaboration led by ICARDA has developed new varieties of durum wheat and barley that show increased resilience to drought conditions. These varieties aim to enhance food security and agricultural sustainability, especially in regions prone to severe droughts (ICARDA, 2023). Understanding and improving drought stress tolerance in wheat and barley is crucial for ensuring food security and agricultural sustainability. Roost system architecture traits such as rooting depth will be important in conferring differences in ability to extract water under depth and hence drought tolerance. Root cortical senescence traits, such as root cortical aerenchyma, cortical cell size and cortical area, are also thought to be important under drought as they may reduce the overall metabolic cost of the roots, permitting increased root growth, and therefore improving water capture at depth.

Continued research and development of drought-resistant crop varieties, along with improved water management practices, are essential strategies to mitigate the adverse effects of drought on crop production (Leng and Hall, 2019; Meise et al., 2019). The present study provides a comprehensive investigation of the effects of drought on root cortical senescence traits in wheat and barley and associated impacts on plant growth, emphasizing the importance of addressing drought stress in these crops to ensure sustainable agricultural practices.

4.2 The specific objectives of this chapter are to:

1- To characterise the root anatomical structures of mutant alleles of the PRT6 gene in spring barley (*prt6k*, *prt6i*, and *prt6 ubrboxc*) and NILs in spring wheat and their parental wildtypes (spring barley Sebastian and spring wheat Paragon) using microscopic and image-based methods, with particular emphasis on the extent and pattern of RCS under controlled drought stress conditions compared to unstressed control plants.

2- To evaluate the physiological responses (e.g., leaf chlorophyll retention, NDVI, biomass , grain yield and yield components) of both barley and wheat genotypes under drought conditions compared to unstressed controls and determine whether RCS expression correlates with above-ground performance.

3- To investigate inter- and intra-species variation in RCS expression between barley and wheat lines, thereby determining whether RCS functions as a conserved or species-specific adaptive trait

4.3 The specific hypotheses tested in this chapter are

- that the three mutant lines *prt6k*, *prt6i* and *prt6 ubrboxc* for the *PRT6* gene increase root cortical senescence and aerenchyma area and this leads to increased water uptake and above-ground biomass under drought compared to the wild type Sebastian parent in barley.

- that there is a relationship between root cortical senescence and expression of the PRT6 gene in the mutant lines affecting the N-degron pathway, such that the mutant lines with reduced expression of the PRT6 gene show greater root cortical senescence, aerenchyma

formation and above-ground biomass than the Sebastian wild type in spring barley in field conditions under drought conditions.

4.4. Materials and methods

4.4.1 Experimental design and treatments

Ten genotypes were grown in the experiments, as described in Chapter 2. Briefly, there were four wheat genotypes: three wheat near-isogenic lines (NILS) in spring wheat 'Paragon' background as well as the Paragon wild type were used in experiments.

The wheat genotypes used were:

The wheat and barley genotypes used in the experiments were as follows:

Species	Genotype
Wheat	Paragon (WT)
	WB TK0018-PFI
	WB TK0019-PFI
	WB TK0020-OG
Barley	Sebastian (WT)
	mutant alleles in PRT6 (*prt6k*, *prt6i*, *prt6ubrboxc*)
	Irina (KWS)
	Sassy (KWS)

The wheat near-isogenic lines were supplied by Dr Simon Griffiths at the John Innes Centre, Norwich, UK. The spring barley wild type Sebastian and three barley mutant alleles in PRT6 (*prt6k*, prt6i and *prt6 ubrboxc*) were provided by Dr Mendiondo's laboratory (Mendiondo et al., 2016). In addition, the commercial spring barley cultivars KWS Irina and Sassy were used as check cultivars.

There were two glasshouse experiments conducted, one in 2021 and another in 2022-23.

Each experiment employed a 'split-plot' design with two irrigation treatment levels (fully irrigated and droughted) and ten genotypes, with irrigation treatments assigned at the 'main plot' level and each treatment replicated four times. The sowing dates were 18 February 2021 and 5 August 2022. Destructive sampling was performed at anthesis (GS61) and at harvest, with two technical replicates for each sampling time. Detailed information on experimental treatments and growing conditions is provided in **Chapter 2.2.1**.

4.4.2. Plant measurements

Full details of the measurements of the root anatomical traits, above-ground physiological traits and biomass, grain yield and yield components are harvest are provided in **Chapter**

2.2.2.

4.5. Results

4.5.1 Root cortical senescence traits

Tables 4.1 and **4.2** present REML analysis results comparing treatment differences in root cortical senescence (RCS) traits in adventitious roots for wheat and barley genotypes under control (fully irrigated) and drought conditions, measured at anthesis in two years. The RCS traits measured were aerenchyma Area (AA), percentage root cortical aerenchyma (percCisA), Cortex cell Area (CCA), percentage metaxylem (percSisMX), total cortical area (TCA), and total stele area (TSA).

In 2021, the root cortical senescence traits differed in control compared to well-irrigated conditions (**Table 4.1; Fig. 4.1**). For the wheat genotypes, there was an effect of drought on percentage aerenchyma ($P<0.001$) and also and effect of genotype ($P<0.001$), and for the interaction between irrigation treatment and genotype ($P< 0.01$). Overall drought increased the percentage aerenchyma to 16% (from 6% under well water conditions). Percentage aerenchyma was higher in the NIL WBTK0020-OG line than in the parent Paragon under drought. There was also an irrigation × genotype interaction for the percentage stele as metaxylem ($P< 0.05$). For other RCS traits there were no significant effects of the irrigation

treatment or genotype or for the irrigation treatment × genotype interaction. In 2022 for wheat genotypes, percentage aerenchyma area was again increased under drought (26%) compared to well-watered conditions (21%) ($P<0.05$). The cortex area was also reduced under drought ($P< 0.05$). There were significant effects for genotype but not for the irrigation treatment × genotype interaction for these RCS traits. Percentage aerenchyma was again higher in the NIL WBTK0020-OG than in the parent Paragon.

In 2021 for the barley genotypes, there was an effect of drought for percentage aerenchyma ($P< 0.01$), total cortical area ($P< 0.05$) and cortex cell area ($P< 0.05$); and an effect of genotype for percentage aerenchyma ($P< 0.01$), aerenchyma area ($P< 0005$) and total cortical area ($P< 0.05$). Again, drought increased the percentage aerenchyma area and decreased the cortical area compared to well-watered conditions. Regarding the effect of genotype for aerenchyma area ($P<0.01$) and percentage aerenchyma area ($P< 0.001$) the mutant lines *prt6k* and *prt6i* showed increases compared to the Sebastian WT. For percentage aerenchyma there was an irrigation treatment × genotype interaction ($P=0.06$) with a greater increase under drought for *prt6i* compared to the Sebastian QT. In 2022, there was an effect of irrigation treatment and genotype for each of percentage aerenchyma, aerenchyma area and total cortical area ($P< 0.05$). The direction of the effects was the same as in 2021. The genotype effect was significant for percentage aerenchyma with a greater value for *prt6k* than the Sebastian WT ($P<0.01$). There was also an irrigation × genotype interaction with *prt6k* showing a smaller response to drought than the other genotypes ($P< 0.05$).

Table 4.1.A Root Cortical Senescence (RCS) traits measured at anthesis for cv. Paragon and three near-isogenic lines of wheat, as well as under control (fully irrigated) and drought conditions. Data were collected during the 2021 and 2022 growing seasons. The traits include: aerenchyma area (AA; mm²), percentage root cortical aerenchyma (percCisA), cortex cell area (CCA; mm²), percentage metaxylem (percSisMX), total cortical area (TCA; mm²), and total stele area (TSA; mm²).

	Year 1												Year 2											
Genotype	**AA**		**CCA**		**PercCisA**		**PercSisMX**		**TCA**		**TSA**		**AA**		**CCA**		**PercCisA**		**PercSisMX**		**TCA**		**TSA**	
	Con	Dro	Con	Dro	Con	Dro	Con	Dro	Con	Dro	Con	Dro	Con	Dro	Con	Dro	Con	Dro	Con	Dro	Con	Dro	Con	Dro
Paragon	8E-05	0.0007	9E-04	0.0009	3.71	17	7.554	5.694	0.0025	0.0039	0.0003	0.00101	0.0167	0.0206	0.0213	0.0117	19.74	25.02	6.742	5.545	0.0822	0.0821	0.0185	0.02225
WB TK0018-PFI	5E-05	0.0062	8E-04	0.0045	2.12	20.47	5.12	6.52	0.0023	0.0268	0.0003	0.00639	0.009	0.021	0.0099	0.015	21.29	23.29	8.567	7.231	0.0407	0.08234	0.0113	0.01717
WB TK0019-PFI	0.0002	0.0004	3E-04	0.0011	11.27	9.43	6.657	5.503	0.0016	0.0046	0.0004	0.00117	0.0182	0.0169	0.0223	0.0163	18.26	24.12	9.291	7.664	0.0985	0.07474	0.0271	0.01824
WB TK0020-OG	0.0042	0.0005	0.006	0.0005	14.3	24.52	6.663	8.53	0.0228	0.0023	0.0022	0.0006	0.0242	0.0221	0.0222	0.0132	22.97	30.18	6.783	10.401	0.1068	0.07315	0.0234	0.02031
Genotype	**0.42**		**0.531**		**0.001**		**0.113**		**0.478**		**0.414**		**0.24**		**0.311**		**0.318**		**0.098**		**0.23**		**0.102**	
Treatment	**0.625**		**0.767**		**0.001**		**0.963**		**0.865**		**0.319**		**0.318**		**0.039**		**0.026**		**0.742**		**0.476**		**0.614**	
Genotype*Treatment	**0.174**		**0.185**		**0.005**		**0.033**		**0.171**		**0.241**		**0.246**		**0.201**		**0.891**		**0.05**		**0.033**		**0.097**	

Table 4.1.B Root Cortical Senescence (RCS) traits measured at anthesis for cv Sebastian and three mutant lines and two elite lines (Sassy and Irina) of barley under control (fully irrigated) and drought conditions. Data were collected during the 2021 and 2022 growing seasons. The traits include: aerenchyma area (AA; mm²), percentage root cortical aerenchyma (percCisA), cortex cell area (CCA; mm²), percentage metaxylem (percSisMX), total cortical area (TCA; mm²), and total stele area (TSA; mm²).

	Year 1												Year 2											
Genotype	**AA**		**CCA**		**PercCisA**		**PercSisMX**		**TCA**		**TSA**		**AA**		**CCA**		**PercCisA**		**PercSisMX**		**TCA**		**TSA**	
	Con	**Dro**	**Con**	**Dro**	**Con**	**Dro**	**Con**	**Dro**	**Con**	**Dro**	**Con**	**Dro**	**Con**	**Dro**	**Con**	**Dro**	**Con**	**Dro**	**Con**	**Dro**	**Con**	**Dro**	**Con**	**Dro**
prt6k	0.0122	0.0119	0.016	0.0106	15.97	21.87	8.116	7.788	0.077	0.0541	0.0127	0.01393	0.0234	0.013	0.0112	0.0078	29.89	26.8	7.329	9.027	0.0779	0.0511	0.0119	0.01007
prt6i	0.0343	0.0169	0.043	0.0102	16.99	31.42	6.967	6.87	0.2172	0.0542	0.0273	0.01195	0.0448	0.0158	0.0398	0.0072	19.32	31.75	8.181	9.626	0.2287	0.0497	0.0303	0.00942
prt6 ubr boxc	0.0032	0.0061	0.009	0.0268	9.16	6.95	8.445	9.497	0.0344	0.0859	0.0064	0.01726	0.0367	0.0426	0.053	0.0246	14.66	23.9	8.911	8.343	0.2542	0.1743	0.048	0.04456
Sebastian (WT)	0.0062	0.006	0.03	0.0107	7.78	16.43	7.431	7.366	0.1029	0.0446	0.0136	0.00666	0.0129	0.0161	0.0119	0.0094	20.36	28.04	7.756	7.322	0.0619	0.0578	0.0103	0.01216
Genotype	**0.001**		**0.121**		**0.001**		**0.082**		**0.017**		**0.013**		**0.001**		**0.001**		**0.001**		**0.507**		**0.001**		**0.001**	
Treatment	**0.27**		**0.0.37**		**0.004**		**0.81**		**0.015**		**0.404**		**0.193**		**0.001**		**0.001**		**0.482**		**0.001**		**0.084**	
Genotype*Treatment	**0.027**		**0.001**		**0.061**		**0.824**		**0.001**		**0.001**		**0.037**		**0.001**		**0.007**		**0.456**		**0.001**		**0.023**	
Irina	0.0776	0.1003	0.04	0.0417	28.54	28.63	7.434	7.7	0.2816	0.3425	0.0458	0.05571	0.0704	0.0986	0.0581	0.033	23.58	31.73	7.124	8.603	0.2893	0.3037	0.0527	0.05764
Sassy	0.0608	0.0649	0.045	0.0405	25.2	23.96	8.526	6.598	0.2356	0.2766	0.0481	0.0644	0.0582	0.0817	0.0415	0.0543	23.65	24.76	7.36	6.893	0.2641	0.3263	0.0558	0.06674
Genotype	**0.001**		**0.044**		**0.001**		**0.981**		**0.001**		**0.001**		**0.001**		**0.001**		**0.456**		**0.865**		**0.001**		**0.001**	
Treatment	**0.501**		**0.208**		**0.34**		**0.435**		**0.899**		**0.486**		**0.059**		**0.39**		**0.009**		**0.956**		**0.336**		**0.233**	
Genotype*Treatment	**0.679**		**0.439**		**0.411**		**0.409**		**0.336**		**0.328**		**0.33**		**0.36**		**0.416**		**0.621**		**0.331**		**0.658**	

Table 4.2.A REML statistics from the cross-experiment analysis for the Root Cortical senescence (RCS) traits for cv Paragon and three near-isogenic lines of wheat under control (fully irrigated) and drought conditions measured at antheses (Values are means from two independent experiments in 2021 and 2022-23). AA (aerenchyma area, mm^2), percCisA (percentage root cortical aerenchyma, mm^2), CCA (cortex cell area, mm^2), percSisMX (percentage metaxylem), TCA (total cortical area, mm^2) and TSA (total stele area, mm^2).

Genotype	Year 1+2											
	AA		CCA		PercCisA		PercSisMX		TCA		TSA	
	Con	Dro	Con	Dro	Con	Dro	Con	Dro	Con	Dro	Con	Dro
Paragon	0.0084	0.0095	0.011	0.0057	11.73	20.56	7.148	5.628	0.0423	0.0387	0.0094	0.01045
WB TK0018-PFI	0.0045	0.0144	0.005	0.0103	11.7	22.04	6.843	6.915	0.0215	0.0577	0.0058	0.01237
WB TK0019-PFI	0.01	0.0148	0.012	0.0144	15.08	22.28	8.094	7.393	0.0545	0.066	0.015	0.01611
WB TK0020-OG	0.0154	0.0113	0.015	0.0068	19.12	27.35	6.73	9.465	0.0695	0.0377	0.014	0.01045
Genotype	0.522		0.487		0.002		0.073		0.483		0.304	
Treatment	0.296		0.386		0.001		0.951		0.87		0.654	
Genotype*Treatment	0.29		0.195		0.187		0.014		0.161		0.625	

Table 4.2.B REML statistics from the cross-experiment analysis for the Root Cortical senescence (RCS) traits for cv Sebastian and three mutant lines and two elite lines (Sassy and Irina) of barley under control (fully irrigated) and drought conditions measured at antheses (Values are means from two independent experiments in 2021 and 2022-23). AA (aerenchyma area, mm^2), percCisA (percentage root cortical aerenchyma, mm^2), CCA (cortex cell area, mm^2), percSisMX (percentage metaxylem), TCA (total cortical area, mm^2) and TSA (total stele area, mm^2).

Genotype	Year 1+2											
	AA		CCA		PercCisA		PercSisMX		TCA		TSA	
	Con	Dro	Con	Dro	Con	Dro	Con	Dro	Con	Dro	Con	Dro
prt6k	0.0097	0.0122	0.021	0.0099	14.44	23.58	7.603	7.339	0.0812	0.0527	0.0119	0.01004
prt6i	0.0168	0.0126	0.014	0.0088	21.7	25.04	7.792	8.584	0.0774	0.0522	0.0124	0.01145
prt6 ubr boxc	0.0401	0.0164	0.041	0.0087	18.29	31.59	7.641	8.248	0.2236	0.052	0.0289	0.01069
Sebastian (WT)	0.0228	0.0229	0.035	0.0258	12.37	14.77	8.717	8.964	0.1626	0.1267	0.0307	0.02986
Genotype	**0.001**		**0.001**		**0.001**		**0.149**		**0.001**		**0.001**	
Treatment	**0.139**		**0.001**		**0.001**		**0.453**		**0.001**		**0.08**	
Genotype*Treatment	**0.033**		**0.014**		**0.102**		**0.806**		**0.001**		**0.056**	
Irina	0.0736	0.0995	0.05	0.0374	25.78	30.18	7.261	8.151	0.2859	0.3231	0.0497	0.05667
Sassy	0.0594	0.0724	0.043	0.0466	24.34	24.32	7.878	6.729	0.2514	0.2987	0.0524	0.06544
Genotype	**0.001**		**0.001**		**0.002**		**0.874**		**0.001**		**0.001**	
Treatment	**0.065**		**0.101**		**0.016**		**0.698**		**0.591**		**0.202**	
Genotype*Treatment	**0.304**		**0.306**		**0.209**		**0.376**		**0.167**		**0.222**	

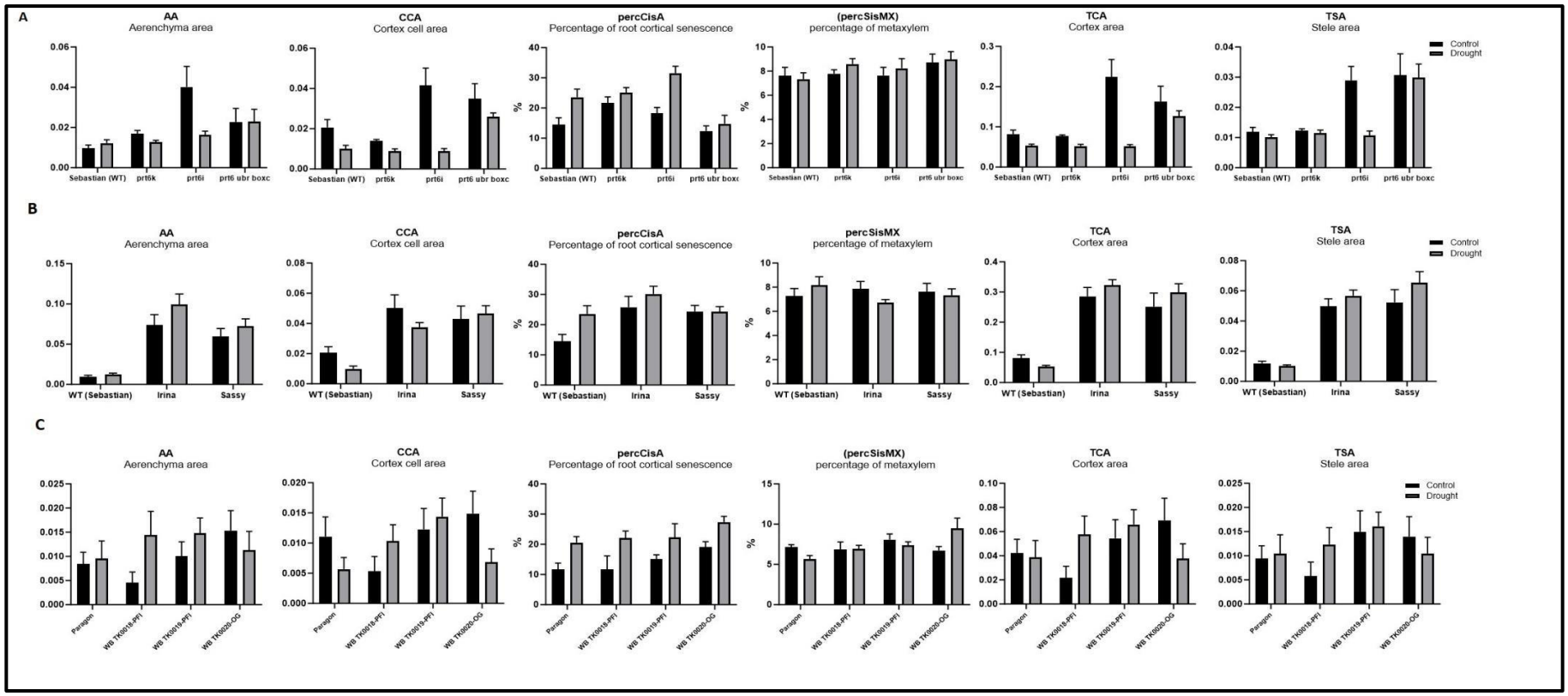

Figure 4.1. Root Cortical Senescence (RCS) traits for *cv. Paragon* and three near-isogenic wheat lines, as well as *cv. Sebastian* and three mutant barley lines, along with two elite barley lines (*Sassy* and *Irina*) in A) 2021, B) 2022-23 and c) cross-experiment mean. Measurements were taken under control (fully irrigated) and drought conditions at anthesis. Traits measured include: aerenchyma area (AA, mm²), percentage root cortical aerenchyma (percCisA, %), cortex cell area (CCA, mm²), percentage metaxylem (percSisMX, %), total cortical area (TCA, mm²), and total stele area (TSA, mm²). Error bars are standard error of the mean. For statistical significance of Drought, Genotype and Drought × Genotype effects see **Tables 4.2 A** and **B.**

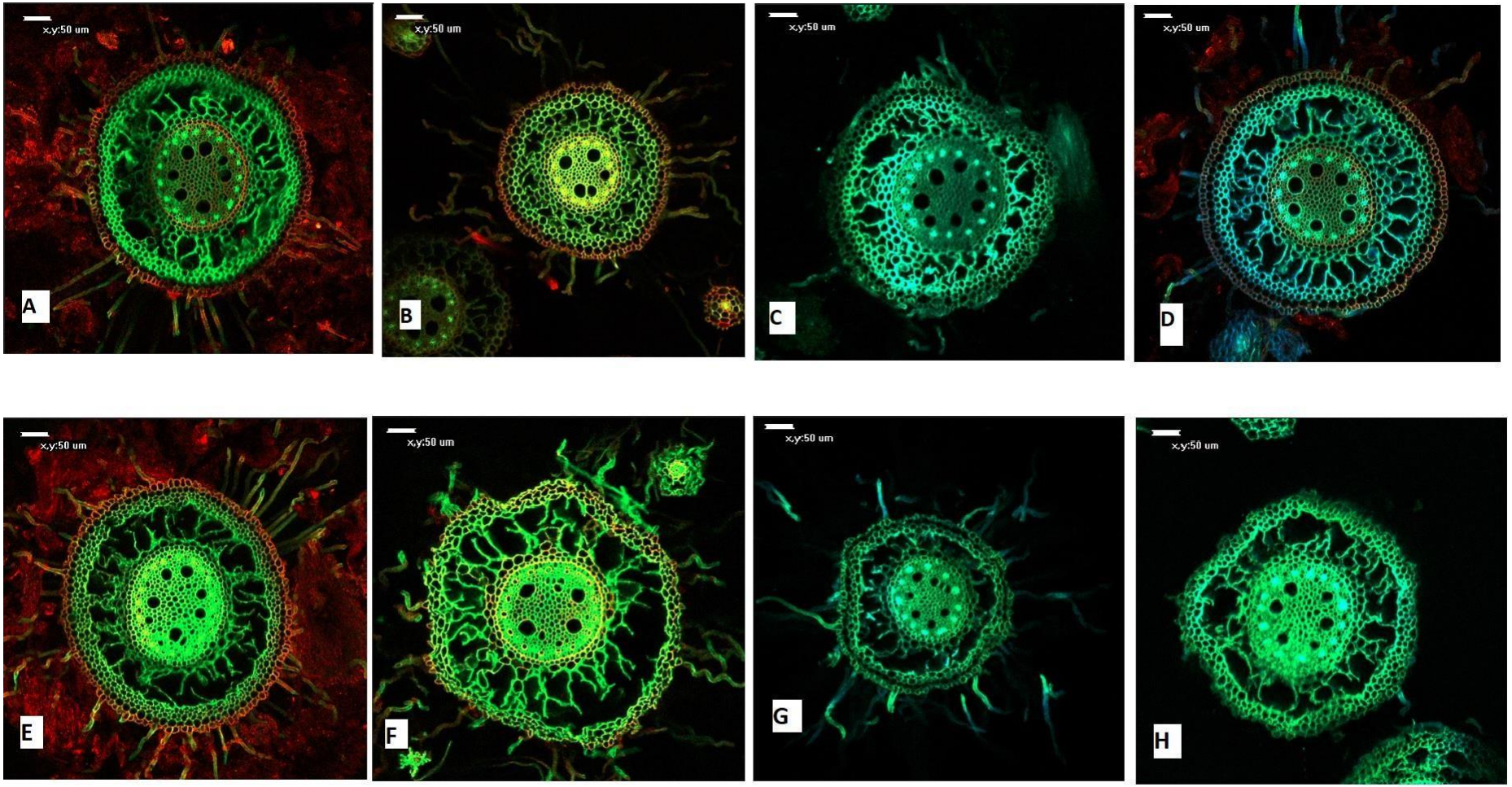

Figure 4.2. Root cross-sections. Top row: Root cross-sections under control (well-irrigated) conditions. Bottom row: Root cross-sections under drought conditions. Images were taken at anthesis using a Nikon microscope. The genotypes shown include the cultivar Paragon (A) and three near-isogenic lines of wheat: WB TK0018-PFI (B), WB TK0019-PFI (C), and WB TK0020-OG (D).

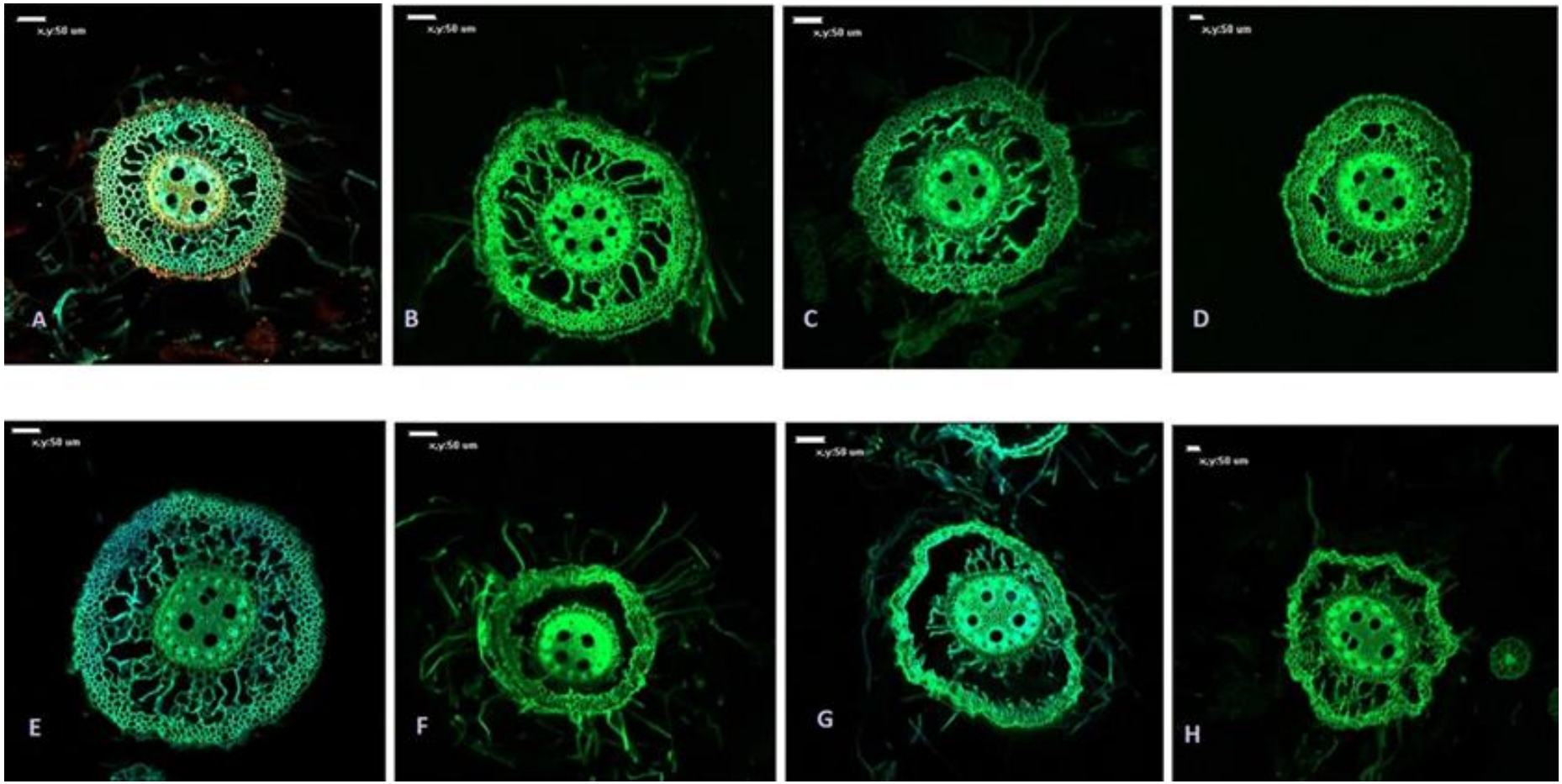

Figure 4.3 Root cross sections at anthesis, captured using a Nikon microscope. The top row shows roots under control (well- irrigated) conditions, while the bottom row depicts roots under drought conditions. Panels: A (WT Sebastian), B (*prt6k*), C (*prt6i*) and D (*prt6 ubrboxc*).

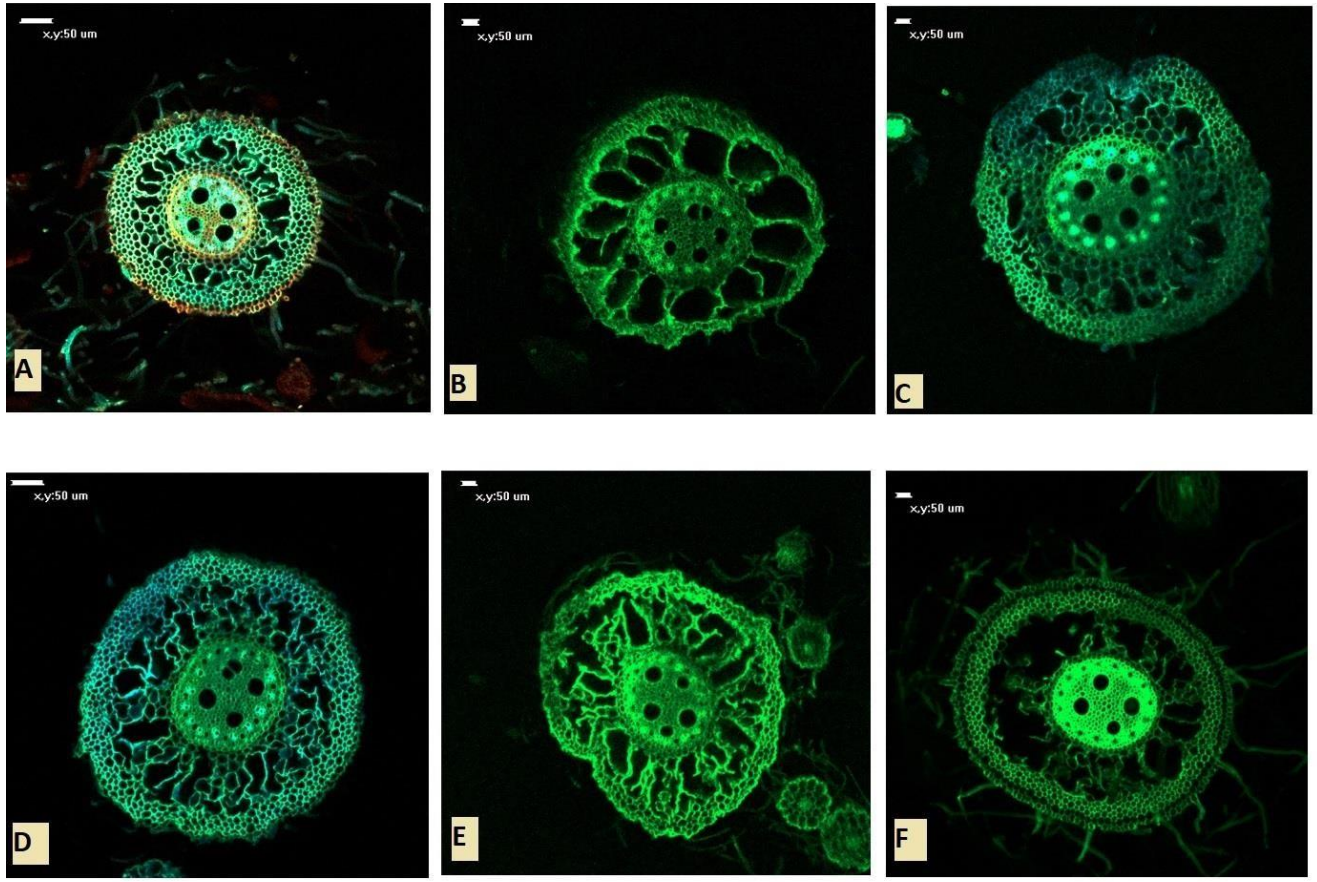

Figure 4.4. Top row showing root cross-section under control conditions (well irrigated) and the bottom row under drought conditions for roots at anthesis using Nikon microscope for two elite lines (Sassy and Irina) A (WT Sebastian), B (Irina), C (Sassy).

4.5.2 Above-ground traits in 2021 experiment

4.5.2 1 Leaf relative chlorophyll content (SPAD)

In 2021, flag-leaf chlorophyll content (measured by SPAD value) decreased under drought conditions across various dates, but this effect was observed only after GS61 compared to well-irrigated conditions (Table 4.3). A significant effect of drought was detected on 11 June ($P < 0.05$). Among the wheat genotypes, the genotype effect was significant only on 11 May ($P = 0.05$), with lower values observed for WB-TK0019 compared to Paragon and WBTK0019. There was no significant interaction between irrigation treatment and genotype on any assessment date.

In barley, the *prt6i* line had a higher value than the Sebastian WT on 7 April but a lower value on 13 May ($P< 0.05$). Overall SPAD values ranged from 36.4 to 47.7 under well-watered conditions and 31.0 to 48.2 under drought. The interaction between irrigation treatment and genotype was not significant at any assessment date.

4.5.2.2 Tillers per plant

The number of tillers per plant in wheat (Paragon and near-isogenic lines) and barley (Sebastian and mutant lines, plus elite lines Sassy and Irina) genotypes under control (well irrigated) and drought conditions from 23 March to 13 May is shown in **Table 4.4**. Tiller

numbers generally showed no significant decrease under drought conditions during this period.

In wheat, initially Paragon had fewer tillers than the NILs on 29 March ($P<0.05$) and 8 April ($P< 0.01$), but thereafter differences between the NILs and Paragon were not statistically significant. In barley, among Sebastian and the mutant lines there were differences on all assessment dates ($P< 0.001$). *prt6i* had fewer tillers per plant than Sebastian. There were irrigation treatment × genotype interaction (among all six barley genotypes) on 8 and 13 April ($P< 0.05$), whereby Irina and *prt6k* had relatively more tillers under drought compared to *prt6 ubr boxc* than under well irrigated conditions.

4.5.2.3 Leaf chlorophyll fluorescence (Quantum Yield)

In wheat, there was no significant effect of drought on leaf QY except for 11 May, when QY decreased by 3-10% under drought (**Table 4.5**). The genotype and irrigation treatment x genotype effects were not statistically significant on any assessment date. In barley, irrigation treatment, genotype and interaction effects were not statistically significant, except for 11 May when leaf QY increased under drought for *prt6k*, *prt6 ubrboxc* and Sebastian, but decreased under drought for *prt6i* ($P< 0.05$).

Table 4.3. Leaf SPAD for Paragon and 3 NILs of wheat; and Sebastian and 3 mutant lines and Sassy and Irina of barley under control (irrigated)and drought in 2021

Genotype	SPAD															
	29-Mar		08-Apr		15-Apr		22-Apr		29-Apr		07-May		13-May		11-Jun	
	Con	Dro	Con	Dro	Con	Dro	Con	Dro	Con	Dro	Con	Dro	Con	Dro	Con	Dro
Paragon	48.2	48.8	54.23	48.25	50	51.35	48.97	49.45	51.38	46.7	51.45	52	47.15	51.7	33.2	0
WB TK0018-PFI	46.35	44.63	50.7	49.5	50.5	53.07	46.73	48.1	46.6	47	47.08	49.33	48.6	56.63	31.02	14.27
WB TK0019-PFI	44.55	49.98	51.12	51.38	52.37	52.1	49.32	52.47	48.33	48.33	50.3	50.1	54.92	53.85	19.02	6.88
WB TK0020-OG	45.23	47.05	51.27	49.05	50.47	50.07	49.67	45.77	48.6	48.08	48.82	52.2	51.62	56.5	18.48	0
Genotype	0.528		0.668		0.265		0.148		0.416		0.053		0.214		0.521	
Treatment	0.327		0.188		0.177		0.709		0.474		0.218		0.148		0.226	
Genotype*Treatment	0.323		0.44		0.123		0.402		0.773		0.886		0.847		0.429	
prt6k	49.93	43.95	47.37	48.77	45.17	45.15	40.07	40.1	48.87	44.1	48.07	43.95	47.76	49.62	0	0
prt6i	44.28	46.32	52.05	52.05	54.85	51.35	47.07	47.58	48.45	47.15	46.52	43.85	39.88	37.05	0	0
prt6 ubr boxc	46.05	41.1	52.38	47.48	48.12	45.62	39.77	38.32	44.17	42.23	46.25	45.88	50.23	48.8	0	0
Sebastian (WT)	43.53	43.68	48.87	48.6	49.23	48.98	41.4	43.67	47.83	47.75	48.37	50.27	49.07	50.82	12.1	0
Genotype	0.778		0.451		0.003		0.016		0.107		0.283		0.037		0.331	
Treatment	0.371		0.568		0.242		0.881		0.189		0.425		0.927		0.241	
Genotype*Treatment	0.56		0.631		0.774		0.913		0.739		0.612		0.931		0.215	
Irina	36.1	47.5	48..8	40.6	53.2	40.3	39.05	37.4	45	44.4	45.25	45.5	44	48.7	0	0
Sassy	40.47	42	50	46.5	46.5	44.95	45.87	42.55	47.4	44.65	46.33	47.77	48.3	51.8	0	0
Genotype	0.71		0.082		0.169		0.13		0.177		0.202		0.012		0.17	
Treatment	0.364		0.003		0.346		0.858		0.304		0.183		0.005		0.002	
Genotype*Treatment	0.564		0.017		0.409		0.168		0.264		0.649		0.087		0.604	

Table 4.4.A Fertile tillers per plant for cv Paragon and three near-isogenic lines of wheat under control (fully irrigated) and drought conditions measured weekly in 2021.

Genotype	Tiller number													
	29-Mar		08-Apr		15-Apr		22-Apr		29-Apr		07-May		13-May	
	Con	Dro	Con	Dro	Con	Dro	Con	Dro	Con	Dro	Con	Dro	Con	Dro
Paragon	6.75	6.5	8.5	8.5	10.5	11	11.25	13	12	14.5	13	16	14.5	18.5
WB TK0018-PFI	8.25	7	9	10.33	10	11.33	11.25	12.33	12.25	12.67	13.25	13.33	14	13.67
WB TK0019-PFI	8.75	9.75	11	11	12	11.75	13.5	12.25	14	13.75	14.75	16.5	17.5	17.25
WB TK0020-OG	7.5	8.75	10.75	10.75	11.5	11.5	13	13	13.5	13.5	14.25	14.25	16.25	15.75
Genotype	0.039		0.03		0.599		0.48		0.786		0.435		0.252	
Treatment	0.669		0.551		0.646		0.741		0.454		0.388		0.838	
Genotype*Treatment	0.339		0.8		0.928		0.582		0.19		0.726		0.563	

Table 4.4.B Fertile tillers per plant for cv Sebastian and three mutant lines and two elite lines (Sassy and Irina) of barley under control (fully irrigated) and drought conditions measured weekly in 2021.

Genotype	Tiller number													
	29-Mar		08-Apr		15-Apr		22-Apr		29-Apr		07-May		13-May	
	Con	Dro	Con	Dro	Con	Dro	Con	Dro	Con	Dro	Con	Dro	Con	Dro
prt6k	16.33	12	19	15.5	23	18	25.33	24.5	30	25.75	33.67	25.5	36.67	28.5
prt6i	7.25	14	8.75	19	11.5	23	13.25	13.5	14.75	12.25	15.5	27.75	17	27.5
prt6 ubr boxc	12.5	7.5	17.75	9.5	22	11.5	25.5	22	28.5	25.5	27	16.25	31.5	20.5
Sebastian (WT)	14.67	11.25	17	16.5	19.67	19.5	22.67	21.75	25.33	23	27	25.75	30	28.25
Genotype	0.001		0.001		0.001		0.001		0.001		0.001		0.001	
Treatment	0.288		0.634		0.218		0.15		0.054		0.542		0.236	
Genotype*Treatment	0.785		0.833		0.6336		0.445		0.495		0.621		0.186	
Irina	10	15	12.5	20	14.5	26	18	27	20	27	22	29	27	30
Sassy	9.67	13	15	17.5	19.67	21	22.33	23	25	25.25	26.33	26	34.33	28
Genotype	0.601		0.554		0.434		0.714		0.577		0.757		0.786	
Treatment	0.481		0.104		0.235		0.365		0.89		0.845		0.368	
Genotype*Treatment	0.143		0.018		0.024		0.193		0.282		0.317		0.543	

Table 4.5.A Leaf chlorophyll fluorescence for cv Paragon and three near-isogenic lines of wheat control (fully irrigated) and drought conditions measured weekly in 2021

Genotype	Chlorophyll Fluorescence (QY)							
	22-Apr		26-Apr		07-May		11-May	
	Con	Dro	Con	Dro	Con	Dro	Con	Dro
Paragon	0.745	0.74	0.7475	0.71	0.745	0.745	0.7675	0.705
WB TK0018-PFI	0.74	0.7733	0.745	0.7233	0.7575	0.6933	0.755	0.7067
WB TK0019-PFI	0.7375	0.6975	0.7475	0.7325	0.6325	0.725	0.7575	0.73
WB TK0020-OG	0.7625	0.7275	0.74	0.73	0.695	0.7275	0.725	0.7175
Genotype	0.197		0.983		0.293		0.294	
Treatment	0.254		0.087		0.437		0.003	
Genotype*Treatment	0.182		0.849		0.183		0.288	

Table 4.5.B Leaf chlorophyll fluorescence for cv Sebastian and three mutant lines and two elite lines (Sassy and Irina) of barley under control (fully irrigated) and drought conditions measured weekly in 2021.

Genotype	Chlorophyll Fluorescence (QY)							
	22-Apr		26-Apr		07-May		11-May	
	Con	Dro	Con	Dro	Con	Dro	Con	Dro
prt6k	0.6567	0.7275	0.7	0.735	0.7133	0.7075	0.7033	0.7225
prt6i	0.6625	0.75	0.6875	0.76	0.6725	0.71	0.69	0.7175
prt6 ubr boxc	0.7333	0.695	0.7433	0.7175	0.7233	0.65	0.7067	0.6875
Sebastian (WT)	0.6233	0.7175	0.6633	0.6975	0.7467	0.7425	0.72	0.7275
Genotype	0.42		0.694		0.227		0.404	
Treatment	0.027		0.184		0.662		0.591	
Genotype*Treatment	0.235		0.242		0.886		0.944	
Irina	0.68	0.74	0.74	0.7	0.73	0.7	0.76	0.69
Sassy	0.7033	0.7525	0.7367	0.74	0.7133	0.7075	0.72	0.745
Genotype	0.322		0.295		0.684		0.732	
Treatment	0.026		0.224		0.145		0.995	
Genotype*Treatment	0.613		0.136		0.605		0.208	

4.5.2.4 Green area and dry matter per main shoot and per plant at anthesis

Averaging over wheat genotypes, green area per main shoot (GA-MS) decreased from 143.1 cm^2 (well irrigated) to 110.2 cm^2 (drought), a 23% reduction ($P < 0.001$), and green area per plant (GA-PL) decreased from 556.4 cm^2 to 357.8 cm^2, a 36% reduction ($P < 0.001$; Table 4.6; Fig. 4.5). The effects of genotype and the irrigation treatment × genotype interaction were not statistically significant. For barley, overall drought decreased green area per MS from 95.1 to 72.0 cm^2 ($P< 0.01$) and green area per plant from 2167 to 1250 cm^2 ($P< 0.001$). Among Sebastian and the mutant lines, *ptr6k* had lower values than other genotypes ($P<0.001$); and for green area per plant *prt6i* had lower values than the WT ($P< 0.001$). The irrigation treatment × genotype interaction was not significant for GA-MS or GA-PL.

For wheat genotypes, drought decreased biomass per main shoot by ca. 20% overall ($P< 0.001$) and biomass per plant by ca. 35%. The genotype effect and the irrigation treatment × genotype effect were not significant. For barley, the irrigation treatment effect was not significant on biomass per main shoot, but biomass per plant decreased under drought ($P< 0.05$). There was a trend for an irrigation treatment × genotype interaction among Sebastian and the mutant lines, with the decrease relatively greater for *prt6k* and *prt6i* than Sebastian ($P = 0.07$).

Table 4.6.A Green area (GA, cm^2) and biomass (g) per main shoot (MS) and per plant (PL) for cv Paragon and three near-isogenic lines of wheat under control (fully irrigated) and drought conditions measured at anthesis in 2021

Genotype	GA-MS		GA-PL		BM-MS		BM-PL	
	Con	Dro	Con	Dro	Con	Dro	Con	Dro
Paragon	143.1	110.2	556.4	357.8	11.37	9.57	44.27	29.6
WB TK0018-PFI	160.3	86.9	1008.2	367.9	10.9	9.93	42.7	34.01
WB TK0019-PFI	165.1	106.8	694.4	382.3	14.49	10.08	49.43	31.37
WB TK0020-OG	140.5	85.1	700.9	395.7	13.63	7.96	49.06	31.79
Genotype	0.698		0.596		0.583		0.323	
Treatment	0.001		0.001		0.007		0.001	
Genotype*Treatment	0.813		0.699		0.393		0.156	

Table 4.6.B Green area (GA, cm^2) and biomass (g) per main shoot (MS) and per plant (PL) for cv Sebastian and three mutant lines and two elite lines (Sassy and Irina) of barley under control (fully irrigated) and drought conditions measured at anthesis in 2021

Genotype	GA-MS		GA-PL		BM-MS		BM-PL	
	Con	Dro	Con	Dro	Con	Dro	Con	Dro
prt6k	139.87	89.62	2225	1403	5.24	6.815	45.29	34.45
prt6i	81.26	78.25	1252	517	5.195	5.462	32.59	23.8
prt6 ubr boxc	86	44.25	2541	1247	5.62	5.512	42.05	36.69
Sebastian (WT)	89.37	77.31	2445	1568	3.967	4.65	39.24	37.96
Genotype	0.009		0.001		0.143		0.001	
Treatment	0.009		0.001		0.229		0.001	
Genotype*Treatment	0.262		0.376		0.64		0.063	
Irina	58.5	102.5	1608	877	3.605	6.21	47.49	34.26
Sassy	120	105.3	2171	1897	6.122	6.77	40.66	34.47
Genotype	0.06		0.01		0.184		0.28	
Treatment	0.078		0.001		0.086		0.042	
Genotype*Treatment	0.047		0.137		0.548		0.243	

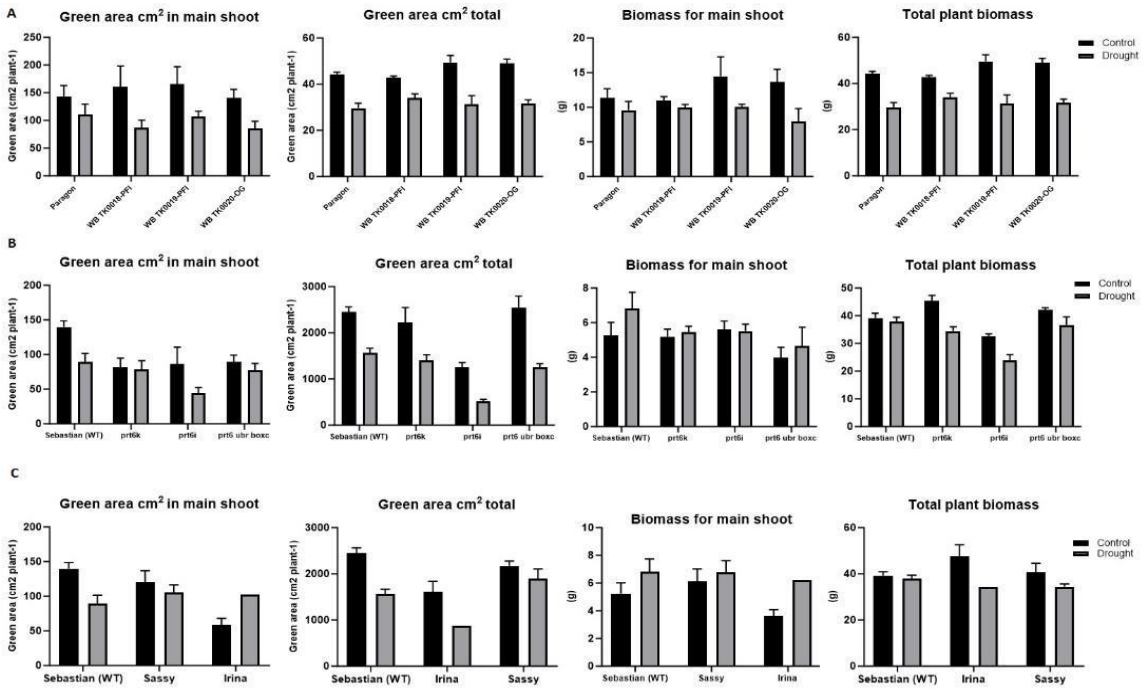

Figure 4.5. Mean green area (cm² per plant) and total biomass (g) per plant for wheat cultivar Paragon and three near-isogenic lines, and for barley cv. Sebastian and three PRT6 mutant alleles (*prt6k, prt6i, prt6 ubrboxc*) alongside elite lines Sassy and Irina, under fully irrigated (control) and drought stress conditions at anthesis in A) cross experiment mean, B) 2021 and C) 2022-23. Error bars represent the standard error of the mean (SEM) across three biological replicates. For statistical significances using REML analysis of Drought, Genotype and Drought × Genotype effects see Tables 4.6A and B; *$p < 0.05$, **$p < 0.01$, ns = not significant.

4.5.2.5 Harvest results

Table 4.7 shows the biomass per main shoot (BM-MS) and per plant (BM-total), the number of fertile (N-F) and infertile (N-INF) tillers, and plant height for the wheat genotypes (Paragon and three near-isogenic lines) and barley (Sebastian and three mutant alelles, along with elite lines Sassy and Irina) under control (well-watered) and drought (Drought) conditions at harvest.

For wheat genotypes, biomass per MS and biomass per plant were decreased by drought

(P=0.09 and P< 0.05, respectively) but there were no significant effects of genotype or the Irrigation × genotype interaction (**Table 4.7**). For barley genotypes, the effects of drought were significant on biomass per plant and fertile tillers per plant (P< 0.001), but not on biomass per main shoot or plant height. There were no significant effects of genotype or for the irrigation × genotype interaction.

For grain number per plant for the wheat genotypes, drought reduced grain per MS, grains per plant, grain weight per MS and grain weight per plant (P<0.01), but the effects of genotype and the irrigation × genotype interaction were not statistically significant (**Table 4.8**). For the barley genotypes, drought significantly reduced grains per plant and grain weight per plant (P< 0.01). There was also an effect of genotype for grains per plant, with the *prt6k* line having more grains per plant than the Sebastian WT under both well-watered and drought conditions (P< 0.05). The interaction between irrigation treatment and genotype was not significantly for either grains per plant or grains per ear.

Table 4.7.A Biomass (g) for main shoot and aboveground plant, number of fertile tillers per plant and plant height (cm) for cv Paragon and three near-isogenic lines of wheat; under control (fully irrigated) and drought conditions measured at harvest in 2021.

Genotype	BM MS g		BM MS Aboveground g		Fert tiller / plant		Plant height cm	
	Con	Dro	Con	Dro	Con	Dro	Con	Dro
Paragon	17.35	14.33	61.29	49.18	5.5	2.5	98.2	83.3
WB-TK0018-PFI	15.38	14.21	57.65	55.58	4.75	3.41	100.8	88.8
WB-TK0019-PFI	16.26	12.67	60.94	49.72	6	3.75	106.8	71.8
WB-TK0020-OG	15.86	13.87	69.68	46.46	6.5	5	69.7	77.6
Genotype (P value)	0.991		0.547		0.577		0.368	
Treatment (P value)	0.094		0.033		0.04		0.775	
Gen x Trt (P value)	0.877		0.348		0.497		0.69	

Table 4.7.B Biomass (g) for main shoot and aboveground plant, number of fertile tillers per plant and plant height for cv Sebastian and three mutant lines and two elite lines (Sassy and Irina) of barley under control (fully irrigated) and drought conditions measured at harvest in 2021

Genotype	BM MS g		BM Aboveground g		Fert tiller / plant		Plant height cm	
	Con	Dro	Con	Dro	Con	Dro	Con	Dro
prt6k	10.64	10.17	70.09	49.16	26.63	14.25	66.9	67.1
prt6i	10.64	8.77	66.97	44.36	29.55	9.98	62	58.6
prt6 ubrboxc	12.21	9.36	44.34	38.07	9.25	3	62.6	61
Sebastian WT	10.49	9.06	63.4	44.06	36	8.75	57.8	51.4
Genotype (P value)	0.136		0.433		0.002		0.336	
Treatment (P value)	0.379		0.138		0.001		0.902	
Gen x Trt (P value)	0.397		0.734		0.054		0.521	
Irina	12.27	10.97	69.76	52.8	26.23	9	46.1	63.3
Sassy	11.45	10.69	66.32	47.1	25.21	3.75	68	58.2
Genotype (P value)	0.486		0.88		0.261		0.88	
Treatment (P value)	0.152		0.22		0.001		0.22	
Gen x Trt (P value)	0.548		0.666		0.352		0.666	

Table 4.8.A Grain number per main shoot, grain number per plant, grain weight per main shoot and grain weight per plant for cv Paragon and three near-isogenic lines of wheat under control (fully irrigated) and drought conditions measured at harvest in 2021.

Genotype	Grains per MS		Grains per plant		GW per MS g		GW per plant g	
	Con	Dro	Con	Dro	Con	Dro	Con	Dro
Paragon	109	57.4	340.5	154.6	2.76	1.36	10.6	3.01
WB-TK0018-PFI	81.8	12.4	312	118.6	3.15	1.2	11.1	5.9
WB-TK0019-PFI	73.3	18.6	314.5	61.6	3.18	1.7	12.1	3
WB-TK0020-OG	59.8	24.8	322.5	61.7	2.27	1.52	14.7	2.9
Genotype (P value)	0.089		0.098		0.81		0.751	
Treatment (P value)	0.001		0.003		0.001		0.001	
Gen x Trt (P value)	0.701		0.687		0.465		0.889	

Table 4.8.B Grain number per main shoot, grain number per plant, grain weight per main shoot and grain weight per plant for cv Sebastian and three mutant lines and two elite lines (Sassy and Irina) of barley under control (fully irrigated) and drought conditions measured at harvest in 2021.

Genotype	Grains per MS		Grains per plant		GW per MS g		GW per plant g	
	Con	Dro	Con	Dro	Con	Dro	Con	Dro
prt6k	17.4	19.6	305.5	103.4	1.16	0.85	13.7	4.2
prt6i	10.5	15.4	216	33.3	0.89	2.22	9.3	0.9
prt6 ubrboxc	8.3	7	95.8	25	0.68	0.79	4.7	1.3
Sebastian WT	14	8	149.3	36.4	0.65	0.48	4.5	1.2
Genotype (P value)	0.093		0.355		0.029		0.068	
Treatment (P value)	0.221		0.146		0.001		0.004	
Gen x Trt (P value)	0.915		0.955		0.271		0.698	
Irina	30.7	19.4	248.9	55.1	1.66	0.91	12.9	0.4
Sassy	21.2	14.8	66.32	277.3	0.96	1.04	68	2.7
Genotype (P value)	0.747		0.929		0.119		0.453	
Treatment (P value)	0.42		0.264		0.001		0.002	
Gen x Trt (P value)	0.991		0.422		0.367		0.399	

4.5.3 Above-ground traits in 2022 experiment

4.5.3.1 Leaf relative chlorophyll content (SPAD)

The leaf chlorophyll content (SPAD value) under drought conditions decreased on several dates compared to well-irrigated conditions (Table 4.9). Among wheat genotypes on 13 September, flag-leaf SPAD values were 45.8 under control and 43.2 under drought. By 16 November, the average values were 44.6 (well irrigated) and 38.45 (drought), indicating a 14.6% decrease under drought ($P < 0.01$). The genotype effect and the interaction between irrigation treatment and genotype were not significant on any assessment date. For barley genotypes, the drought effect was significant on all assessment dates ($P< 0.10$) apart from 2 November, with a decrease under drought compared to well-watered conditions. The genotype effect was statistically significant on most assessment dates with *prt6i* showing higher values than the Sebastian WT ($P< 0.05$), However, the interaction between irrigation treatment and genotype was not significant on any assessment date.

Table 4.9.A Leaf chlorophyll content (SPAD) for cv Paragon and three near-isogenic lines of wheat; under control (fully irrigated) and drought conditions measured weekly in 2022

Genotype	SPAD																	
	13-Sep		20-Sep		28-Sep		12-Oct		19-Oct		26-Oct		02-Nov		09-Nov		16-Nov	
	Con	Dro	Con	Dro	Con	Dro	Con	Dro	Con	Dro	Con	Dro	Con	Dro	con	Dro	Con	Dro
Paragon	49.9	45.65	44.23	45.57	44.07	44.77	44.33	46.2	47.42	46.4	46.4	46.47	46.1	51.42	46.02	48.15	43.92	46.55
WB TK0018-PFI	44.23	37.05	42.67	43.35	40.88	42.98	42.8	43.07	43.67	44.12	44.65	45.58	35.35	47.27	46.38	46.78	48.35	44.15
WB TK0019-PFI	43.9	43.73	45.15	43.92	44.38	41.1	43.05	42.4	44.55	44.3	46.12	45.22	48.45	46.02	47.2	50.85	46.45	36.48
WB TK0020-OG	46.73	46.25	47.25	44.42	44.07	44.48	43.85	45.27	45.78	46.7	36.9	46.83	45.12	46.98	45.83	45.55	48.9	41.75
Genotype	0.334		0.169		0.528		0.348		0.132		0.635		0.308		0.625		0.639	
Treatment	0.308		0.523		0.989		0.532		0.98		0.354		0.157		0.428		0.109	
Genotype*Treatment	0.803		0.364		0.573		0.864		0.908		0.46		0.358		0.872		0.442	

Table 4.9.B Leaf chlorophyll content (SPAD) for cv Sebastian and three mutant lines and two elite lines (Sassy and Irina) of barley under control (fully irrigated) and drought conditions measured weekly in 2022

Genotype	SPAD																	
	13-Sep		20-Sep		28-Sep		12-Oct		19-Oct		26-Oct		02-Nov		09-Nov		16-Nov	
	Con	Dro	Con	Dro	Con	Dro	Con	Dro	Con	Dro	Con	Dro	Con	Dro	con	Dro	Con	Dro
prt6k	49.9	46.17	46.2	43.82	41.53	43.7	45.85	44.5	48.08	47.3	46.08	45.05	43.82	40.95	41.98	35.83	38.05	36.1
prt6i	54	53.62	50.08	51.12	50	50.27	50	50.33	50.12	51.5	49.4	43.7	43.42	39.2	43.33	32.9	39.35	20.73
prt6 ubr boxc	47.62	45.8	44	40.57	42.58	40.1	44.9	40.57	48.43	44.3	50.2	41.27	50.08	49.8	45.5	48.77	39.15	42.47
Sebastian (WT)	47.5	48.77	43.08	46.7	38.2	43.67	46.35	47.07	47.62	51.3	46.73	44.35	47.37	42.83	40.85	40.38	37.17	31.22
Genotype	0.013		0.002		<0.001		0.007		0.3		0.093		0.964		0.079		0.063	
Treatment	0.454		0.401		0.336		0.434		0.906		0.152		0.022		0.14		0.029	
Genotype*Treatment	0.67		0.246		0.319		0.546		0.405		0.952		0.431		0.234		0.047	
Irina	45.77	35.95	39.1	39.35	42.15	36.92	46.1	41.33	46.05	42.15	44.85	32.7	45.3	43.17	41.62	33.02	37.78	23.63
Sassy	45.73	50.52	42.73	44.1	43.95	41.38	42.3	45.88	49.7	46.85	47.35	42.78	43.15	43.6	35.67	40.7	41.1	35.3
Genotype	0.206		0.002		0.122		0.699		0.202		0.152		0.785		0.972		0.348	
Treatment	0.436		0.8826		0.15		0.572		0.22		0.065		0.527		0.558		0.115	
Genotype*Treatment	0.286		0.392		0.155		0.09		0.807		0.329		0.822		0.562		0.526	

Table 4.10.A Fertile tillers per plant for cv Paragon and three near-isogenic lines of wheat under control (fully irrigated) and drought conditions measured weekly in 2022

Genotype	Tiller number																	
	13-Sep		20-Sep		28-Sep		12-Oct		19-Oct		26-Oct		02-Nov		09-Nov		16-Nov	
	Con	Dro	Con	Dro	Con	Dro	Con	Dro	Con	Dro	Con	Dro	Con	Dro	con	Dro	Con	Dro
Paragon	5.5	5.25	9.25	9.5	11	12.5	11.75	12.5	11.75	12.5	12	12.75	10.5	12.25	10.5	19	10.25	17.5
WB TK0018-PFI	4.75	4	8.25	7.25	8.5	9.5	9.25	9.75	9.25	9.75	9.25	9	9	8.5	8	8.75	6.5	9.5
WB TK0019-PFI	4.5	4.25	7.5	8	10	9.75	10.25	11	10.25	11.25	9.25	10.75	8.75	9.5	8	9.5	8	8.75
WB TK0020-OG	5.25	5.75	10	9	11.5	12.5	12	14.25	11.75	14.25	10.75	14.25	10.5	13.5	10.75	12	10	11
Genotype	0.281		0.105		0.022		0.003		0.009		0.002		0.005		0.062		0.136	
Treatment	0.726		0.633		0.284		0.108		0.103		0.052		0.107		0.102		0.125	
Genotype*Treatment	0.87		0.766		0.858		0.849		0.746		0.267		0.496		0.373		0.6	

Table 4.10.B Fertile tillers per plant for cv Sebastian and three mutant lines and two elite lines (Sassy and Irina) of barley under control (fully irrigated) and drought conditions measured weekly in 2022

Genotype	Tiller number																	
	13-Sep		20-Sep		28-Sep		12-Oct		19-Oct		26-Oct		02-Nov		09-Nov		16-Nov	
	Con	Dro	Con	Dro	Con	Dro	Con	Dro	Con	Dro	Con	Dro	Con	Dro	con	Dro	Con	Dro
prt6k	15.25	13.5	18.75	18	25	21.25	25.75	22.5	25.75	23	25.5	23.75	25.75	25	26.5	27.75	26.5	35.25
prt6i	11	11	16	14	17.75	18.5	20.75	19	21.75	19	23.25	20	26.5	21.5	30.5	29.25	37.75	36.75
prt6 ubr boxc	6.75	6.67	8.25	8.67	11.75	10.33	12.5	11	13.5	12	14.25	14	15	16.5	15.5	18.33	17	23
Sebastian (WT)	13.75	9.75	16.25	13.25	22.5	19	24.25	20.25	25	20.5	25.25	21.25	25.5	23.75	26.5	28.5	31.5	41
Genotype	**<0.001**		**<0.001**		**<0.001**		**<0.001**		**<0.001**		**<0.001**		**<0.001**		**0.007**		**0.013**	
Treatment	**0.11**		**0.118**		**0.09**		**0.021**		**0.012**		**0.038**		**0.221**		**0.651**		**0.134**	
Genotype*Treatment	**0.379**		**0.551**		**0.461**		**0.819**		**0.807**		**0.645**		**0.479**		**0.946**		**0.737**	
Irina	11.25	10	13.75	12	16.5	15.25	17.75	17.25	18.75	17	19	17.25	21.5	18.25	22.25	21.5	22.25	27.75
Sassy	13.25	10.25	17.25	12.75	21.25	18.25	23	18.25	23.25	18.25	24	18.75	24.75	19.25	28	25.5	41.5	29.75
Genotype	**0.033**		**0.005**		**<0.001**		**<0.001**		**0.003**		**0.003**		**0.043**		**0.23**		**0.164**	
Treatment	**0.083**		**0.66**		**0.055**		**0.031**		**0.027**		**0.038**		**0.071**		**0.806**		**0.85**	
Genotype*Treatment	**0.798**		**0.429**		**0.726**		**0.368**		**0.596**		**0.464**		**0.514**		**0.85**		**0.146**	

4.5.3.2 Tillers per plant

Table 4.10 shows the tillers per plant for the wheat and barley genotypes under well irrigated and drought conditions measured weekly. The irrigation treatment effect was not statistically significant. The genotype effect was significant on most assessment dates with WB TH018-PFI and WBI-TH019-PFI having fewer tillers per plant than the Sebastian WT ($P< 0.05$). The interaction between irrigation treatment and genotype was not significant on any assessment date.

4.5.3.3 Leaf chlorophyll fluorescence (QY)

Table 4.11 presents the leaf chlorophyll fluorescence (QY) measurements for different wheat and barley lines under control (well irrigated) and drought conditions, recorded weekly. For wheat and barley genotypes, there were no significant genotype effects or irrigation treatment × genotype interaction on any assessment date.

Table 4.11.A Leaf chlorophyll fluorescence (quantum yield, QY) for cv Paragon and three near-isogenic lines of wheat; under control (fully irrigated) and drought conditions measured weekly in 2022

					Chlorophyll Fluorescence (QY)							
Genotype	**13-Sep**		**04-Oct**		**12-Oct**		**26-Oct**		**02-Nov**		**09-Nov**	
	Con	**Dro**	**Con**	**Dro**	**Con**	**Dro**	**Con**	**Dro**	**Con**	**Dro**	**Con**	**Dro**
Paragon	0.7133	0.71	0.7317	0.7317	0.7233	0.7358	0.7608	0.7508	0.7583	0.7633	0.76	0.76
WB TK0018-PFI	0.7125	0.7083	0.7375	0.7217	0.7333	0.7258	0.7692	0.7642	0.7575	0.7658	0.7225	0.7467
WB TK0019-PFI	0.7089	0.725	0.7325	0.725	0.725	0.7192	0.7733	0.7617	0.7525	0.755	0.7492	0.7425
WB TK0020-OG	0.7208	0.7192	0.7233	0.7517	0.715	0.7417	0.7642	0.7575	0.7625	0.6475	0.7492	0.6983
Genotype	**0.935**		**0.789**		**0.888**		**0.453**		**0.391**		**0.322**	
Treatment	**0.925**		**0.853**		**0.417**		**0.167**		**0.359**		**0.558**	
Genotype*Treatment	**0.94**		**0.13**		**0.378**		**0.974**		**0.302**		**0.316**	

Table 4.11.B Leaf chlorophyll fluorescence (quantum yield, QY) for cv Sebastian and three mutant lines and two elite lines (Sassy and Irina) of barley under control (fully irrigated) and drought conditions measured weekly in 2022.

Genotype	Chlorophyll Fluorescence (QY)											
	13-Sep		04-Oct		12-Oct		26-Oct		02-Nov		09-Nov	
	Con	Dro	Con	Dro	Con	Dro	Con	Dro	Con	Dro	Con	Dro
prt6k	0.7117	0.6983	0.7417	0.735	0.7192	0.7367	0.7783	0.7817	0.7417	0.7425	0.7433	0.6967
prt6i	0.6983	0.6825	0.7333	0.7125	0.7308	0.72	0.7733	0.7733	0.7217	0.6667	0.735	0.6425
prt6 ubr boxc	0.7111	0.7044	0.7142	0.7233	0.7292	0.7433	0.7617	0.7644	0.7542	0.7333	0.7267	0.7522
Sebastian (WT)	0.7108	0.68	0.7217	0.74	0.7283	0.7308	0.7692	0.7608	0.7783	0.7508	0.7475	0.7333
Genotype	**0.88**		**0.177**		**0.903**		**0.073**		**0.085**		**0.292**	
Treatment	**0.341**		**0.96**		**0.562**		**0.89**		**0.201**		**0.116**	
Genotype*Treatment	**0.968**		**0.185**		**0.703**		**0.815**		**0.777**		**0.269**	
Irina	0.7267	0.74	0.7258	0.7367	0.735	0.72	0.7483	0.7633	0.7558	0.6667	0.7358	0.6833
Sassy	0.7383	0.6958	0.725	0.7217	0.7167	0.735	0.7617	0.7533	0.7692	0.74	0.705	0.7083
Genotype	**0.493**		**0.286**		**0.975**		**<0.001**		**0.581**		**0.919**	
Treatment	**0.469**		**0.971**		**0.401**		**0.449**		**0.27**		**0.265**	
Genotype*Treatment	**0.505**		**0.606**		**0.186**		**0.115**		**0.564**		**0.672**	

4.5.3.4 Green area and dry matter per main shoot and per plant at anthesis

Table 4.12 shows results on the green area (GA) and biomass (BM) per main shoot (MS) and the total plant for the wheat and barley genotypes under control (fully irrigated) and drought conditions at anthesis. For wheat genotypes, the drought reduced green area per plant and biomass per plant ($P< 0.05$). However, the genotype effect and irrigation treatment × genotype interaction were not statically significant ($P< 0.05$).

For barley genotypes the drought effect decreased green area per plant, but increased biomass per MS ($P< 0.05$). The green area per plant and the biomass per plant were lower in *prt6i* than WT Sebastian ($P< 0.05$). The irrigation treatment × genotype interaction was not statically significant for any parameter.

Table 4.12 Green area (GA, cm^2) and biomass (BM, g) per main shoot and per plant (total) for cv Paragon and three near-isogenic lines of wheat; and for cv Sebastian and three mutant lines and two elite lines (Sassy and Irina) of barley under control (fully irrigated) and drought conditions measured at anthesis in 2022.

Genotype	GA-MS		GA-Total		BM-MS		BM-total	
	Con	Dro	Con	Dro	Con	Dro	Con	Dro
Paragon	151.1	143.2	929	470.9	3.232	3.34	24.44	13.8
WB TK0018-PFI	283.1	216.4	952.5	623.4	6.695	4.678	24.32	14.7
WB TK0019-PFI	147	169	891.5	569	3.33	4.527	21.61	14.7
WB TK0020-OG	137.9	108.2	970.5	543.1	3.459	2.475	24.06	16.25
Genotype	**0.048**		**0.489**		**0.019**		**0.687**	
Treatment	**0.524**		**<0.001**		**0.478**		**<0.001**	
Genotype*Treatment	**0.793**		**0.562**		**0.264**		**0.679**	
prt6k	73.71	57.68	1320.1	766.9	1.02	1.607	24	22.25
prt6i	156.71	70.24	894.7	579.3	1.409	3.795	17.14	11.61
prt6 ubr boxc	82.1	57.55	1330.7	772.1	1.34	2.112	24.14	19.04
Sebastian (WT)	93.04	74.99	1118.5	986.2	1.65	1.585	29.2	24.68
Genotype	**0.41**		**0.022**		**0.221**		**0.022**	
Treatment	**0.106**		**0.001**		**0.046**		**0.118**	
Genotype*Treatment	**0.627**		**0.183**		**0.277**		**0.955**	
Irina	98.34	62.97	816.9	642.7	3.479	2.416	27.27	20.33
Sassy	82.82	51.22	1468	706.8	1.903	1.405	29.27	14.96
Genotype	**0.401**		**0.034**		**0.007**		**0.607**	
Treatment	**0.003**		**0.013**		**0.126**		**0.023**	
Genotype*Treatment	**0.653**		**0.102**		**0.509**		**0.504**	

4.5.3.5 Harvest results

For wheat genotypes, drought decreased biomass per plant, fertile tillers per plant and plant height ($P < 0.001$; Table 4.13). There was an effect of genotype on biomass per plant, fertile tiller number and plant height ($P < 0.001$). Biomass per plant was greater in Paragon than WB TH019-PFI and plant height was greater in WB TH019-PFI than Paragon. The irrigation treatment × genotype interaction was not significant for any trait. For barley genotypes, drought decreased biomass per MS, biomass per plant, fertile tillers per plant and plant height ($P < 0.01$). There was an effect of genotype for biomass per plant ($P < 0.01$) and fertile tillers per plant ($P = 0.06$). The biomass per plant and the tillers per plant were lower for the *prt6i* line than for the Sebastian WT.

Table 4.13 Biomass (g) for main shoot and total of plant, number of fertile and infertile tillers and plant height for cv Paragon and three near-isogenic lines of wheat; and for cv Sebastian and three mutant lines and two elite lines (Sassy and Irina) of barley under control (fully irrigated) and drought conditions measured at harvest in 2022.

Genotype	BM-MS		BM-total		N-F		N-INF		Plant high	
	Con	Dro	Con	Dro	Con	Dro	Con	Dro	Con	Dro
Paragon	4.362	4.207	27.8	17.52	6	2.5	1.75	6.25	75.22	69.55
WB TK0018-PFI	5.635	5.03	26.66	16.26	4.25	2.5	1.25	7.25	87.38	71.78
WB TK0019-PFI	4.852	5.35	25.17	16.47	5	2.25	2	4.75	91.57	76.93
WB TK0020-OG	5.103	3.935	31.06	17.07	6.25	4.75	2	5.25	87.22	67.6
Genotype	0.259		0.041		<0.001		0.927		0.028	
Treatment	0.391		<0.001		<0.001		<0.001		<0.001	
Genotype*Treatment	0.538		0.146		0.119		0.666		0.303	
prt6k	3.237	1.845	29.51	19.61	17	7	14.75	23	67.8	53.5
prt6i	2.64	2.17	23.94	12.64	12.5	3.33	8	16.33	74	56.33
prt6 ub boxc	3.143	2.35	31.07	19.22	22.5	11.5	7.75	23.25	66.88	56.57
Sebastian (WT)	2.54	2.072	36.74	21.68	22	6.75	5.75	26.25	67.38	53.15
Genotype	0.744		0.003		0.06		0.663		0.55	
Treatment	0.015		<0.001		<0.001		0.003		<0.001	
Genotype*Treatment	0.667		0.721		0.74		0.653		0.89	
Irina	3.71	3.41	36.46	22.76	15.5	6.75	21.25	15.25	63.92	58.4
Sassy	2.54	2.072	36.74	21.68	22	6.75	5.75	26.25	67.38	53.15
Genotype	0.026		0.901		0.347		0.776		0.775	
Treatment	0.1		<0.001		<0.001		0.024		<0.001	
Genotype*Treatment	0.655		0.634		0.365		0.046		0.228	

Grain number per plant and grain weight per plant were significantly decreased by drought in both the wheat and barley genotypes ($P<0.05$; Table 4.14). For barley, the genotype effect was significant for grain number per plant ($P=0.07$) and grain weight per plant ($P=0.07$), but the irrigation treatment × genotype interaction was not significant. The grains per plant and the grain weight per plant were greater for the Sebastian WT than the *prt6k* and *prt6i* lines. For both wheat and barley, the irrigation × treatment interactions for GN-PL and GW-PL were not significant.

Table 4.14. Grain number for main shoot, total of grain number per plant, grain weight (g) in main shoot and total of grain weight (g) per plant and harvest index for cv Paragon and three near-isogenic lines of wheat; and for cv Sebastian and three mutant lines and two elite lines (Sassy and Irina) of barley under control (fully irrigated) and drought conditions measured at harvest in 2022.

Genotype	GN-MS		GN-PL		GW-MS		GW-PL		HI	
	Con	Dro	Con	Dro	Con	Dro	Con	Dro	con	Dro
Paragon	16.5	18.5	172.25	29.5	0.6262	0.691	5.734	0.937	0.2064	0.0546
WB TK0018-PFI	20.25	13	85.25	46	0.9693	0.603	3.466	1.94	0.1247	0.1508
WB TK0019-PFI	14.75	31.5	104.25	72	1.0704	1.0841	4.983	2.525	0.195	0.1188
WB TK0020-OG	30.5	13	182	74.25	0.8739	0.427	5.311	2.89	0.1735	0.1759
Genotype	**0.799**		**0.155**		**0.399**		**0.825**		0.814	
Treatment	**0.786**		**<0.001**		**0.36**		**<0.001**		0.027	
Genotype*Treatment	**0.181**		**0.137**		**0.728**		**0.433**		0.402	
prt6k	12	6.75	85.2	46.2	0.7789	0.4627	4.045	1.808	0.1988	0.0824
prt6i	12.75	11.5	114.5	10.3	0.824	0.587	5.662	0.72	0.2804	0.0584
prt6 ubr boxc	13	12.75	226.5	35.5	0.4829	0.8049	7.415	1.737	0.2307	0.0883
Sebastian (WT)	16.25	10.5	266.2	58.2	0.9127	0.6963	11.133	2.846	0.3193	0.1327
Genotype	**0.583**		**0.069**		**0.74**		**0.074**		0.379	
Treatment	**0.165**		**<0.001**		**0.42**		**<0.001**		<0.001	
Genotype*Treatment	**0.77**		**0.155**		**0.302**		**0.301**		0.803	
Irina	20.75	15.75	221.2	125.5	1.351	1.149	11.613	9.017	0.3294	0.3606
Sassy	18.75	16.25	145.5	84	1.247	1.12	7.196	4.9	0.2047	0.1914
Genotype	**0.124**		**0.317**		**0.012**		**0.054**		0.056	
Treatment	**0.039**		**<0.001**		**0.133**		**0.005**		0.266	
Genotype*Treatment	**0.784**		**0.185**		**0.943**		**0.17**		0.187	

4.5.4 Grain ionomics in 2021 and 2022

Grains of the main shoots for the barley mutant lines and the Sebastian WT in both experiments were analysed to evaluate the elemental accumulations under control and drought treatments (**Fig. 4.6**). Calcium (Ca), Magnesium (Mg), Potassium (K), and Phosphorus (P) had higher concentrations, while Copper (Cu), Boron (B), Manganese (Mn), and Zinc (Zn) had lower concentrations among the mutants. Significant differences in elements were observed due to the irrigation treatment, notably for Cu and Zn ($p < 0.001$ for both); however, no differences among the mutants were found in this study. The rest of the elements shown in Figure 4.6 did not present significant differences between the treatments; however, differences among the mutants were observed. Specifically, the concentrations of B, Ca, K, Mg, and Mn were significantly different among the genotypes/mutants ($p < 0.001$, $p = 0.028$, $p = 0.009$, $p < 0.001$, and $p < 0.04$, respectively). In these elements, the *prt6k* mutant had higher concentrations than the WT, whereas the *prt6i* mutant tended to have lower concentrations than the WT and the other mutants. Iron showed a marginally significant variation ($p = 0.051$), with all mutants exhibiting higher Fe levels than the WT.

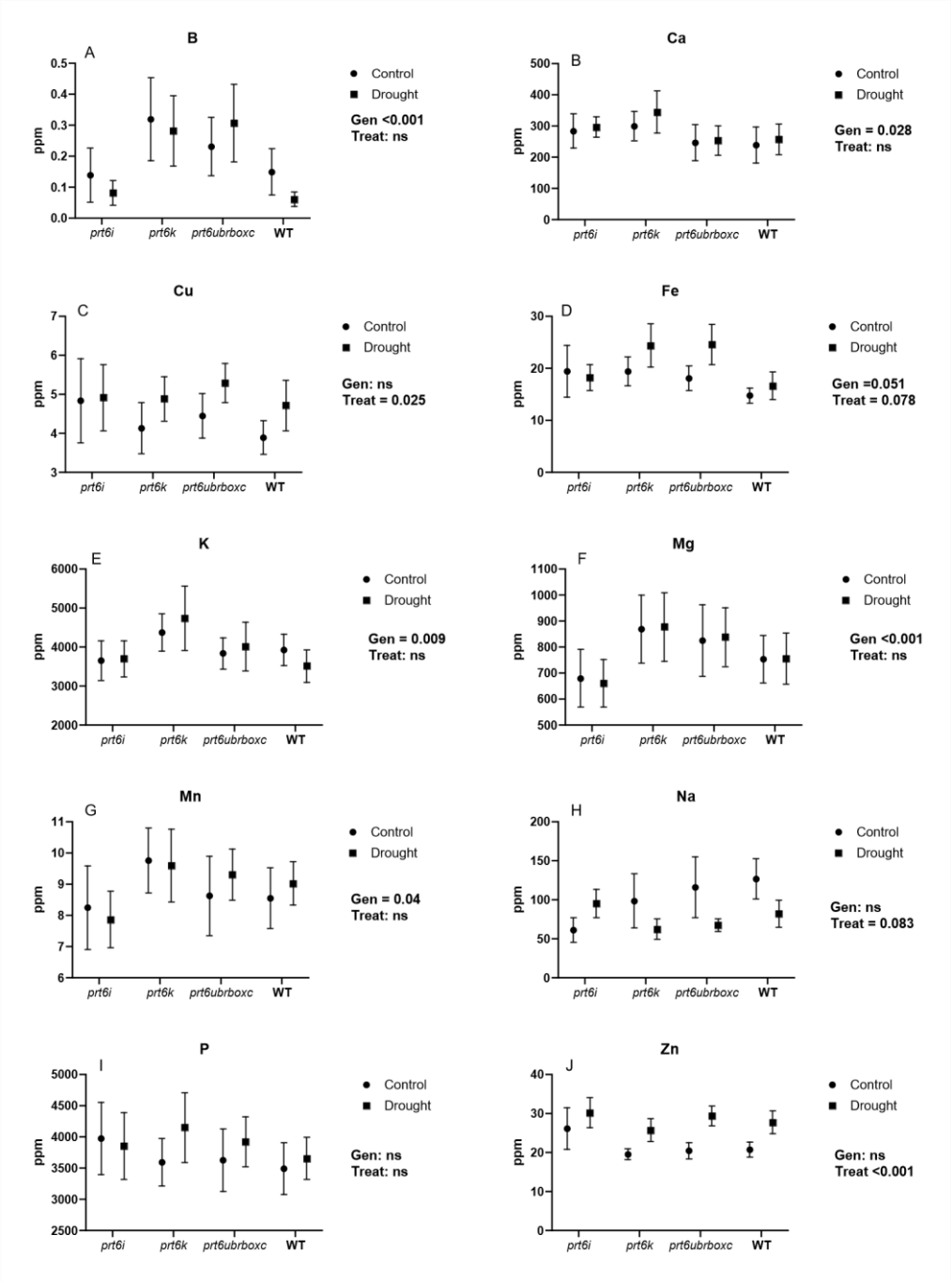

Figure 4.6. Mineral content in barley grain: cv Sebastian and three PRT6 mutant lines under drought and control conditions A) boron (B), B) calcium (Ca), C) cooper (Cu), D) iron (Fe), E) potassium (K), F) magnesium (Mg), G) manganese (Mn), H) sodium (Na), I) phosphorus (P), J) zinc (Zn) in a glasshouse experiment over 2021 and 22 under control (C) and drought treatment (T). ppm: parts per million (ppm). Error bars represent standard error of difference of the means (S.E.D)

Correlations between the concentrations of the elements under control and drought conditions are shown in Table 4.15. Similar positive correlations were found in the two treatments; however, stronger correlations between the elements were found under drought conditions. Under drought, Mg was positively correlated with B ($r = 0.74$, $p < 0.001$), Ca ($r = 0.65$, $p < 0.01$), Fe ($r = 0.82$, $p < 0.001$), K ($r = 0.68$, $p < 0.01$), Mn ($r = 0.75$, $p < 0.001$) and P ($r = 0.55$, $p < 0.05$). Ca was also positively correlated with Fe ($r = 0.50$, $p < 0.05$), K ($r = 0.51$, $p < 0.05$), P ($r = 0.71$, $p < 0.01$). Fe was positively related to B ($r = 0.86$, $p < 0.001$), K ($r = 0.73$, $p < 0.001$), Mn ($r = 0.62$, $p < 0.05$) and P ($r = 0.55$, $p < 0.05$). Zn was only correlated with Cu ($r = 0.89$, $p < 0.001$) and P ($r = 0.64$, $p < 0.050$).

Table 4.15 Correlations between the concentrations of different elements in the barley grains under (A) control and (B) drought conditions. *p < 0.05, **p < 0.01, ***p < 0.001, italics < 0.10.

Ionomics

(A) Control

	1	2	3	4	5	6	7	8	9	10
1 B	-									
2 Ca	0.15	-								
3 Cu	0.27	0.34	-							
4 Fe	0.52*	0.39	0.83***	-						
5 K	0.05	0.52*	-0.03	0.24	-					
6 Mg	0.64**	0.34	0.02	0.16	0.24	-				
7 Mn	0.64**	0.63**	0.54*	0.74***	0.34	*0.49*	-			
8 Na	-0.41	0.18	-0.57*	*-0.43*	0.57*	-0.05	-0.22	-		
9 P	-0.19	0.69**	0.54*	0.42	0.50*	0.12	0.41	0.07	-	
10 Zn	-0.03	0.37	0.82***	0.72**	0.13	-0.27	0.43	-0.39	0.71**	-

(B) Drought

	1	2	3	4	5	6	7	8	9	10
1 B	-									
2 Ca	0.51*	-								
3 Cu	0.17	0.19	-							
4 Fe	0.86***	0.50*	0.26	-						
5 K	0.60*	0.51*	0.08	0.73**	-					
6 Mg	0.74***	0.65**	0.14	0.82***	0.68**	-				
7 Mn	0.51*	0.42	-0.26	0.62*	0.41	0.75***	-			
8 Na	-0.51*	*-0.43*	-0.16	-0.31	-0.35	-0.36	-0.33	-		
9 P	0.52*	0.71**	*0.49*	0.55*	0.71**	0.55*	0.18	*-0.49*	-	
10 Zn	0.25	0.38	0.89***	0.23	0.12	0.18	-0.31	-0.25	0.64**	-

4.6 Discussion

The results of this study highlight the impact of drought stress on various root cortical senescence (RCS) and physiological and morphological parameters of the wheat and barley genotypes, including genetically mutated lines. The primary focus was on RCS characteristics and biomass production with additional data collected on tiller numbers and leaf senescence. This discussion links the findings to previous studies, providing a comprehensive understanding of the genotypic responses to drought and the potential mechanisms of drought tolerance.

RCS involves the programmed death of root cortical cells, leading to the formation of air spaces (aerenchyma). This process enhances root efficiency by reducing the metabolic costs associated with maintaining living root cells, thereby conserving energy and resources. Increased aerenchyma formation (as indicated by AA and percCisA) under drought conditions was a common response among the genotypes, particularly in the mutant barley lines. Aerenchyma enhances root aeration, facilitating oxygen diffusion to the root system and improving root survival in anaerobic soil conditions (Colmer, 2003). Moreover, aerenchyma reduces root metabolic costs by replacing living cortical cells with air spaces, significantly lowering the oxygen demand and nutrient consumption by roots under stress conditions (Evans, 2004).

While increased AA under drought conditions can enhance root aeration and reduce metabolic costs, it may also potentially negatively affect water transport efficiency. Aerenchyma formation reduces the overall density of root tissue, which could decrease the hydraulic conductivity of the root system, potentially limiting water uptake and transport (Lynch, 2013). This trade-off between enhanced root metabolic cost and reduced water transport efficiency must be carefully managed to optimize drought tolerance.

4.6.1 Root Cortical Senescence (RCS) responses to drought

Root adaptations, such as increased aerenchyma area (AA) and percentage root cortical aerenchyma (PercCisA), were observed under drought conditions in the barley mutant lines and some wheat genotypes compared to the parental wild types. Greater responses for increased percentage aerenchyma were also observed from some barley mutant lines

compared to the wild type. These adaptations are potentially important for enhancing water and nutrient-uptake efficiency. Previous studies by Lynch (2013) and Saengwilai et al. (2014) demonstrated that the formation of aerenchyma and changes in root cortical structure are important for improving root hydraulic conductivity and reducing metabolic costs under drought.

In this study, increased aerenchyma formation (as indicated by AA and PercCisA) under drought conditions compared to the WT was observed in mutant barley lines. Aerenchyma reduces root metabolic costs by replacing living cortical cells with air spaces, significantly lowering the oxygen demand and nutrient consumption by roots under stress conditions (Evans, 2004). This may allow additional root growth and increased root length density under drought, facilitating water uptake.

The reduction in cortex cell area (CCA) observed under drought conditions across most genotypes suggests a strategic response to minimize metabolic activity and conserve energy. As roots face water deficits, the reduction in CCA can help decrease the respiration rate of root cells, thereby conserving carbohydrates that can be redirected to maintain growth and essential physiological functions (Henry et al., 2012).

In wheat, the percentage of aerenchyma overall increased with drought in both years but this was more pronounced in year 2 and there were some apparent differences between genotypes. For instance, in 2021 wheat line 19 showed no increase in aerenchyma under drought, while other genotypes did. In year 2, there were interactions for TCA, highlighting the complex response mechanisms to drought stress.

For barley, line *prt6i* showed a larger response in percentage aerenchyma under drought than Sebastian in 2021. In 2022, both the *prt6i* and *prt6 ubrboxc* mutants exhibited larger responses compared to Sebastian. Mutant lines generally displayed larger responses than Sebastian in 2022. These observations suggest that mutations in the PRT6 gene may accelerate the formation of aerenchyma. Potential mechanisms could include altered hormonal signaling pathways that regulate cell death and differentiation, facilitating the development of aerenchyma under stress conditions. This accelerated formation of aerenchyma could enhance the ability of roots to adapt to low oxygen environments and improve water uptake efficiency under drought.

The observed root cortical adaptations, including increased aerenchyma formation and reduced cortex cell area, highlight the complex and dynamic responses of roots to drought conditions. These changes are likely crucial for maintaining root function and overall plant resilience under water stress. Further investigation into the genetic and physiological mechanisms underlying these adaptations will provide deeper insights into improving crop performance under drought conditions.

Increased aerenchyma formation (as indicated by AA and percCisA) under drought conditions was a common response among the genotypes, particularly in mutant barley line *prt6i*. Aerenchyma enhances root aeration, facilitating oxygen diffusion to the root system and improving root survival in anaerobic soil conditions (Colmer, 2003). Moreover, aerenchyma reduces root metabolic costs by replacing living cortical cells with air spaces, which can significantly lower the oxygen demand and nutrient consumption by roots under stress conditions (Evans, 2004).

The reduction in cortex cell area (CCA) observed under drought conditions across most genotypes suggests a strategic response to minimize metabolic activity and conserve energy. As roots face water deficits, the reduction in CCA can help decrease the respiration rate of root cells, thereby conserving carbohydrates that can be redirected to maintain growth and essential physiological functions (Henry et al., 2012).

The integration of our findings with previous studies on the N-degron pathway underscores the critical role of both below-ground traits in determining drought tolerance. These results provide valuable insights for breeding programmes aimed at developing drought-resilient crop varieties, supporting sustainable agricultural practices in water-limited environments.

4.6.2 Biomass responses

In these experiments the wheat and the barley genotypes did not respond significantly differently to the drought stress, in spite of the increase in AA% in the individual barley mutant lines compared to the parental wild type. This suggests that AA% alone is not a sufficient indicator of drought tolerance without taking into consideration other root and above-ground physiological traits. Future studies should explore the complex interactions between aerenchyma formation and other physiological processes to understand their comprehensive

impact on drought resilience. One possible explanation for the lack of drought tolerance despite increased AA% could be related to the impact of AA% on water transport in xylem vessels. Aerenchyma plays a role in facilitating gas exchange in roots, but its increase might interfere with the hydraulic conductivity of xylem vessels. This could happen if the formation of aerenchyma reduces the mechanical strength of roots or alters their ability to transport water efficiently from roots to shoots (Tyree & Zimmermann, 2013).

Furthermore, if the increased AA% is not contributing to enhanced drought tolerance mechanisms, it could lead to suboptimal water utilization under drought conditions (Serraj & Sinclair, 2002). The lack of improvement in biomass retention despite increased AA% might indicate that other physiological traits or metabolic pathways are more critical for drought tolerance, such as efficient water-use efficiency, better root system architecture traits, or enhanced antioxidant defense mechanisms (Turner, 2019).

4.6.3 Grain ionomics responses

Several studies of barley crops have been reported under different environmental conditions for a more sustainable solution for the challenges due to climate change. These investigations normally show advances in grain yield and yield components but not many also include the grain nutrient content. The present study evaluated different elements in the barley grains under the control and drought treatment and assessed correlations and possible trade-offs between the elements among the different mutants. Most of the micro and macro elements did not show a significant difference between the irrigation treatment levels; however, differences between mutant lines were found. Elements concentrations were higher in all the mutants than the WT. For instance, these results showed these barley mutants do not compromise the nutrient concentration in grain under water stress. Plants under water stress might enhance nutritious concentration in barley but with the appropriate soil conditioners and foliar sprays (Wahab et al., 2022). The finding mentioned above agreed with the present results. Similar results were stated by Lan et al. (2024) in wheat and Mahmoud et al. (2021) in barley. Notwithstanding, Zn (an essential heavy metal) was higher in drought than control by 6.55 ppm. A study by Joshi et al. (2010) mentioned significant Genotype x Environment interaction (G x E) for Fe and Zn in wheat. In fact, research in wheat proposed the importance of soil pH for the accumulation of B, Fe, Na, P, Pb and Zn in the grain (higher pH soil = higher

nutritional deficiencies) (Caldelas et al., 2023). However, pH was not measured in this study to confirm the relationship between pH and ionomics in grains. Therefore, the evaluation of elements in grains at different conditions (glasshouse, field trial) and different soil pH is recommended to see if differences in concentrations of elements in grains are found between these environments and to evaluate their correlation with grain yield.

Chapter 5: Spring barley mutant lines: Assessing physiological traits and greenhouse Gas emissions in field experiments

Abstract

The world's changing climate threatens crop yields and the security of the global food supply. Research into breeding strategies for maintaining yield in the face of climate change is key for future food security. In plants, the Ubiquitin-mediated proteolysis, through the Plant Cysteine Oxidase (PCO) branch of the PRT6 N-degron pathway was identified as a key regulator of plant developmental and environmental responses. Much of the molecular understanding in the PRT6 N-degron pathway has been established in the genetic model *Arabidopsis thaliana*. However, there is also evidence that at least some of the molecular components of this pathway are conserved in cereals, e.g. its involvement in sensing low oxygen levels during waterlogging in barley. Also, it has been shown that this pathway may control barley response to drought. This pathway therefore has the potential to stabilize crop yields in the face of abiotic stresses if we understand the key proteins involved in this process and how they are regulated. Drought is one of the most devastating abiotic stresses affecting barley crops worldwide. The present study examined the performance of different barley mutants alleles for the PRT6 gene in barley in two field experiments at the University of Nottingham farm, UK in 2022 and 2023. The aim of this study was: i) to evaluate the genetic variation of physiological traits, yield, and greenhouse gas emissions in the field trial. In near-isogenic lines in the field experiment, the mutant alleles *prt6h*, *prt6i* and Sebastian (wild type) showed grain yield of 910 g/m^2, 913 g/m^2 and 917 g/m^2, respectively. However, biomass at maturity was higher in *prt6k* compared to WT by 4%. Differences in the impact of greenhouse gas emissions were found in the field. CO_2 and N_20 was higher in *prt6k* compared to the WT by 34% and 20%, respectively. Trade-offs between grain yield and other physiological traits with GHG emissions were found for *prt6k*. For instance, further studies and the development of new barley varieties with high grain yield, resistant to drought stress and that doesn't cause higher GHG emissions are needed.

5.1 Introduction

Agricultural production is under threat from climate change (Habib-ur-Rahman et al., 2022) with adverse effects such as drought and extreme heat having negative effects on crop

production worldwide (Furtak & Wolińska, 2023). These effects may cause a change in the water availability/distribution and changes in the plant phenological development (Gray &

Brady, 2016). One of the challenges this century is rising food demand with a population of ~11 billion people by 2100. Therefore, new approaches to improve food security in the face of changing climatic conditions are being assessed (Ingram, 2011; International Programs Center at the U.S., 2019). As such, it is critical to develop new breeding strategies to stabilize yield under environmental stresses. Currently there is insufficient understanding of how crops sense and respond to abiotic stresses at a molecular level and new understanding is required to combat these challenges. In plants, the N-degron pathways were identified as key regulator of plant developmental and environmental responses (Pryor *et al.* 2013; Bita, *et al*. 2013; Gourdji, *et al*. 2013; Gibbs *et al.* 2014; Gibbs, *et al.* 2014). The molecular understanding of the N-degron pathways has been established in the genetic model *Arabidopsis thaliana*. There is evidence that at least some of the molecular components of the N-degron pathways are conserved in cereals (Bita, *et al*. 2013; Gibbs *et al.* 2014; Gibbs, *et al.* 2014).

Barley is the second most important crop in the UK (Yawson et al., 2017) that provides a considerable amount of protein, fibre, b-glucans and it is widely used for multiple purposes: staple food for humans, animal feed and brewing material (Geng et al., 2022; Pejcz et al., 2017; Škrbić et al., 2009). Drought is the most serious abiotic stress affecting barley globally, leading to significant reductions in grain yield (Samarah et al., 2009; Forster et al., 2004). For example, a study evaluating barley genotypes under different drought treatment in the field found a yield reduction of 68-87% (Samarah et al., 2009). Studies have shown how drought alters barley crops at different phenological stages, for example, reduction of biomass production, plant height, leaf green area, number of tillers, ear size, grain weight, photosynthesis, nutrients, yield and yield components (Askarnejad et al., 2021; DaszkowskaGolec et al., 2019; Francia et al., 2013; F. Li et al., 2020; L. Li & Wang, 2023; Samarah et al., 2009). To respond to climate change, it is crucial to develop resilient agricultural practices and crop varieties, including barley, that can resist drought stress via genetic improvement. Plant-soil interactions are important regulators of soil biogeochemical cycling e.g. via roots inputs of labile substances into the rhizosphere. Plant-soil interactions are also important regulators of CO_2, CH_4 and N_2O emissions from agricultural soils. In this context N_2O emissions are of particular importance, N_2O being the major contributor to GHG gas emitted from agricultural crops

(Snyder et al., 2009). N_2O results by denitrification through the activity of soil microorganisms (Hassan et al., 2022). Nitrification is the microbial oxidation of ammonium (NH_4+) to nitrate ($N0_3$-) (Wang et al., 2021). In the denitrification process, the nitrate (NO_3 – N) is reduced to nitrite (NO_2 – N), nitric oxide (NO), nitrous oxide (N_2O), and finally dinitrogen gas (N_2) (Yang et al., 2018). CO_2 emissions from root and soil microbial respiration and CH_4 are generated by methanogenesis under waterlogged conditions, however, well drained soils act as CH_4 sinks via CH_4 oxidation by soil bacteria (Van Zandvoort et al., 2017). Different reasons for greenhouse gases in field production are water and substrate availability, soil texture, precipitation, temperature (Ball, 2013; HernandezRamirez et al., 2009; Karanjekar et al., 2015; Martins et al., 2021; Snyder et al., 2009). Generally, uptake of CH_4 from cereal fields is expected to be more prevalent in drier soils where volumetric water content does not exceed 35% and emissions to be exponentially greater where soils become waterlogged. In the present context, mutant lines with reduced root cortical senescence may exhibit reduced root respiration contributing to mitigation of GHGs. Other factors which influence GHG are formulation and rate fertilizer and cropping system (Hernandez-Ramirez et al., 2009). In fact, soil cultivation and growing different crops annually can often accelerate the conversion soil C to carbon dioxide by soil microbes (Vergé et al., 2007). Therefore, some agricultural operations may have scope as potential approaches for mitigation as greenhouse gases such as fertilization, tillage and crop rotation (Alskaf et al., 2021; Chataut et al., 2023). However, given the role of roots for GHG dynamics, altered root structure and function can impact GHG emissions.

In the present study, two field experiments were carried out in the UK over two years, 2022 and 2023, both experiments assessing mutant barley lines. The specific objective of this chapter is to assess the agronomic implications of RCS expression in the context of plant performance and stress tolerance in field experiments, and explore whether lines exhibiting enhanced RCS in controlled-environments maintain superior growth under field conditions.; and to test whether genotypes showing differences in RCS traits differ in the flux of green-house gases (CO_2, N_2O and CH_4) from the soil in the field.

A key hypothesis tested in this chapter is that there is a relationship between **r**oot cortical senescence and expression of the *PRT6* gene in the mutant lines affecting the CO_2 production by root maintenance respiration, such that the mutant lines with reduced expression of the

PRT6 gene show greater root cortical senescence, aerenchyma formation and hence reduced CO_2 emissions associated with maintenance compared to the Sebastian wild type in barley.

5.2 Materials and methods

5.2.1 Experimental design

Field experiments were carried out in 2022 and 2023 at the University Nottingham Farm, Sutton Bonington campus, Nottinghamshire, UK. The soil type for both years was sandy loam from the Dunnington Heath Series (FAO class Stagno Gleyic Luvisol). In each year, a completely randomised design was implemented for 5 barley genotypes with four replicates.

The plant material utilized comprised the mutant barley lines for PRT6 alleles described in **Chapter 2** in a Sebastian spring barley background, *prt6k*, *prt6i*, *prt6 ubrboxc* and the Sebastian WT. The mutations for PRT6 were identified in an EMS TILLING population and then backcross into cv Sebastian. The material was backcrossed to BC3 in a Sebastian background by AB InBev (Fort Collins Colorado). The subplots were 1.2 m long and 1.0 m wide with a 0.20 m gap in between in both years. The sowing dates were 5 April in 2022 and 18 April in 2023 at the rate of 300 seeds m^{-2}. In 2022, fertilizers added were 60 Kg ha^{-1} of Nitram on 24 March 2022, 60 kg N/ha of Nitram on 26 April 2022, 2.5 L ha^{-1} of Opte Man and Master Mag + TE. In 2023, only 60 kg N/ha was added. The average temperature during the cycle in 2022 was 15.5°C and 14.5°C in 2023 (Appendix **Table 5.1**). Harvest dates were 12 August 2022 and 21 August 2023 using a combine harvester. Herbicides and fungicides were applied as necessary to minimize the effects of weeds and diseases.

5.2.2. Crop measurements

5.2.2.1 Sampling and growth analysis

Growth stages were taken according to Zadoks et al. (1974). Plant establishment was measured 3 weeks after sowing by counting the number of plants in a 1 m row. Five plants were selected for growth analysis at physiological maturity by cutting at ground level, avoiding the border area and the external rows. Ten days after anthesis, plant height was measured

from ground level to peduncle using a ruler. The number of shoots (main shoot (as tallest shoot) and fertile and infertile tillers) was measured at physiological maturity. Plant height, spike length, number of spikelets per spike, and above-dry weight biomass were measured on all fertile shoots. Dry weights of straw and grain were recorded after drying for 40 h at 70°C. After physiological maturity, machine-harvested grain yield was measured in each plot using a combine harvester and values were further adjusted to moisture percentage measured in each plot.

5.2.2.2 Normalized Difference Vegetation Index

Normalized Difference Vegetation Index was measured in each plot using a handheld Green Seeker spectroradiometer (Trimble Agriculture, CO, USA) placing the instrument approximately 50 cm above the level of the crop. The NDVI measurements provided additional information on canopy green area and senescence profiles. NDVI was measured twice per week from onset of stem elongation (GS31) to heading (GS55) and once per week from heading (GS55) to physiological maturity. NDVI was calculated from measurements of reflectance in the red (680 nm) and near infrared (NIR, 800 nm) regions of the spectrum using equation (1):

$$\mathrm{NDVI} = \frac{(\mathrm{R800}-\mathrm{R\ 680})}{(\mathrm{R800}+\mathrm{R680})} \quad (1)$$

where R680 and R800 are the reflectance at 680 and 800 nm, respectively.

5.2.2.3 Greenhouse gas fluxes

GHG fluxes were measured three times during the growing season in 2023 (19-20 June, 28-29 June, 12-13 July) from flowering to grain-filling period in the genotypes Sebastian (WT), *prt6k* and *prt6ubrboxc*. The closed chamber method was used for determining GHG fluxes. For this method PVC collars were inserted into the ground in between rows. The collars were then sealed with lids fitted with suba seals during sampling. The PVC collars were 10 cm diameter

and ca 10 cm above the soil surface. The tubes were inserted 30 cm into the soil and had two 10*10 cm openings cut out between 10 and 20 cm depth to allow for root ingrowth.

Two chambers were inserted in each plot, one near the front of the plot and one at the back. The samples were taken at intervals of 0, 15, 30 and 60 minutes in each chamber by inserting the needle of the 20 ml syringe through the rubber septum fixed and stored in 20 ml glass vials (Alskaf et al., 2021). The air inside the chamber was mixed before taking the measurements, using a 20 ml syringe. A gas chromatograph (GC) was used to analyse the concentration of atmospheric greenhouse gases: methane (CH_4), carbon dioxide (CO_2) and nitrous oxide (N_2O).

5.2.4 Statistical analysis

Analysis of variance (ANOVA) was performed using GenStat (23rd edition, VSN International Ltd, UK). In the field experiment genotype was used as the fixed effect. Phenotypic correlations between traits were Pearson's correlation coefficient calculated using two-year genotype means. Data was checked for normality and homogeneity of variance using residual plots.

5.3 RESULTS

5.3.1 Meteorological data

The two field experiments were sown on similar dates in April in the two years with only 13 days' difference. However, the conditions varied significantly in both years, with higher mean temperature and less rainfall in 2022 than in 2023 (**Appendix Table 5.1)** for meteorological data. Therefore, in some cases, results are shown separately in each year for a better understanding of the data.

5.3.2. Physiological traits

Across the two years, grain yield showed genetic variation from 636 to 917 g/m^2 ($p < 0.001$) (**Fig. 5.1**). The mutant *prt6h (910 g/m^2)* and *prt6i* (913 g/m^2) showed a similar grain yield compared to Sebastian (wild type "WT") (917 g/m^2), whereas the lower grain yield was

observed for *prt6 ubrboxc* (636 g/m^2). Plant height varied from 46.8 to 52.1 cm (p = 0.009); most of the mutants performed similarly to the WT, however, *prt6 ubrbox* showed lower plant height, 46.8 cm. Infertile shoots per plant did not differ significantly among the genotypes, with 3 – 4 infertile shoots per plant for all genotypes. Biomass per main shoot varied from 1.37 to 1.62 (p = 0.045). The *prt6k* mutant had greater biomass (1.62 g) compared to the WT (with highest grain yield per main shoot; 1.55 g) followed by prt6h (1.54 g). *prt6 ubrbox* had the lowest biomass, 1.37 g per plant.

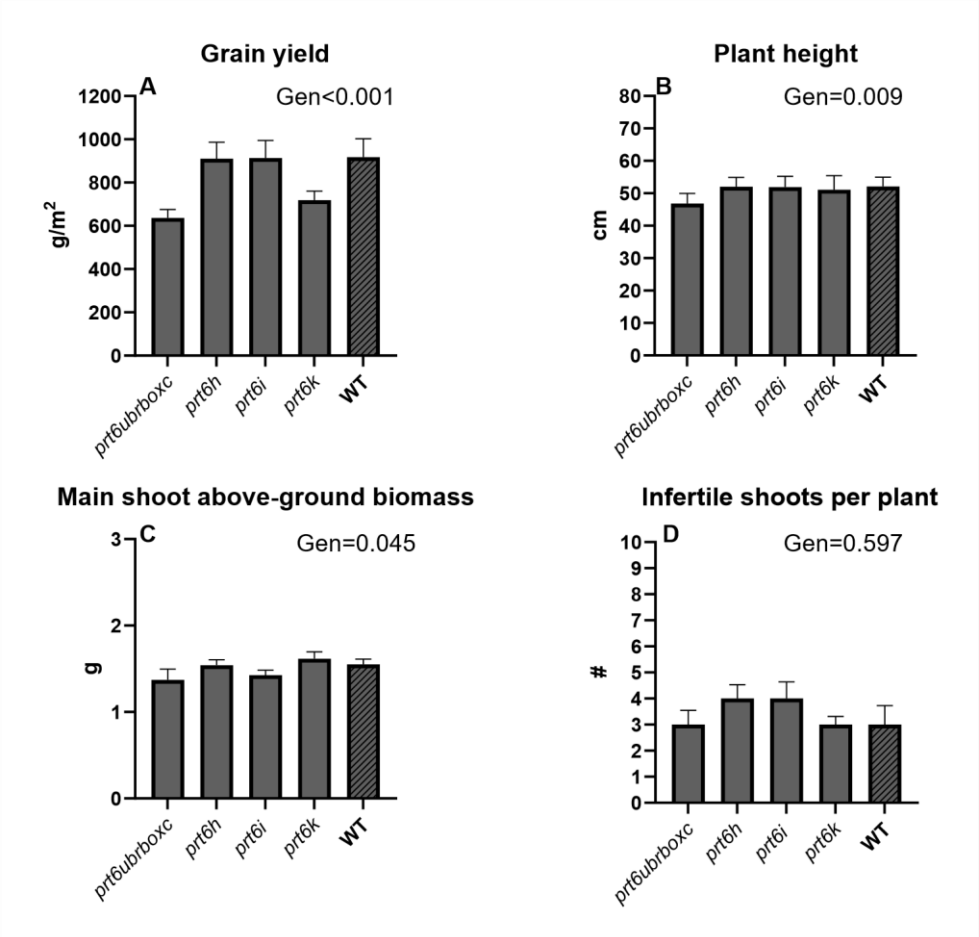

Figure 5.1. Mean across the 2 years for A) grain yield, B) plant height, C) biomass of main shoot at physiological maturity and D) infertile shoots per plant at physiological maturity**.** Error bars represent standard error of mean.

Above-ground biomass at physiological maturity did not show a genetic variation when considering the whole plant or the fertile tillers (**Appendix Fig. 5.1**). Spike length was measured at physiological maturity in two ways, including or not the awns (**Appendix Fig. 5.1**), only the measurement including the awns showed a significant genetic variation ($p < 0.001$). WT showed higher spike length (with awns) of 18.8 cm compared to *prt6k* at 16.5 cm.

The number of spikelets per ear did not show significant genetic variation. Normalized Difference Vegetation Index (NDVI) was measured from early vegetative stage to grain filling in each year (**Figure 5.2**). In this case, data are shown separately for each year. In 2022, during the vegetative stage, the WT and mutants performed similarly. However, from anthesis, *prt6k* decreased more rapidly compared to the WT and the other mutants. NDVI for *prt6i* was greater during the crop cycle than the WT. In 2023, NDVI for *prt6k* declined from its peak value more rapidly compared to the other mutants. *prt6k* canopy greenness was prolonged during grain filling compared to the WT. Results for each year showed a consistency in NDVI with regard to genotype differences; however, NDVI values were slightly higher in 2022 compared to 2023.

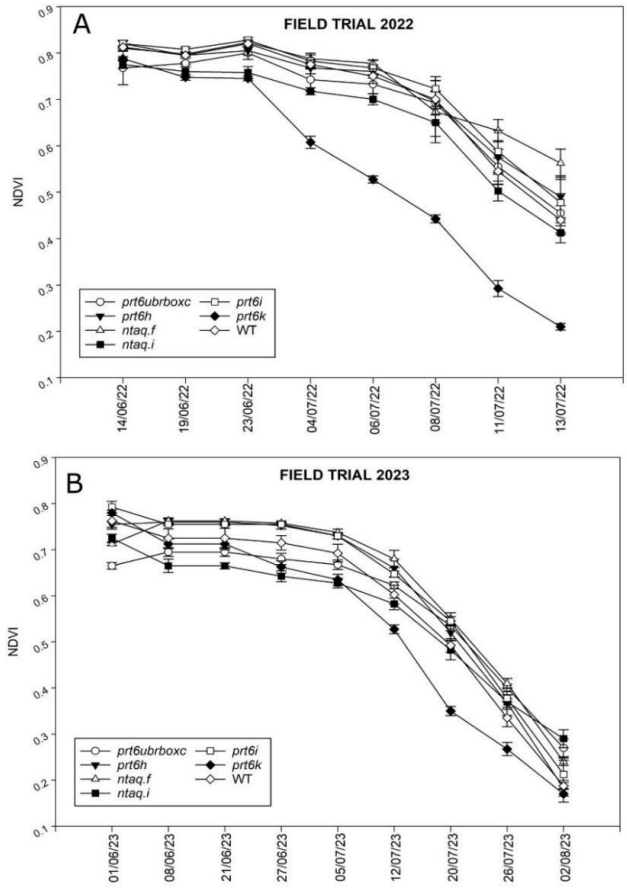

Figure 5.2 Normalized Difference Vegetation Index (NDVI) for WT Sebastian and three mutant lines of barley (*prt6k*, *prt6i*, *prt6ubrboxc*) for the PRT6 gene during grain filling in field trials in A) 2022 and B) 2023. Error bars represent the Standard Error of the Mean (SEM). Legends indicate the genotype for the barley PRT6 mutant lines and the Sebastian wildtype . NDVI values were used as a proxy for canopy greenness.

5.3.3 GHG fluxes

Soil-CO_2 fluxes differed among the WT and mutants in the field trial across the measurements taken during flowering-grain filling period ($p < 0.001$) (**Figure 5.3.A**). *prt6k* showed greater CO_2 fluxes than Sebastian (WT), 761.6 mg CO_2 m^{-2} h^{-1}, with a difference of 256.6 mg CO_2 m^{-2} h^{-1} between them. In contrast, prt6 ubrboxc had lower CO_2 than WT (353.4 mg CO_2 m^{-2} h^{-1}) and the mutant with the lowest psoil-CO_2 was *prt6 ubrboxc* with 45.1 mg CO_2 m^{-2} h^{-1} . Methane fluxes were negative and showed a similar pattern compared to the CO_2 fluxes, however, no

significant difference was found between the WT and mutants (**Figure 3.B**). Regarding N_2O fluxes, the mutant prt6k showed higher µg m^{-2} h^{-1} than the others (32.41 µg m^{-2} h^{-1}), followed by the WT (25.81 µg m^{-2} h^{-1}) and prt6ubrboxc (2.51 µg m^{-2} h^{-1}) (p = 0.008) (**Figure 5.3.C)**.

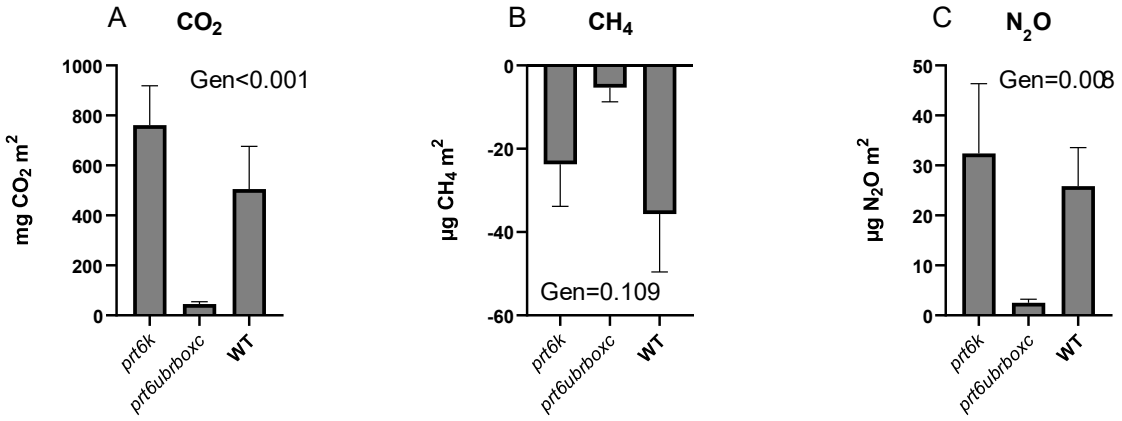

Figure 5.3 Fluxes of greenhouse gases (CO_2, CH_4, and N_2O; µmol m^{-2} h^{-1}) measured during the grain filling period in the 2023 field experiment for Sebastian WT and barley mutant lines (*prt6k*, *prt6i*, *prt6ubrboxc*) of the PRT6 gene. Values are displayed as means ± Standard Error of the Means (SEM). Statistical analysis was conducted using REML to assess genotype effects. Data provide insight into the environmental footprint of different barley lines.

5.4 Discussion

In this study, mutants were evaluated in the field over two years to evaluate how they perform in the UK environment. These mutants were also studied in glasshouse conditions to assess them under drought treatments (see **Chapter 4**). The study included several traits, e.g., physiological traits and soil green-house gas emissions. In some cases, experiments in control environments (glasshouse, growth-rooms) do not scale to the canopy and field performance. Therefore, this field study facilitated a more representative evaluation of the mutants and the relations and trade-offs between the traits under different conditions.

Across the two years, *prt6i* showed very similar grain yield to Sebastian (WT). Interestingly, taller mutants showed greater grain yield; e.g., *prt6ubrbox* was the smaller mutant with the lowest grain yield whereas the WT and *prt6i* were the taller mutants with higher grain yield. The mutations showed similar total above-ground biomass compared to the WT, however, significant differences were presented in the main shoot in which the higher biomass was shown in the WT and the *prt6i* and *prt6k* mutations. The differences in biomass can be explained by larger spikes in the mutants mentioned above. Differences in grain yield could be related to the differences in the peduncle and main shoot length in the main shoot in tall mutants, e.g. WT, *prt6i* and *prt6h* showed the higher main shoot length than the other mutants evaluated with a considerably higher grain yield compared to the WT. However, some research in wheat found that competition for assimilates during the "rapid spike growth" (from mid stem elongation to late anthesis) between stem and spike plays an important role in determining grain number (Slafer & Rawson, 1994). Nevertheless, some other possible mechanisms that could explain the present results are the conclusions found by Sierra-Gonzalez et al. (2021), where shorter stem internodes 2 and 3 allow more assimilates to be allocated to the spike and hence higher grain number is reached.

Mutants were tested in 2022 and 2023 in the field; however, there were meteorological differences across the two years, 2022 was a hotter summer with less rainfall whereas 2023 was colder with more rainfall during the season. The contrasting weather caused differences in NDVI during the two crop cycles. Mutants performed similarly relative to each other across the two years; however, in the first year due to lower rainfall mutants showed an early senescence compared to the second season. The *prt6i* mutant tended to stay green for longer

than the WT in both years. Interestingly, this mutant showed slightly higher grain yield in the study. These contrasting conditions allowed for a comparative analysis of mutant performance, revealing differences in the NDVI (Normalized Difference Vegetation Index) throughout the crop cycle. While the mutants generally performed similarly across both years, early senescence was observed in the first year due to insufficient rainfall. However, mutant *prt6i* exhibited delayed senescence compared to WT, which is associated with extended photosynthetic activity and increased assimilate accumulation during grain filling (Thomas & Howarth, 2000). This trait has been a target in breeding programmes for cereals like wheat and barley, as it can enhance grain yields under both optimal and stressed conditions (Gregorczyk et al., 2020).

Soil-gas emissions were evaluated three times in the field trial in 2023 from anthesis to the grain-filling period. Significant differences in the three gases were found among the mutants and WT. The *prt6k* mutation showed higher CO_2, CH_4 and N_20 whereas *prt6 ubrboxc* had the lowest values. Additionally, *prt6k* presented lower grain yield than WT and did not have greater grain concentrations of elements analysed in the glasshouse experiments in Chapter 4 if compared with WT and the other mutants. In this instance, a trade-off in *prt6k* was found in different traits; even if grain yield was not much compromised vs WT, growing *prt6k* may cause higher impact for global warming compared with the WT. This could imply that nitrate uptake was lower for *prt6k* compared the WT, possibly associated with greater percentage aerenchyma in root compared to the WT. However, there are other factors that should be considered. For example, soil respiration is influenced by soil temperature and soil moisture (Mi et al., 2018; Snyder et al., 2009). Measurements were taken during the summer when the crops reached anthesis-grain-filling; not many differences in soil temperature were observed in the experiments carried out. However, dry soil conditions prior to soil GHG measurements may have contributed to the negative soil fluxes for CH_4 in the present study, restricting the action of biogenic processes of methanogens (methane-emitting microorganisms), which are predominant in anaerobic conditions. Overall, however, N_2O emissions from agricultural soils (327 Tg CO_2 equivalents) are far more important than their sink function than is the case for CH_4 (6.3 Tg CO_2 equivalents). A study in organic barley found similar results in which N_20 was much higher due to wet soils during summer season. Other studies have published the influence of soil moisture and temperatures on GHG emissions (Mi et al., 2018; S. Wang et al.,

2016). Simionescu et al. (2019) explained that CO_2 and CH_4 reach high concentrations via respiration by root and microorganisms. It was also mentioned that the high CH_4 emissions occur because of anaerobic methane-producing bacteria (Simionescu et al., 2019). This complements our research, in which the mutant with lower root length (*prt6ubrbox*; root length data not shown) showed lower gas emissions in the field trial. However, a potential trade-off can be seen between a reduced impact of cereal production on greenhouse gas emissions and lower grain production in the present field experiments.

The observed trade-off between grain yield and GHG emissions, particularly in *prt6k*, highlights the broader agricultural challenge of balancing food production with environmental sustainability. While *prt6k* did not drastically reduce grain yield compared to WT, its higher GHG emissions suggest that more nuanced breeding approaches are required to address both productivity and environmental impact (Tilman et al., 2011). To mitigate the environmental footprint of high-yielding crops, sustainable agricultural practices, such as optimizing N-use efficiency, cover cropping, and reduced tillage, should be considered (Galloway et al., 2008).

These experiments provide critical insights into the performance of barley mutants under field conditions, emphasizing the importance of field trials in assessing both yield potential and environmental sustainability. The results underscore the complexity of balancing agronomic performance with environmental concerns, particularly in the context of climate change.

Future research should focus on the mechanisms underlying these trade-offs, especially in relation to soil interactions and microbial activity, to develop crop varieties that meet both food security and environmental sustainability goals.

Appendix

Appendix Table 5.1 Meteorological data during the crop trial in 2022 and 2023.

	Average Temp (ʃ)	Average Min Temp (ʃ)	Average Max Temp (ʃ)	Rainfall (mm)
2022:				
April	10.4	4.9	15.4	0.04
May	13.8	5.2	23.6	7.6
June	15.6	4.6	30.6	11.7
July	18.9	7.0	31.0	3.6
August	19.0	6.4	31.0	0.4
2023:				
April	10.4	7.6	13.7	30.6
May	12.4	7.9	16.6	22.8
June	16.4	11.4	21.6	43.6
July	16.1	12.3	19.9	38.8
August	17.0	12.9	21.3	14.5

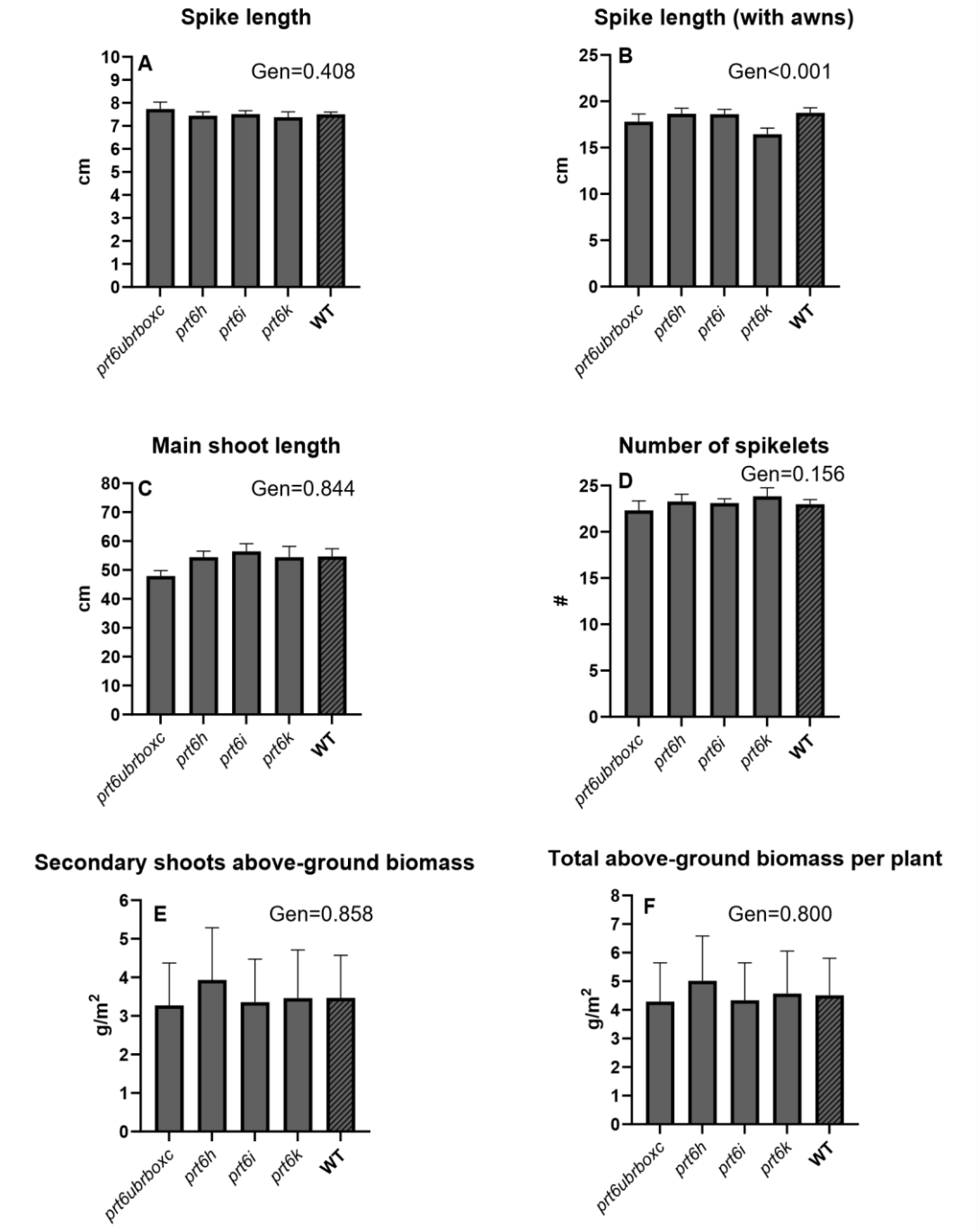

Appendix Figure 5.1. Histograms showing the genetic variation and standard error between WT and mutants across the 2 years data for: A) spike length (cm) B) spike length considering the awns length (cm), C) main shoot length (cm) and D) number of spikelets, E) above-ground biomass in secondary shoots at physiological maturity (g), F) Total above-ground biomass at physiological maturity (g). Measurements taken at physiological maturity. Error bars represent standard error of differences of the means (S.E.D).

Chapter 6: General Discussion

This general discussion aims to synthesize critically the major findings of the thesis in the context of the initial objectives and hypotheses outlined in **Chapter 1**. The study set out to investigate the anatomical and physiological mechanisms underpinning waterlogging and drought tolerance in wheat and barley, focusing particularly on the PRT6 N-degron pathway and its influence on root cortical senescence (RCS) and related root anatomical traits.

Specifically, the research sought to (1) characterize the genetic variation in RCS traits associated with three barley *prt6* mutant alleles under contrasting water logging and unstressed control regimes; (2) evaluate above-ground physiological traits and yield-related parameters in barley and wheat NIL lines under drought and well-watered conditions; and (3) assess the environmental and physiological performance of PRT6 barley mutants in the field, including greenhouse gas (GHG) fluxes. These objectives were formulated in response to key gaps in the literature regarding the role of the N-degron pathway in monocot stress responses, and the integration of root anatomy with agronomic performance under abiotic stress.

A primary challenge in crop improvement is ensuring optimal performance under abiotic stress conditions, exacerbated by climate change. This study evaluated multiple barley and wheat genotypes, including genetically mutated alleles lines, to investigate their physiological and morphological responses to waterlogging and drought. Across three separate studies, we explored the roles of root cortical senescence (RCS), aerenchyma formation, and biomass production in contributing to crop resilience under these abiotic stresses.

6.1 Review of project hypotheses

The study was guided by several hypotheses focused on the genetic variation in root cortical senescence (RCS) traits and how these traits interact with above-ground physiological responses and crop performance under abiotic stress conditions. The primary hypothesis was that allelic variation in PRT6 gene was associated with expression of the RCS traits, which would lead to enhanced resilience under waterlogging and drought conditions. Thus, it w*as hypothesized that the variation in the mutant lines for the PRT6 gene, prt6k, prt6i and prt6ubrboxc,* would correlate with the expression of RCS traits and ultimately influence

biomass, yield and yield components under waterlogged conditions (**Chapter 1**, Hypotheses 1 and 2) and droughted conditions (**Chapter 1**, Hypotheses 1 and 3) (Mendiondo et al., 2016 and Vicente et al 2017). Furthermore, it was hypothesized that the three near-isogenic lines introgressing genes from landraces would show favourable RCS traits to enhance water uptake, biomass and yield under droughted conditions compared to the wheat wild type Paragon (Chapter 1, objective 3). Understanding these genotype x environment interactions and how the effects of the three barley mutant alleles of PRT6 gene are expressed at the field scale and affect GHG emissions by the roots in the field (Chapter 1, Hypotheses 4 and 5) is central to determining the potential for breeding more resilient crop varieties (Reynolds et al., 2012).

6.2 The *PRT6* gene and Root Cortical Senescence (RCS) and aerenchyma formation. A central focus of these studies was the role of RCS, a form of programmed cell death found in root cortical cells, which leads to the formation of air spaces known as aerenchyma. It was hypothesised that root cortical senescence RCS and aerenchyma formation are vital adaptations under waterlogging and drought conditions, as they help improve root aeration and reduce metabolic costs by replacing living cells with air spaces (Colmer & Voesenek, 2009). This reduction in metabolic activity lowers the oxygen demand and nutrient consumption of root tissues, allowing plants to conserve energy and resources in suboptimal growing environments (Evans, 2004).

Under waterlogged conditions, the present results revealed that prt6 barley mutants, particularly *prt6i*, exhibited increased root cortical senescence (RCS) compared to wild-type (WT) plants. This enhanced RCS response suggests a potential mechanism contributing to the *prt6* mutants alleles improved resilience on water excess (low-oxygen environments) and water deficit (drought conditions) as well.

However, although increased aerenchyma area was observed in the waterlogging experiments the expected benefits in chlorophyll retention and shoot growth were not observed in this study. The development of aerenchyma and the increase in root crosssectional area under waterlogging, as seen in some of the *PRT6* mutants alleles, aligns with previous research indicating that aerenchyma formation is an adaptive response to facilitate gas exchange and improve root survival in hypoxic soils (Jackson and Armstrong, 1999).

Similarly, in the drought-focused experiments, increased aerenchyma formation was a common response across barley and wheat genotypes under drought, with some of the *PRT6* lines showing a greater increase in RCS compared to WT. This adaptation was particularly pronounced in the *prt6i* barley mutant allele, where enhanced RCS development likely contributed to better root aeration and reduced metabolic cost of roots (Lynch, 2013). However, it is important to note that increased RCS formation, while reducing root metabolic costs, could also reduce water transport efficiency, presenting a possible trade-off between conserving energy and maintaining hydraulic conductivity under drought stress (Henry et al., 2012).

6.3 RCS traits and biomass: Grain yield responses to abiotic stress

Interestingly, while aerenchyma formation and RCS may be beneficial for root adaptations, the present findings suggested that these traits alone are not sufficient to explain the full extent of drought or waterlogging tolerance. Instead, it appeared a combination of factors, including root structure, plant height, photosynthetic efficiency, and the ability to retain chlorophyl, contributed to overall plant performance. The reduction in cortex cell area (CCA) observed under drought conditions highlights a strategic shift to conserve energy by minimizing root respiration, allowing carbohydrates to be redirected toward essential physiological functions (Henry et al., 2012).

The field experiments also revealed the complex relationship between biomass production, plant height and grain yield under stress conditions. For instance, under waterlogged or drought conditions, *PRT6* mutants did not demonstrate significant improvements in biomass retention or chlorophyll content compared to the WT, contrary to previous studies (Mendiondo et al., 2016) performance in Control Environment Room (CER). However, when evaluating the above-ground biomass in field conditions, some mutants displayed enhanced biomass production, suggesting that RCS and aerenchyma formation might have facilitated better nutrient uptake and root capacity at the field scale (Reynolds et al., 2012).

In field trials, taller genotypes generally produced higher grain yields, reinforcing the well documented relationship between plant height and yield potential (Reynolds et al., 2012). This observation was more generally consistent across both waterlogged and drought conditions,

where taller plants tended exhibited larger spikes and higher biomass accumulation. In contrast, shorter mutants, such as *prt6ubrboxc,* had reduced grain yields and biomass, confirming the importance of plant stature in optimizing yield under stress.

6.4 Soil Greenhouse gas emissions and environmental Sustainability

A novel aspect of this study was the evaluation of soil greenhouse gas (GHG) emissions in the field experiments, particularly in relation to the trade-off between crop productivity and environmental impact. The results revealed significant differences in CO_2, CH_4, and N_2O emissions between the barley mutants alleles and WT, with the *prt6k* allele producing the highest emissions than WT for CO_2 and N_2O although less for CH_4. This observation suggests that while *prt6k* did not drastically reduce grain yield, its higher GHG emissions pose a potential environmental concern. The relationship between soil moisture, microbial activity, and GHG emissions has been well established (Snyder et al., 2009; Mi et al., 2018), and these findings emphasize the need for breeding programs to consider not only yield potential but also the environmental footprint of crop.

Reducing GHG emissions from agricultural soils is essential for mitigating climate change, and the identification of genotypes such as *prt6 ubrbox*, which had lower emissions, could provide valuable insights for developing more sustainable crop varieties. Interestingly, we hypothesized that the *prt6 ubrbox* allele carries a significant mutation within the UBR BOX domain. This domain is crucial for the PRT6 E3 ligase to interact with and destabilize target substrates under normal conditions. While the identification and manipulation of PRT6 N-degron substrates are beyond the scope of this project, Mendiondo's lab has identified several GVII-ERFs as substrates *in vitro* in barley, including BERF and RAF (Alasami, unpublished). BERF1 and RAF are well-established regulators of plant stress responses. For example, ectopic expression of *RAF* in *A. thaliana* promotes resistance to *Ralstonia solanacearum* and enhances tolerance to salt stress (Jung et al., 2007). *BERF1* is involved in the ethylene-mediated fine-tuning of *knox3 (Bkn3*) and is expressed in root tissue in barley (Osnato et al., 2010). Schneider *et al.* (2018) demonstrated the upregulation of *RAF* and *BERF1* in a transcriptional analysis, highlighting their importance in root cortical senescence (RCS) development. These results highlight the broader challenge of balancing food production with environmental

sustainability, particularly as agriculture seeks to meet the demands of a growing global population while minimizing its ecological impact**.**

6.5 Scaling controlled environment and glasshouse results to the field

In the controlled environments and glasshouse experiments, the traits were studied at the individual plant level, whereas in the field they were studied at the crop level (a population of plants). Therefore, some traits which are measured at a population level in the field such as biomass per m^2 may not correlate well to the biomass of a single plant in the glasshouse. However, single shoot traits which are measured in the controlled environment, glasshouse and field may scale across the different experiments better. One of the benefits of performing a CE or glasshouse experiment is potentially a more precise estimation of the genetic variation with a more uniform environmental background. In the present experiments it is encouraging that the differences among the genotypes in the RCS traits, such as percentage aerenchyma, were consistently observed across experiments and did scale between the controlled environment and glasshouse experiments. The RCS traits were not measured in the field experiments (**Table 6.1 and 6.2**).

Table 6.1 Summary of glasshouse and field experiments results

Variable	Glasshouse Results	Field Results	Comments	Academic References
Grain Yield	Mutants *prt6i* performed similarly to WT; prt6ubroxc showed lower yield	Mutants *prt6i* : prt6ubrbox showed lower yield	Genetic performance for grain yield is consistent across both environments, suggesting stable genetic performance in mutants.	Pang et al. (2004); Setter et al. (2003)
Plant Height (cm)	No significant differences in plant height among most mutants	Mutant *prt6 ubrbox* showed lower height: 46.8 cm	The field experiment showed lower plant height for prt6ubrbox, indicating this trait might be more environment-sensitive.	Rajhi et al. (2011); Setter et al. (1999)
Biomass (g)	*prt6k* showed the greatest biomass (1.62 g)	*prt6k* also had higher biomass in field experiments	Biomass results across environments reinforces the genetic advantage of prt6k under waterlogged or stressed conditions.	Colmer (2003); Yamauchi et al. (2017)
Infertile Shoots	3–4 infertile shoots per plant, no significant difference	Consistent infertile shoots across all genotypes in field trials	Infertile shoot results are stable across environments, indicating no significant genotype-environment interaction.	Visser et al. (1995)
NDVI (Normalized Difference Vegetation Index)	Consistency in NDVI across two years; prt6k dropped significantly during the crop cycle	Consistent NDVI patterns over two years. prt6i outperformed WT in terms of green canopy retention	NDVI variability underlines the dynamic responses to environmental factors, especially during later growth stages.	Qi et al. (2019); Yamauchi et al. (2017)

Table 6.2 Summary of root cortical senescence trait responses across experiments (values represent means of three barley mutant genotypes and WT Sebastian)

RCS Trait responses	Greenhouse (well watered) to stress	Greenhouse (Drought)	Controlled Env (Control)	Controlled Env (Waterlogging)	Comment
AA mm²	0.1	0.15	0.0053	0.0314	AA shows a slightly higher increase in under WL, suggesting better adaptability to waterlogging. This is consistent with the findings of Colmer (2003) and Pang et al. (2004), which indicated positive effects on aerenchyma formation under stress in environments (Mano et al., 2008; Rajhi et al., 2011).
CCA mm²	0.245	0.145	0.3276	0.9945	CCA values are consistent but show slightly higher response under WL, suggesting that controlled environments may favour cortical cell area expansion. This aligns with findings from Setter et al. (2003) and Rajhi et al. (2011) on cell area expansion under water stress.
percCisA %	12.5	19.2	1.79	15.8	percCisA shows a greater increase in under WL than drought, indicating stronger root senescence response under waterlogging. This matches findings by Yamauchi et al. (2017) and Setter et al. (2003), which highlighted enhanced root senescence in controlled conditions.
percSisMX %	7.2	8.4	8.9	10.1	percSisMX exhibits minor variations across abiotic stress environments. This is similar to results observed by Yamauchi et al. (2017) and Qi et al. (2019), where metaxylem formation was slightly enhanced under controlled waterlogged conditions.
TCA mm²	0.108	0.059	0.221	0.228	TCA shows marginal differences, with controlled environments slightly favoring cortex restriction under water stress. This observation is supported by Kreuzwieser and Rennenberg (2014) and Yu et al. (2019), who found that cortex area tends to expand under waterlogged stress.
TSA mm²	0.015	0.012	0.035	0.042	TSA showed small inconsistent effects across both stress environments.

6.6 Future work

6.4.1 Validation of results across a wider range of genotypes and environments

Future studies should focus on validating the effects of the *PRT6* mutant alleles across a broader spectrum of environmental conditions and genotypes, including barley germplasm collections and breeding panels from various regions worldwide. This will help to ensure that the observed effects are not limited to a specific genetic background and are applicable to a diverse range of barley varieties. Additionally, testing these mutant alleles under a wider range of environmental conditions, such as different climates, soil types, and water availability scenarios, is crucial to assess their stability and effectiveness in enhancing stress tolerance across diverse agro-ecological zones. This approach will provide a more comprehensive understanding of the potential applications of *PRT6* mutant alleles in barley improvement programs globally.

6.4.2 Application of RCS Traits and *PRT6* mutant alleles in plant breeding for waterlogging and drought Tolerance

The integration of RCS traits and PRT6 mutant alleles into breeding programs holds significant promise for improving both waterlogging and drought tolerance in crops. Integrating RCS into breeding programs can improve water and nutrient use efficiency by reducing metabolic costs associated with maintaining non-essential root tissues. By promoting more efficient root systems, RCS can help crops like barley or wheat better adapt to resource-limited environments, ultimately improving yield stability and sustainability. Plant breeders could leverage molecular markers linked to these favourable alleles to facilitate marker-assisted selection (MAS), enabling the efficient identification of plants with enhanced root aeration, water retention, and stress signalling pathways. By incorporating these traits into breeding pipelines, it would be possible to develop barley varieties with greater resilience to waterlogging and drought, supporting more sustainable crop production in regions susceptible to these stresses. Utilising molecular markers for RCS traits in marker-assisted selection (MAS) could accelerate the development of stress-tolerant cultivars, particularly when combined with modern genomic tools like GWAS and genomic selection, leading to more robust crop varieties capable of withstanding diverse environmental challenges.

Conclusion

Overall, the findings from these studies underscore the complexity of plant responses to abiotic stress and the importance of integrating multiple traits, such as root cortical senescence, aerenchyma formation, plant height, biomass production, and soil GHG emissions, when evaluating crop performance. While RCS and aerenchyma formation are vital adaptations under both waterlogged and drought conditions, they must be considered in conjunction with other physiological and morphological traits to develop truly resilient crop varieties.

These insights are critical for breeding programs aimed at improving crop tolerance to abiotic stress. The potential trade-offs between yield, water transport efficiency, and environmental impact must be carefully managed to achieve both food security and sustainability. Future research should explore the genetic and physiological mechanisms underlying these adaptations, particularly in relation to the N-degron pathway and hormonal signalling, to enhance our understanding of how crops can be optimized for growth under increasingly challenging environmental conditions.

In addressing the above objectives, the research provides nuanced insights into the functional role of the *PRT6* gene in mediating anatomical and physiological stress responses. The results demonstrated that prt6 alleles exhibit consistent effects on RCS traits across stress environments, particularly in enhancing aerenchyma development. However, these anatomical advantages did not universally translate into improved shoot growth, biomass accumulation, or yield, indicating that the benefits of enhanced RCS are highly context-dependent and influenced by additional physiological factors.

Importantly, the wheat NIL lines exhibited differential above-ground responses to drought without clear corresponding changes in root anatomy, suggesting species-specific mechanisms of drought tolerance. In field conditions, prt6k mutants showed modest improvements in biomass and heightened GHG emissions, highlighting the importance of assessing trade-offs between productivity and environmental sustainability.

Overall, this thesis supports the hypothesis that the PRT6 N-degron pathway is a significant regulatory node in stress adaptation in cereals. However, the evidence also points to the complexity of translating root anatomical traits into agronomic benefits. Future studies

incorporating molecular validation, transcriptomic analysis, and multi-season field trials will be critical to fully harness the breeding potential of *PRT6* alleles. The integration of root anatomical phenotypes with holistic plant performance metrics remains a promising but challenging frontier in the development of climate-resilient crops.

7. References

Achard, P., et al. (2006). Integration of plant responses to environmentally activated phytohormonal signals. *Science, 311*(5757), 91–94. https://doi.org/10.1126/science.1118642

Ahmed, F., Rai, M., Ismail, M. R., Juraimi, A. S., Rahim, H. A., Asfaliza, R., & Latif, M. A. (2013). Waterlogging tolerance of crops: Breeding, mechanism of tolerance, molecular approaches, and future prospects. *BioMed Research International, 2013*, Article ID 963525. https://doi.org/10.1155/2013/963525

Allah Wasaya, Zhang, X., Fang, Q., & Yan, Z. (2018). Root phenotyping for drought tolerance: A review. *Agronomy, 8*(11), 241. https://doi.org/10.3390/agronomy8110241

Alskaf, K., Mooney, S. J., Sparkes, D. L., Wilson, P., & Sjögersten, S. (2021). Short-term impacts of different tillage practices and plant residue retention on soil physical properties and greenhouse gas emissions. *Soil & Tillage Research, 206*, 104803. https://doi.org/10.1016/j.still.2020.104803

Askarnejad, M., Soleymani, A., & Javanmard, H. (2021). Barley (*Hordeum vulgare* L.) physiology including nutrient uptake affected by plant growth regulators under field drought conditions. *Journal of Plant Nutrition, 44*(1), 1–17. https://doi.org/10.1080/01904167.2021.1889593

Bailey-Serres, J., & Voesenek, L. A. C. J. (2008). Flooding stress: Acclimations and genetic diversity. *Annual Review of Plant Biology, 59*, 313–339. https://doi.org/10.1146/annurev.arplant.59.032607.092752

Bailey-Serres, J., Fukao, T., Gibbs, D. J., Holdsworth, M. J., Lee, S. C., Licausi, F., Perata, P., Voesenek, L. A. C. J., & van Dongen, J. T. (2012). Making sense of low oxygen sensing. *Trends in Plant Science, 17*(3), 129–138. https://doi.org/10.1016/j.tplants.2011.12.004

Bailey-Serres, J., Lee, S. C., & Brinton, E. (2012). Waterproofing crops: Effective flooding survival strategies. *Plant Physiology, 160*(4), 1698–1709. https://doi.org/10.1104/pp.112.208173

Bailey-Serres, J., et al. (2012). Plant responses to flooding stress. *Plant Physiology, 160*(4), 1698–1709. https://doi.org/10.1104/pp.112.201715

Baker, N. R., & Rosenqvist, E. (2004). Applications of chlorophyll fluorescence can improve crop production strategies: An examination of future possibilities. *Journal of Experimental Botany, 55*(403), 1607–1621. https://doi.org/10.1093/jxb/erh196

Bakker, D., Hamilton, G., Houlbrooke, D., & Spann, C. (2005). The effect of raised beds on soil structure, waterlogging, and productivity on duplex soils in Western Australia. *Soil Research, 43*(5), 575–585. https://doi.org/10.1071/SR03118

Ball, B. C. (2013). Soil structure and greenhouse gas emissions: A synthesis of 20 years of experimentation. *European Journal of Soil Science, 64*(3), 357–373. https://doi.org/10.1111/ejss.12013

Barnabás, B., Jäger, K., & Fehér, A. (2008). The effect of drought and heat stress on reproductive processes in cereals. *Plant, Cell & Environment, 31*(1), 11–38. https://doi.org/10.1111/j.1365-3040.2007.01727.x

Bindraban, P. S., Stoorvogel, J. J., Jansen, D. M., Vlaming, J., & Groot, J. J. R. (2012). Assessing the impact of soil degradation on food production. *Current Opinion in Environmental Sustainability, 4*(5), 478–485. https://doi.org/10.1016/j.cosust.2012.09.015

Bita, C. E., & Gerats, T. (2013). Plant tolerance to high temperature in a changing environment: Scientific fundamentals and production of heat stress-tolerant crops. *Frontiers in Plant Science, 4*, 273. https://doi.org/10.3389/fpls.2013.00273

Blum, A. (2011). *Plant breeding for water-limited environments*. Springer. https://doi.org/10.1007/978-1-4419-7491-4

Blum, A. (2011). Drought resistance—is it really a complex trait? *Functional Plant Biology, 38*(10), 753–757. https://doi.org/10.1071/FP11101

Bos, M. G., & Boers, T. M. (1994). Land drainage: Why and how? In H. P. Ritzema (Ed.), *Drainage principles and applications* (pp. 23–32). International Institute for Land Reclamation & Improvement.

Boudiar, R., Cabeza, A., Fernández-Calleja, M., Pérez-Torres, A., Casas, A. M., González, J. M., Mekhlouf, A., & Igartua, E. (2021). Root trait diversity in field-grown durum wheat and comparison with seedlings. *Agronomy, 11*(12), 2545. https://doi.org/10.3390/agronomy11122545

Boyer, J. S., et al. (2013). Global food security: Perspectives from science and policy. *Global Food Security, 2*(3), 139–143. https://doi.org/10.1016/j.gfs.2013.08.002

Burton, A. L., Brown, K. M., & Lynch, J. P. (2013). Phenotypic diversity of root anatomical and architectural traits in *Zea* species. *Crop Science, 53*(3), 1042–1055. https://doi.org/10.2135/cropsci2012.07.0440

Caldelas, C., Rezzouk, F. Z., Aparicio Gutiérrez, N., Diez–Fraile, M. C., & Araus Ortega, J. L. (2023). Interaction of genotype, water availability, and nitrogen fertilization on the mineral content of wheat grain. *Food Chemistry, 404*, 134565. https://doi.org/10.1016/j.foodchem.2022.134565

Chandio, A. S., Lee, T. S., & Mirjat, M. S. (2013). Simulation of horizontal and vertical drainage systems to combat waterlogging problems along the Rohri Canal in Khairpur District, Pakistan. *Journal of Irrigation and Drainage Engineering, 139*(9), 710–717. https://doi.org/10.1061/(ASCE)IR.1943-4774.0000590

Chapman, S. R., & Carter, L. P. (1976). *Barley*. In *Crop production principles and practices* (pp. 311–323). W. H. Freeman and Company. ISBN: 0-7167-0581-8

Chataut, G., et al. (2023). Greenhouse gas emissions from agricultural soil: A review. *Journal of Agriculture and Food Research, 11*, 100533. https://doi.org/10.1016/j.jafr.2023.100533

Chen, Y., Palta, J., Prasad, P. V. V., et al. (2020). Phenotypic variability in bread wheat root systems at the early vegetative stage. *BMC Plant Biology, 20*, 185. https://doi.org/10.1186/s12870-020-02390-8

Chimungu, J. G., Brown, K. M., & Lynch, J. P. (2014). Large root cortical cell size improves drought tolerance in maize. *Plant Physiology, 166*(4), 2166–2178. https://doi.org/10.1104/pp.114.250449

Colmer, T. D. (2003). Long-distance transport of gases in plants: A perspective on internal aeration and radial oxygen loss from roots. *Plant, Cell & Environment, 26*(1), 17–36. https://doi.org/10.1046/j.1365-3040.2003.00991.x

Colmer, T. D., & Voesenek, L. A. C. J. (2009). Flooding tolerance: Suites of plant traits in variable environments. *Functional Plant Biology, 36*(8), 665–681. https://doi.org/10.1071/FP09144

Comas, L., Becker, S., Cruz, V. M., Byrne, P. F., & Dierig, D. A. (2013). Root traits contributing to plant productivity under drought. *Frontiers in Plant Science, 4*, 442. https://doi.org/10.3389/fpls.2013.00442

Conrad, R. (2009). The global methane cycle: Recent advances in understanding the microbial processes involved. *Environmental Microbiology Reports, 1*(5), 285–292. https://doi.org/10.1111/j.1758-2229.2009.00038.x

Daszkowska-Golec, A., et al. (2019). Genetic and physiological dissection of photosynthesis in barley exposed to drought stress. *International Journal of Molecular Sciences, 20*(24), 6341. https://doi.org/10.3390/ijms20246341

Díaz, A. S., Aguiar, G. M., Pereira, M. P., et al. (2018). Aerenchyma development in different root zones of maize genotypes under water limitation and different phosphorus nutrition. *Biologia Plantarum, 62*(3), 561–568. https://doi.org/10.1007/s10535-018-0773-8

Dissmeyer, N. (2019). Conditional protein function via N-degron pathway–mediated proteostasis in stress physiology. *Annual Review of Plant Biology, 70*, 83–117. https://doi.org/10.1146/annurev-arplant-050718-095937

Dutta, C., & Sarma, R. N. (2022). Role of root traits and root phenotyping in drought tolerance. *International Journal of Environment and Climate Change, 12*, 1–14.

Evans, D. E. (2004). Aerenchyma formation. *New Phytologist, 161*(1), 35–49. https://doi.org/10.1046/j.1469-8137.2003.00907.x

Fahad, S., Bajwa, A. A., Nazir, U., Anjum, S. A., Farooq, A., Zohaib, A., Sadia, S., Nasim, W., Adkins, S., Saud, S., Ihsan, M. Z., Alharby, H., Wu, C., Wang, D., & Huang, J. (2017). Crop production under drought and heat stress: Plant responses and management options. *Frontiers in Plant Science, 8*, 1147. https://doi.org/10.3389/fpls.2017.01147

Fahad, S., et al. (2019). Crop production under drought and heat stress: Plant responses and management options. *Frontiers in Plant Science, 10*, 1147. https://doi.org/10.3389/fpls.2019.01147

Fan, X., et al. (2021). Cross-talks between macro- and micronutrient uptake and signaling in plants. *Frontiers in Plant Science, 12*, 663477. https://doi.org/10.3389/fpls.2021.663477

Farooq, M., Wahid, A., Kobayashi, N., Fujita, D., & Basra, S. M. A. (2009). Plant drought stress: Effects, mechanisms and management. *Agronomy for Sustainable Development, 29*(1), 185–212. https://doi.org/10.1051/agro:2008021

Fischer, R. A., & Turner, N. C. (1978). Plant productivity in the arid and semiarid zones. *Annual Review of Plant Physiology, 29*, 277–317. https://doi.org/10.1146/annurev.pp.29.060178.001425

Forster, B. P., et al. (2004). Genotype and phenotype associations with drought tolerance in barley tested in North Africa. *Annals of Applied Biology, 144*(2), 157–168. https://doi.org/10.1111/j.1744-7348.2004.tb00329.x

Francia, E., et al. (2013). Determinants of barley grain yield in drought-prone Mediterranean environments. *Italian Journal of Agronomy, 8*(1), e1. https://doi.org/10.4081/ija.2013.e1

Furtak, K., & Wolińska, A. (2023). The impact of extreme weather events as a consequence of climate change on soil moisture and on the quality of the soil environment and agriculture – A review. *CATENA, 231*, 107378. https://doi.org/10.1016/j.catena.2023.107378

Gibbs, D. J., Bailey, M., Tedds, H. M., & Holdsworth, M. J. (2016). From start to finish: Amino-terminal protein modifications as degradation signals in plants. *New Phytologist, 211*(4), 1188–1194. https://doi.org/10.1111/nph.14047

Gibbs, D. J., Lee, S. C., Isa, N. M., Gramuglia, S., Fukao, T., Bassel, G. W., Correia, C. S., Corbineau, F., Theodoulou, F. L., Bailey-Serres, J., & Holdsworth, M. J. (2011). Homeostatic response to hypoxia is regulated by the N-end rule pathway in plants. *Nature, 479*(7373), 415–418. https://doi.org/10.1038/nature10534

Gibbs, D. J., et al. (2014). N-end rule pathway components in Arabidopsis control the hypoxic response via regulatory oxygen sensing. *Molecular Cell, 53*(3), 369–379. https://doi.org/10.1016/j.molcel.2013.12.020

Gibbs, D. J., et al. (2014). Oxygen-dependent proteolysis regulates the hypoxic response in *Arabidopsis thaliana*. *Trends in Cell Biology, 24*(11), 603–611. https://doi.org/10.1016/j.tcb.2014.07.005

Giuntoli, B., & Perata, P. (2018). Group VII ethylene response factors in Arabidopsis: Regulation and physiological roles. *Plant Physiology, 176*(2), 1143–1155. https://doi.org/10.1104/pp.17.01783

Gourdji, S. M., et al. (2013). An assessment of climate change impacts on crop productivity using the DSSAT-CERES-Wheat model. *Environmental Research Letters, 8*(2), 024041. https://doi.org/10.1088/1748-9326/8/2/024041

Hacke, U. G., Sperry, J. S., Wheeler, J. K., & Castro, L. (2006). Scaling of angiosperm xylem structure with safety and efficiency. *Tree Physiology, 26*(6), 689–701. https://doi.org/10.1093/treephys/26.6.689

Harwood, J. (2016). *Biotechnology of major cereals*. CAB International.

Henry, A., & Lynch, J. P. (2012). Root architecture and plant productivity in response to drought stress: Optimizing root water uptake. *Plant Physiology, 160*(4), 1706–1719. https://doi.org/10.1104/pp.112.202230

Henry, A., Gowda, V. R. P., Torres, R. O., McNally, K. L., & Serraj, R. (2012). Variation in root system architecture and drought response in rice (*Oryza sativa*): Phenotyping of the OryzaSNP panel in rainfed lowland fields. *Field Crops Research, 120*(2), 205–214. https://doi.org/10.1016/j.fcr.2010.07.002

Henry, R. J., et al. (2020). Genomic approaches to enhancing stress tolerance for food security in the face of climate change. *Plant Biotechnology Journal, 18*(8), 1676–1685. https://doi.org/10.1111/pbi.13348

Hirabayashi, Y., et al. (2013). Global flood risk under climate change. *Nature Climate Change, 3*(9), 816–821. https://doi.org/10.1038/nclimate1911

Holdsworth, M. J., Vicente, J., Sharma, G., & Abbas, M. (2020). The plant N-degron pathways of ubiquitin-mediated proteolysis. *Journal of Integrative Plant Biology, 62*(1), 70–89. https://doi.org/10.1111/jipb.12882

Holdsworth, M. J., Gibbs, D. J., & Vicente, J. (2019). Regulation of plant developmental processes by the ubiquitin-proteasome system. *Journal of Experimental Botany, 70*(15), 3727–3745. https://doi.org/10.1093/jxb/erz209

Hörtensteiner, S., & Feller, U. (2002). Nitrogen metabolism and remobilization during senescence. *Journal of Experimental Botany, 53*(370), 927–937. https://doi.org/10.1093/jexbot/53.370.927

Hossain, M. A., et al. (2019). Plant responses to hypoxia—Is survival a balancing act? *Trends in Plant Science, 24*(9), 813–825. https://doi.org/10.1016/j.tplants.2019.06.006

Jackson, M. B., & Armstrong, W. (1999). Formation of aerenchyma and the processes of plant adaptation to soil waterlogging. *Journal of Experimental Botany, 50*(337), 445–455. https://doi.org/10.1093/jxb/50.337.449

Jaramillo, R. E., Nord, E. A., Chimungu, J. G., Brown, K. M., & Lynch, J. P. (2013). Root cortical traits for improved water and nutrient acquisition: Physiological and genetic strategies. *Journal of Experimental Botany, 64*(12), 3559–3572. https://doi.org/10.1093/jxb/ert208

Joshi, A. K., Crossa, J., Arun, B., Chand, R., Trethowan, R., Vargas, M., & Ortiz-Monasterio, I. (2010). Genotype × environment interaction for zinc and iron concentration of wheat grain in eastern Gangetic plains of India. *Field Crops Research, 116*(3), 268–277. https://doi.org/10.1016/j.fcr.2010.01.004

Jung, Y., Park, K., Jensen, K. H., Kim, W., & Kim, H. Y. (2019). A design principle of root length distribution of plants. *Journal of the Royal Society Interface, 16*(150), 20190556. https://doi.org/10.1098/rsif.2019.0556

Kant, S., et al. (2017). Nitrogen nutrition impacts on yield and protein concentration in wheat. *Crop Science, 57*(1), 327–331. https://doi.org/10.2135/cropsci2016.02.0112

Kaur, G., Singh, G., Motavalli, P. P., Nelson, K. A., Orlowski, J. M., & Golden, B. R. (2020). Impacts and management strategies for crop production in waterlogged or flooded soils: A review. *Agronomy Journal, 112*(3), 1476–1501. https://doi.org/10.1002/agj2.20093

Kim, J., et al. (2020). CRISPR/Cas9: A novel weapon in the arsenal to combat plant diseases. *Frontiers in Plant Science, 11*, 40. https://doi.org/10.3389/fpls.2020.00040

Klein, S. P., Schneider, H. M., Perkins, A. C., Brown, K. M., & Lynch, J. P. (2020). Multiple integrated root phenotypes are associated with improved drought tolerance. *Plant Physiology, 183*(3), 1011–1025. https://doi.org/10.1104/pp.20.00211

Kozlic, A., Winter, N., Telser, T., Reimann, J., Rose, K., Nehlin, L., Berckhan, S., Sharma, G., Dambire, C., Boeckx, T., Holdsworth, M. J., & Bachmair, A. (2022). A yeast-based functional assay to study plant N-degron–N-recognin interactions. *Frontiers in Plant Science, 12*, 806129. https://doi.org/10.3389/fpls.2021.806129

Lan, Y., Kuktaite, R., Chawade, A., & Johansson, E. (2024). Chasing high and stable wheat grain mineral content: Mining diverse spring genotypes under induced drought stress. *PLOS ONE, 19*(2), e0298350. https://doi.org/10.1371/journal.pone.0298350

Lesmes-Vesga, R. A., Cano, L. M., Ritenour, M. A., Sarkhosh, A., Chaparro, J. X., & Rossi, L. (2023). Variation in the root system architecture of peach × (peach × almond) backcrosses. *Plants, 12*(9), 1874. https://doi.org/10.3390/plants12091874

Li, X., et al. (2021). Genetic modification for plant adaptation to flooding stress. *Current Opinion in Plant Biology, 56*, 124–130. https://doi.org/10.1016/j.pbi.2020.11.002

Licausi, F., Kosmacz, M., Weits, D. A., Giuntoli, B., Giorgi, F. M., Voesenek, L. A. C. J., Perata, P., & van Dongen, J. T. (2011). Oxygen sensing in plants is mediated by an N-end rule pathway for protein destabilization. *Nature, 479*(7373), 419–422. https://doi.org/10.1038/nature10536

Loreti, E., et al. (2016). Gibberellins, jasmonate, and abscisic acid modulate the response of plants to submergence and drought. *Frontiers in Plant Science, 7*, 1451. https://doi.org/10.3389/fpls.2016.01451

Lynch, J. P. (2013). Steep, cheap and deep: An ideotype to optimize water and N acquisition by maize root systems. *Annals of Botany, 112*(2), 347–357. https://doi.org/10.1093/aob/mcs293

Lynch, J. P., Chimungu, J. G., & Brown, K. M. (2014). Root anatomical phenes associated with water acquisition from drying soil: Targets for crop improvement. *Journal of Experimental Botany, 65*(21), 6155–6166. https://doi.org/10.1093/jxb/eru162

Lynch, J. P., Strock, C. F., Schneider, H. M., et al. (2021). Root anatomy and soil resource capture. *Plant and Soil, 466*(1), 21–63. https://doi.org/10.1007/s11104-021-05010-y

Mahmoud, A. W. M., Hassan, A. Z. A., Mottaleb, S. A., Rowezak, M. M., & Salama, A. M. (2021). The role of nano-silicon and other soil conditioners in improving physiology and yield of drought-stressed barley crop. *Agriculture (Pol'nohospodárstvo), 67*(3), 124–143. https://doi.org/10.2478/agri-2021-0012

Manik, S. M. N., Pengilley, G., Dean, G., Field, B., Shabala, S., & Zhou, M. (2019). Soil and crop management practices to minimize the impact of waterlogging on crop productivity. *Frontiers in Plant Science, 10*, 140. https://doi.org/10.3389/fpls.2019.00140

Mendiondo, G. M., Gibbs, D. J., Szurman-Zubrzycka, M., Korn, A., Marquez, J., Szarejko, I., Maluszynski, M., & Holdsworth, M. J. (2016). Enhanced waterlogging tolerance in barley by manipulation of the N-end rule pathway. *Plant Biotechnology Journal, 14*(1), 40–50. https://doi.org/10.1111/pbi.12334

Mendiondo, G. M., Gibbs, D. J., Szurman-Zubrzycka, M., & Holdsworth, M. J. (2016). Drought tolerance and crop growth enhancement by N-degron pathway-mediated plant signaling. *Nature Biotechnology, 34*(1), 73–78. https://doi.org/10.1038/nbt.3415

Mi, N., Bai, H., & Liang, C. (2018). Effects of waterlogging stress on greenhouse gas emissions from agricultural soils. *Agricultural and Forest Meteorology, 252*, 1–10. https://doi.org/10.1016/j.agrformet.2018.01.012

Moore, F. C., & Lobell, D. B. (2015). The fingerprint of climate trends on European crop yields. *Proceedings of the National Academy of Sciences, 112*(9), 2670–2675. https://doi.org/10.1073/pnas.1409606112

Paez-Garcia, A., Motes, C. M., Scheible, W. R., Chen, R., Blancaflor, E. B., & Monteros, M. J. (2015). Root traits and phenotyping strategies for plant improvement. *Plants, 4*(2), 334–355. https://doi.org/10.3390/plants4020334

Pais, I. P., Moreira, R., Semedo, J. N., Ramalho, J. C., Lidon, F. C., Coutinho, J., Maçãs, B., & Scotti-Campos, P. (2023). Wheat crop under waterlogging: Potential soil and plant effects. *Plants, 12*(1), 149. https://doi.org/10.3390/plants12010149

Pan, J., Sharif, R., Xu, X., & Chen, X. (2021). Mechanisms of waterlogging tolerance in plants: Research progress and prospects. *Frontiers in Plant Science, 11*, 627331. https://doi.org/10.3389/fpls.2020.627331

Pirasteh-Anosheh, H., & Emam, Y. (2019). The role of plant growth regulators in enhancing crop yield under saline conditions: From theory to practice. *Iranian Society of Crops and Plant Breeding Sciences*. Corpus ID: 219817085.

Pryor, S. C., Barthelmie, R. J., Young, D. T., Takle, E. S., Arritt, R. W., Flory, D., Gutowski, W. J., Nunes, A., & Roads, J. (2013). Wind speed trends over the contiguous United States. *Climatic Research, 56*(1), 61–72. https://doi.org/10.3354/cr01139

Rajhi, I., Yamauchi, T., Takahashi, H., Nishiuchi, S., Shiono, K., Watanabe, R., Mliki, A., Nagamura, Y., & Nishizawa, N. K. (2011). Root cortical senescence decreases root respiration and improves waterlogging tolerance in Triticeae. *New Phytologist, 190*(2), 351–363. https://doi.org/10.1111/j.1469-8137.2010.03581.x

Ray, D. K., Gerber, J. S., MacDonald, G. K., & West, P. C. (2015). Climate variation explains a third of global crop yield variability. *Nature Communications, 6*, 5989. https://doi.org/10.1038/ncomms6989

Raza, A., Razzaq, A., Mehmood, S. S., Zou, X., Zhang, X., Lv, Y., & Xu, J. (2019). Impact of climate change on crops adaptation and strategies to tackle its outcome: A review. *Plants, 8*(2), 34. https://doi.org/10.3390/plants8020034

Reynolds, M. P., Pask, A. J. D., & Mullan, D. M. (2012). *Physiological breeding I: Interdisciplinary approaches to improve crop adaptation*. CIMMYT.

Robinson, D. (1990). Resource capture by root systems. In W. R. Gardner, D. Robinson, & A. J. Watson (Eds.), *Root growth and function in nutrient environments* (pp. 99–116). Springer.

Saengwilai, P., Tian, X., & Lynch, J. P. (2014). Low crown root number enhances nitrogen acquisition from low-nitrogen soils in maize. *Plant Physiology, 166*(2), 581–589. https://doi.org/10.1104/pp.113.232603

Schmitt, J., Offermann, F., Söder, M., Frühauf, C., & Finger, R. (2022). Extreme weather events cause significant crop yield losses at the farm level in German agriculture. *Food Policy, 112*, 102359. https://doi.org/10.1016/j.foodpol.2022.102359

Schneider, H. M., Wojciechowski, T., Postma, J. A., Brown, K. M., Lücke, A., Zeisler, V., Schreiber, L., & Lynch, J. P. (2017). Root cortical senescence improves growth under suboptimal availability of N, P, and K. *Plant Physiology, 174*(4), 2333–2347. https://doi.org/10.1104/pp.17.00763

Serraj, R., & Sinclair, T. R. (2002). Osmolyte accumulation: Can it really help increase crop yield under drought conditions? *Plant, Cell & Environment, 25*(2), 333–341. https://doi.org/10.1046/j.0016-8025.2001.00899.x

Shabala, S. (2011). Physiological and molecular bases of stress tolerance in plants. *Current Opinion in Plant Biology, 14*(3), 267–273. https://doi.org/10.1016/j.pbi.2011.03.001

Shan, Q., Wang, Y., Li, J., & Gao, C. (2014). Targeted genome modification of crop plants using a CRISPR-Cas system. *Nature Protocols, 9*(10), 2395–2410. https://doi.org/10.1038/nprot.2014.157

Sharma, A., Garg, S., Sheikh, I., & Vyas, P. (2020). Effect of wheat grain protein composition on end-use quality. *Journal of Food Science and Technology, 57*(8), 2771–2785. https://doi.org/10.1007/s13197-020-04353-0

Shukla, V., Yadav, R., Tyagi, A., Jha, A., Sharma, S., & Kumar, D. (2019). Root system architecture and abiotic stress tolerance: Current knowledge in root and tuber crops. *Frontiers in Plant Science, 10*, 1291. https://doi.org/10.3389/fpls.2019.01291

Slack, S. (2018). Identifying rooting traits and their genetic bases for improved drought tolerance in winter wheat (Doctoral dissertation). University of Nottingham, UK.

Smith, D. L., Dijak, M., Bulman, P., Ma, B. L., & Hamel, C. (1999). Barley: Physiology of yield. In V. O. Sadras & D. Calderini (Eds.), *Crop yield: Physiology and processes* (pp. 67–92). Springer.

Snyder, C. S., Bruulsema, T. W., Jensen, T. L., & Fixen, P. E. (2009). Review of greenhouse gas emissions from crop production systems and fertilizer management effects. *Agriculture, Ecosystems & Environment, 133*(3–4), 247–266. https://doi.org/10.1016/j.agee.2009.04.021

Supek, F., Bošnjak, M., Škunca, N., & Šmuc, T. (2011). Multiple statistical tests for de novo mutation discovery in bacterial genomes. *PLoS ONE, 6*(7), e21800. https://doi.org/10.1371/journal.pone.0021800

Talebnia, F., Karakashev, D., & Angelidaki, I. (2010). Production of bioethanol from wheat straw: An overview on pretreatment, hydrolysis and fermentation. *Bioresource Technology, 101*(13), 4744–4753. https://doi.org/10.1016/j.biortech.2009.11.080

Tian, L. X., Zhang, Y. C., Chen, P. L., Zhang, F. F., Li, J., Yan, F., Dong, Y., & Feng, B. L. (2021). How does the waterlogging regime affect crop yield? A global meta-analysis. *Frontiers in Plant Science, 12*, 634898. https://doi.org/10.3389/fpls.2021.634898

Tsegay, A., Raes, D., Geerts, S., Vanuytrecht, E., Abraha, B., Deckers, J., Bauer, H., & Gebrehiwot, K. (2011). Unravelling crop water productivity of tef (*Eragrostis tef* (Zucc.) Trotter) through AquaCrop in northern Ethiopia. *Experimental Agriculture, 48*(2), 222–237. https://doi.org/10.1017/S0014479711001104

Turner, N. C. (2019). Water use efficiency in crop plants: Lessons from the past and research opportunities for the future. *Functional Plant Biology, 46*(12), 1034–1043. https://doi.org/10.1071/FP19176

Tyree, M. T., & Zimmermann, M. H. (2013). *Xylem structure and the ascent of sap*. Springer Science & Business Media. https://doi.org/10.1007/978-3-662-10048-3

USGCRP (United States Global Change Research Program). (2014). Hatfield, J., Takle, G., Grotjahn, R., Holden, P., Izaurralde, R. C., Mader, T., Marshall, E., & Liverman, D. Agriculture. In J. M. Melillo, T. C. Richmond, & G. W. Yohe (Eds.), *Climate change impacts in the United States: The third national climate assessment* (pp. 150–174). U.S. Global Change Research Program. https://doi.org/10.7930/J02Z13FR

Vanhees, D. J., Loades, K. W., Bengough, A. G., Mooney, S. J., & Lynch, J. P. (2020). Root anatomical traits contribute to deeper rooting of maize under compacted field conditions. *Journal of Experimental Botany, 71*(15), 4243–4257. https://doi.org/10.1093/jxb/eraa165

Varshavsky, A. (2019). N-degron and C-degron pathways of protein degradation. *Proceedings of the National Academy of Sciences, 116*(2), 358–366. https://doi.org/10.1073/pnas.1816596116

Vicente, J., Mendiondo, G. M., Movahedi, M., Peirats-Llobet, M., Juan, Y. T., Filippou, P., … Holdsworth, M. J. (2017). The Cys-Arg/N-end rule pathway is a general sensor of abiotic

stress in flowering plants. *Current Biology, 27*(22), 3183–3190.e4. https://doi.org/10.1016/j.cub.2017.09.048

Voesenek, L. A. C. J., & Bailey-Serres, J. (2015). Flood adaptive traits and processes: An overview. *New Phytologist, 206*(1), 57–73. https://doi.org/10.1111/nph.13209

Wahab, A., Mahmoud, M., Mottaleb, A., Rowezak, M., Salama, A., & Mahmoud, A. (2022). The role of nano-silicon and other soil conditioners in improving physiology and yield of drought-stressed barley crop. *Agriculture (Pol'nohospodárstvo), 67*(3), 124–143. https://doi.org/10.2478/agri-2021-0012

Weits, D. A., Kunkowska, A. B., Kamps, N. C. W., Portz, K. M. S., Packbier, N. K., Pedersen, O., … Licausi, F. (2020). Plant oxygen sensors: A breath of fresh air. *Journal of Experimental Botany, 71*(7), 2002–2010. https://doi.org/10.1093/jxb/eraa033

White, M. D., Klecker, M., Hopkinson, R. J., Weits, D. A., Mueller, C., Naumann, C., … Flashman, E. (2017). Plant cysteine oxidases are dioxygenases that enable arginylation of N-end rule targets. *Nature Communications, 8*, 14690. https://doi.org/10.1038/ncomms14690

Wu, Q., Pagès, L., & Wu, J. (2016). Relationships between root diameter, root length and root branching along lateral roots in adult, field-grown maize. *Annals of Botany, 117*(3), 379–390. https://doi.org/10.1093/aob/mcv185

Xiong, W., Reynolds, M., & Xu, Y. (2022). Climate change challenges plant breeding. *Current Opinion in Plant Biology, 70*, 102308. https://doi.org/10.1016/j.pbi.2022.102308

Xu, K., Xu, X., Fukao, T., Canlas, P., Maghirang-Rodriguez, R., Heuer, S., … Bailey-Serres, J. (2020). Understanding the genetic mechanisms of plant resistance to flooding stress. *Advances in Genetics, 104*, 127–155. https://doi.org/10.1016/bs.adgen.2019.12.002

Zhu, J., Mickelson, S. M., Kaeppler, S. M., & Lynch, J. P. (2010). Detection of QTL for adventitious root formation in maize (*Zea mays* L.) under differential phosphorus availability. *Theoretical and Applied Genetics, 121*(5), 721–731. https://doi.org/10.1007/s00122-010-1332-3

Zong, Y., Wang, Y., Li, C., Zhang, R., Chen, K., Ran, Y., … Gao, C. (2017). Precise base editing in rice, wheat and maize with a Cas9-cytidine deaminase fusion. *Nature Biotechnology, 35*(5), 438–440. https://doi.org/10.1038/nbt.3811